ELSEVIER

FEMS Microbiology Reviews 23 (1999) 179–230

FEMS MICROBIOLOGY REVIEWS

Physico-chemistry of initial microbial adhesive interactions – its mechanisms and methods for study

Rolf Bos *, Henny C. van der Mei, Henk J. Busscher

Department of Biomedical Engineering, University of Groningen, Bloemsingel 10, 9712 KZ Groningen, The Netherlands

Received 26 August 1998; accepted 10 February 1999

Abstract

In this review, initial microbial adhesive interactions are divided into adhesion to substratum surfaces, coaggregation between microbial pairs and co-adhesion between sessile and planktonic microorganisms of different strains or species. The physico-chemical mechanisms underlying the adhesive interactions are described and a critical review is given of currently employed methods to study microbial adhesive interactions, with an emphasis on the use of the parallel plate flow chamber. Subsequently, for each of the three microbial adhesive interactions distinguished, the role of Lifshitz-van der Waals, acid-base and electrostatic interactions is described based on existing literature.

Keywords: Microbial adhesion; Hydrophobicity; Contact angle; Zeta potential; Flow chamber; Biofilm

1. Introduction

''Give your evidence'', the King repeated angrily, ''or I'll have you executed.''
Lewis Carroll: Alice in Wonderland

Microorganisms have a strong tendency to become associated with surfaces [1]. Once microorganisms are attached to a substratum surface, a multistep process starts leading to the formation of a complex, adhering microbial community that is termed a 'biofilm'. A biofilm can be defined as a layer of prokaryotic or eukaryotic cells, anchored to a substratum surface and embedded in an organic matrix of biological origin. Biofilms can be beneficial, for instance, to degrade environmental hazardous substances in the soil [2,3] or in a bioreactor [4] or as bioflocculants in the separation of coal particles from associated mineral matter [5], but also detrimental as on food [6–10] and slaughterhouse equipment [11,12], ship hulls [13], biomaterials implants [14], or in the oral cavity [15].

Whereas in many biotechnological applications it is attempted to maintain biofilm adhesion in an optimal spatial arrangement of different microbial species in order to stimulate efficient degradation of xenobiotics in a bioreactor [16], in the medical and dental fields research is focused most often on how to prevent and control formation of an infectious, pathogenic biofilm, and on how to keep the com-

* Corresponding author. Tel.: +31 (50) 3633 140; Fax: +31 (50) 3633 159; E-mail: r.bos@med.rug.nl

0168-6445/99/$20.00
PII: S0168-6445(99)00004-2

a	microbial radius, [m], [μm]
a_h	hydrodynamic microbial radius, [m], [μm]
A	Hamaker constant, [J], [kT]
A_1	blocked area, [m^2], [μm^2]
b	half depth of the parallel plate flow chamber, [m], [cm]
c	microbial density in suspension, [m^{-3}], [cm^{-3}]
d	distance, [m], [cm]
d_0	distance of closest approach between two surfaces, generally taken to be 1.57 Å, [m], [Å]
D_∞	microbial diffusion coefficient, [$m^2\ s^{-1}$], [$cm^2\ s^{-1}$]
e	electron charge, 1.6021×10^{-19} C, [C]
F_d	viscous drag force on an adhering spherical microorganism, [N]
F_l	lift force on an adhering spherical microorganism, [N]
F_γ	surface tension force on a spherical microorganism, [N]
g(r)	radial pair distribution function
g(x,y)	local pair distribution function
G	interaction energy, [J], [kT]
j (t)	deposition rate at t, [$m^{-2}\ s^{-1}$], [$cm^{-2}\ s^{-1}$]
j_0	initial deposition rate, [$m^{-2}\ s^{-1}$], [$cm^{-2}\ s^{-1}$]
j_0^*	initial deposition rate according to Smoluchowski-Levich, [$m^{-2}\ s^{-1}$], [$cm^{-2}\ s^{-1}$]
$j_{ads}(t)$	adsorption rate at t, [$m^{-2}\ s^{-1}$], [$cm^{-2}\ s^{-1}$]
$j_{des}(t)$	desorption rate at t, [$m^{-2}\ s^{-1}$], [$cm^{-2}\ s^{-1}$]
k	Boltzmann constant, 1.3807×10^{-23} J K^{-1}, [J K^{-1}]
Le	establishment length for laminar flow, [m], [cm]
N_A	Avogadro's constant, 6.0225×10^{23} mol^{-1}, [mol^{-1}]
n(t)	number of adhering microorganisms at t, [m^{-2}], [cm^{-2}]
n_∞	number of adhering microorganisms in a stationary end-point, [m^{-2}], [cm^{-2}]
Pe	Péclet number
Q	volumetric flow rate, [$m^3\ s^{-1}$], [$cm^3\ s^{-1}$]
Re	Reynolds number
R_0	initial removal rate of microorganisms in MATH or MATS, [s^{-1}], [min^{-1}]
t	time, [s]
T	absolute temperature, 298 K for room temperature, [K]
v	velocity, [m s^{-1}], [cm s^{-1}]
w	width of the parallel plate flow chamber, [m], [cm]
x	longitudinal distance from the entrance of the parallel plate flow chamber, [m], [cm]
z	height above the bottom plate of the parallel plate flow chamber, [m], [cm]
α_d	deposition efficiency
β	desorption rate coefficient, [s^{-1}]
$\beta(t-\tau)$	desorption rate coefficient as a function of residence time, [s^{-1}]
β_0	initial desorption rate coefficient, [s^{-1}]
β_∞, β_f	final desorption rate coefficient, [s^{-1}]
γ^{LW}	apolar or Lifshitz-van der Waals component of the surface free energy, [mJ m^{-2}]
γ^{AB}	polar or acid-base component of the surface free energy, [mJ m^{-2}]
$\gamma^{\ominus}$	electron-donating parameter of the acid-base component, [mJ m^{-2}]
$\gamma^{\oplus}$	electron-accepting parameter of the acid-base component, [mJ m^{-2}]
γ_{ij}	interfacial free energy, [mJ m^{-2}]
δ	reciprocal relaxation time for bond aging, [s^{-1}]
δ_d	diffusion boundary layer thickness, [m], [nm]
ΔG_{adh}	free energy of adhesion, [mJ m^{-2}]
$\Delta G_{(co)agg}$	free energy of (co)aggregation, [mJ m^{-2}]
ΔG_{co-adh}	free energy of co-adhesion, [mJ m^{-2}]
ε ($\varepsilon_0\varepsilon_r$)	permittivity, 6.96×10^{-10} J m^{-1} V^{-2} for water, [J m^{-1} V^{-2}]
ε_0	permittivity of vacuum, 8.85×10^{-12} J m^{-1} V^{-2}, [J m^{-1} V^{-2}]
ε_r	relative permittivity or dielectric constant, 78.2 for water
θ	(microbial) contact angle, [degrees]
κ^{-1}	double layer thickness, [m], [Å]
λ	correlation length of molecules in a liquid, [m], [nm]
μ	absolute viscosity, 10^{-3} kg m^{-1} s^{-1} for water, [kg m^{-1} s^{-1}]
ρ	fluid density, 10^3 kg m^{-3} for water, [kg m^{-3}]

ρ_0	average density of adhering microorganisms, [m^{-2}], [cm^{-2}]	τ	time of arrival of adhering microorganisms, [s]
$\rho(r,dr)$	local density of adhering microorganisms in a shell with thickness dr at a distance r, [m^{-2}], [cm^{-2}]	χ	ratio between local and non-local deposition rate
σ	wall shear rate, [s^{-1}]	ζ	zeta potential, [mV]

mensal microflora of the skin, urinary and intestinal tracts, or oral cavity intact and free of potential pathogens [17,18]. In the oral cavity, daily tooth brushing is required in order to remove dental plaque and prevent the formation of a cariogenic or periodontopathogenic biofilm. However, despite extensive brushing, not all microorganisms adhering to the tooth surfaces will be removed, because removal is difficult from gingival pockets, interproximal spaces and other retention sites, such as cracks and fissures. These adhering or sessile microorganisms may stimulate the adhesion of planktonic microorganisms present in saliva in vast amounts (10^8 CFU ml^{-1}), as the onset of a new, potentially pathogenic plaque [15,19,20]. In dairy processing, adhesion of thermophilic streptococcal strains on heat exchanger plates in the downward section of pasteurizers may lead to the contamination of already pasteurized products with adverse effects on their taste [6,21]. Microbial adhesion also forms the onset of biofouling on ship hulls and it has been estimated [13] that biofilms, several hundred micrometers in thickness, yield an increase in fuel consumption for an average US Naval vessel of around 20%, corresponding with US$ 400 h^{-1} at 26 knots (48 km h^{-1}).

Although the function and appearance of biofilms in various environments may be different, all biofilms originate from the same sequence of events [22,23]. Fig. 1 schematically presents the initial steps in the formation of a complex, multispecies biofilm. When microorganisms and substratum surfaces are in an aqueous environment, in which organic matter is present (e.g. sea water, milk, tear fluid, urine, blood or saliva), substratum surfaces will first become covered with a layer of adsorbed, organic molecules, generally called 'conditioning film' [24,25], before microorganisms adhere, simply because transport and adsorption of molecules to a substratum proceed relatively fast compared to that of microorganisms [22,24]. Transport of microorganisms towards a substratum surface, as the second step in biofilm formation (see Fig. 1), can be by different mechanisms, depending on the system under consideration, and may include Brownian motion, gravitation, diffusion, convection, or the intrinsic motility of a microorganism. Alternatively, also microorganisms in suspension may be transported towards each other and microbial (co)aggregates can be formed. Subsequently, microbial adhesion (either of single organisms or of (co)aggregates) may occur which is often initially reversible and becomes irreversible in time, amongst others through excretion of exopolymeric substances by the adhering microorganisms [26,27]. Sometimes the excreted, exopolymeric substance adsorbs to a substratum surface to form a microbially derived conditioning film [28], as opposed to host or environmentally derived conditioning films. When a conditioning film is present, an adhering microorganism is usually not in contact with the actual substratum surface and the strength of biofilm formation becomes dependent upon the cohesiveness of the conditioning film, rather than upon its direct interaction with the bare substratum surface [29,30]. Only a few adhering, sessile microorganisms can stimulate the adhesion of other, still suspended planktonic microorganisms. This may occur by sessile microorganisms slowing down an approaching, planktonic microorganism, thus increasing its chance of adhering to the substratum surface, as is frequently observed under flow [31,32] or through strong attractive interactions between sessile and planktonic microorganisms, a phenomenon known as 'co-adhesion' [33–36]. Eventually, adhering microorganisms start growing, which is the major factor contributing to the accumulation of a high number of cells on a substratum surface. Of course, the model as presented in Fig. 1 is simplified and ignores aspects of biofilm formation, such as biosurfactant release by adhering microor-

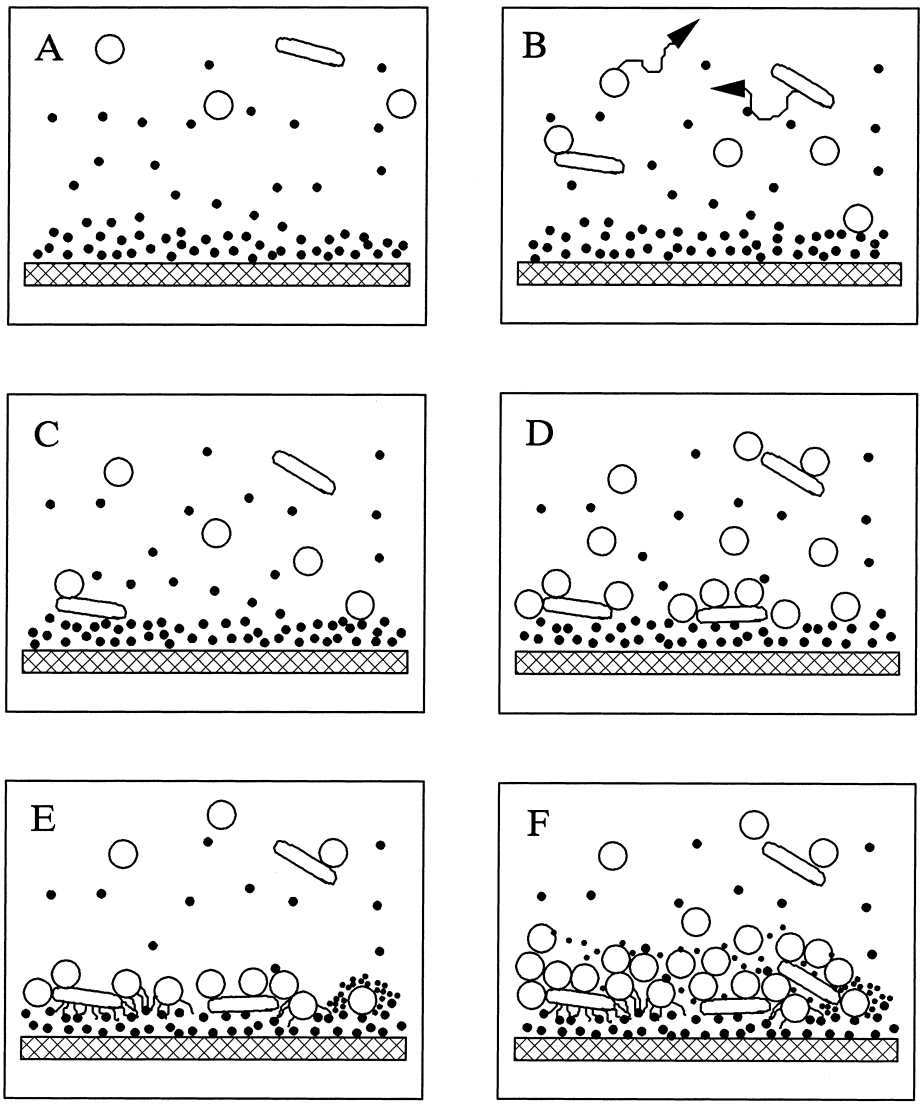

Fig. 1. Schematic, sequential presentation of the initial steps in biofilm formation. A: Adsorption of conditioning film components; B: microbial transport and coaggregation; C: (reversible) adhesion of single organisms and of microbial coaggregates; D: co-adhesion between microbial pairs; E: anchoring or the establishment of firm, irreversible adhesion through exopolymer production; F: growth.

ganisms [37,38], the prevailing nutrient [39,40] or hydrodynamic conditions [41], roughness [42,43] and undoubtedly several other, unknown factors. It is envisaged, however, that the initial events as summarized above will determine the final structure and microbial composition of a mature biofilm [44,45].

Roughness has an influence on biofilm formation [43,46], but with regard to initial adhesion roughness appears to be a minor factor [42,47]. Micrographs of organisms adhering to substratum surfaces seldom show a preference of microorganisms to adhere in scratches or grooves [48]. The influence of surface roughness on biofilm formation is likely more related to the difficulties involved in cleaning rough surfaces [49], resulting in rapid re-growth of a biofilm [43], rather than to being a contributing factor on its own. From a physico-chemical, mechanistic point of view, a rough surface is a folded, flat surface with an ex-

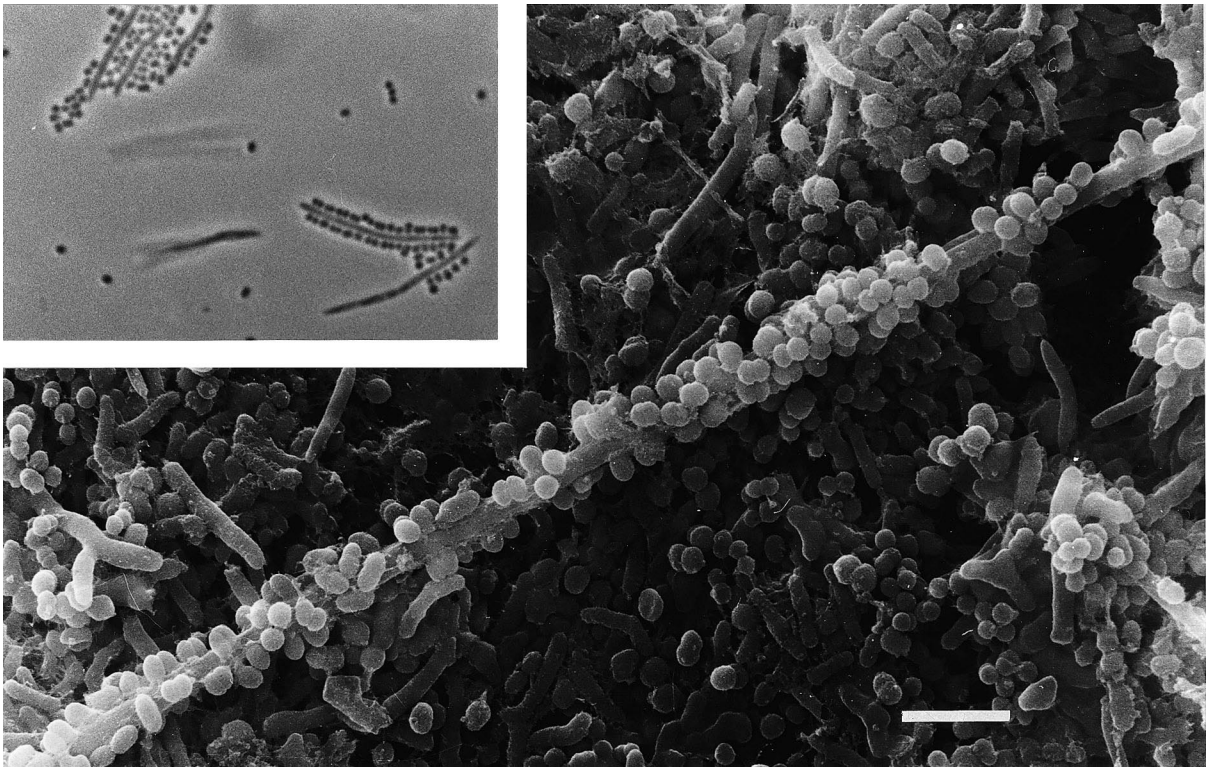

Fig. 2. Scanning electron micrograph (courtesy of Dr. W.L. Jongebloed) of so-called corn-cob structures, as observed frequently in dental plaque, showing close associations between different microorganisms that came into existence either by 'coaggregation' or by 'co-adhesion'. The bar indicates 5 μm. The inset shows a light micrograph (courtesy of Dr. P.E. Kolenbrander) of coaggregates between fusobacteria and streptococci formed in suspension as the onset of corn-cob formations found in vivo.

tended surface area [42] from which similar interaction forces arise as from a smooth surface.

Especially in environments with large numbers of planktonic microorganisms, as in the oral cavity, interspecies binding is believed to be a significant factor in the development of biofilms [15]. Actually, it has long been suggested that interspecies binding occurs solely between microbial species in the oral cavity [50], but examples of interspecies binding outside the oral cavity have been described as well, most notably between pathogenic and commensal microorganisms of the urinary tract [51,52], serving possibly as a clearing mechanism or a means to enhance lactobacillus interference with uropathogen adhesion. Recently [53], also coaggregation between aquatic bacteria has been reported, with *Micrococcus luteus* being mentioned as a bridging organism in the development of aquatic biofilms owing to its ability to coaggregate with many aquatic heterotrophs. Nevertheless, the relevance of interspecies binding in the development of dental plaque is best documented and becomes immediately obvious from electron micrographs of dental plaque, showing close associations between microbial pairs often referred to as so-called corn-cob structures (see Fig. 2). Interspecies binding between oral microbial pairs was first reported by Gibbons and Nygaard [54], observing that certain pairs of planktonic, oral microorganisms displayed fast and extensive coaggregation upon mixing in a test tube, whereas others did not. Subsequently, other investigators have demonstrated that each microbial strain or species has its own specific coaggregation partner [55]. This non-random, specific coaggregation obviously leads to the ordered, corn-cob structures in dental plaque as shown in Fig. 2 [56] and is said to be mediated by stereo-chemical interactions between specific surface components on the interacting microbial cell surfa-

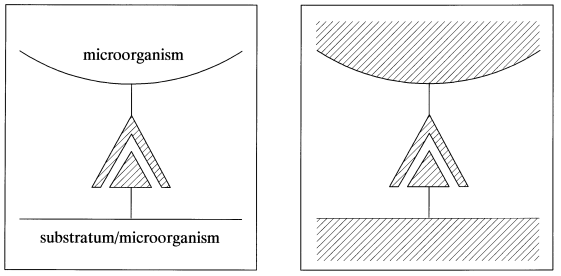

Fig. 3. Both specific and non-specific interactions originate from the same fundamental, physico-chemical forces. In the case of so-called specific interactions, only those forces between highly localized, stereochemical molecular groups are considered (left), whereas the forces between the entire body of the interacting surfaces, whether microbial or not, constitute the so-called non-specific interaction (right). The shaded areas indicate the regions from where the interaction forces are assumed to originate.

ces, such as lectin-carbohydrate interactions [55,57,58].

Although microbial adhesion to inert substratum surfaces as well as to other microbial cell surfaces (i.e. coaggregation or co-adhesion) is frequently described in terms of specific interactions between localized, specific molecular groups and sometimes even in terms of specific forces as being a separate class of fundamental interaction forces, it is important to realize that all interaction forces originate from the same fundamental forces [59,60], including the ever present Lifshitz-van der Waals forces, electrostatic forces, and acid-base interactions. Moreover, whereas specific interactions are highly directional, spatially confined between molecular groups and consequently operative over small distances, say smaller than 5 nm, the so-called non-specific association in microbial adhesion arises from interaction forces between all molecules of the entire cell and substratum and are consequently of a more long-range character. Therefore, in order to adequately describe microbial adhesive interactions, either between two microbial species or between a microorganism and a substratum surface, both the overall, long-range, and non-specific fundamental interaction forces and short-range, specific interactions, as a corollary of the same fundamental forces, now between microscopic stereo-chemical groups, must be taken into consideration [61–63], as schematically indicated in Fig. 3. In fact, once the general macroscopic interaction forces have allowed two surfaces to interact, complementary stereochemical groups may attract each other from a distance of several nanometers, with an attractive interaction energy by far exceeding the general macroscopic interaction [64].

The aim of this review is firstly to summarize physico-chemical approaches frequently employed in modelling microbial adhesive interactions and to try to embed these approaches in our current biochemical and microbiological knowledge of adhesion mechanisms. Secondly, methods generally used to study microbial adhesion to substratum surfaces, microbial coaggregation and co-adhesion will be critically reviewed. The method considered most elegant by the authors, i.e. the parallel plate flow chamber

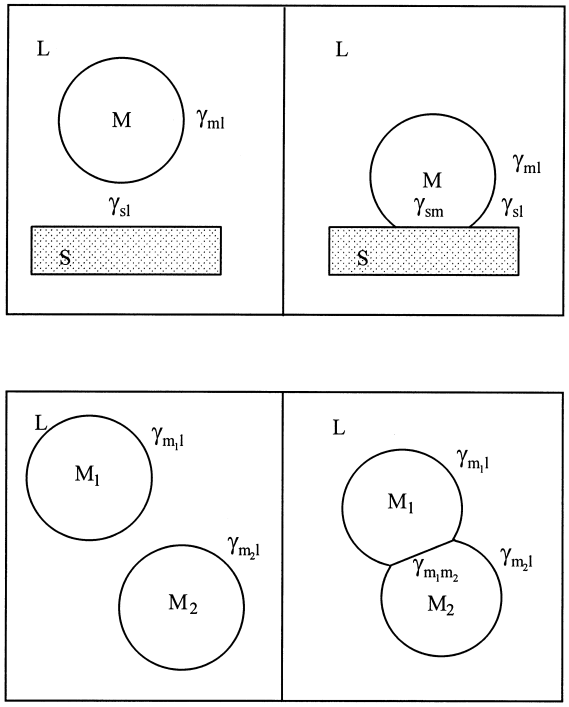

Fig. 4. Schematic presentation of the interfacial free energies γ_{ij} involved in the adhesion of a microorganism (M) to a solid substratum surface (S) from a liquid suspension (L) and for the adhesive interaction between two microorganisms 1 and 2 ('coaggregation' or 'co-adhesion'). Dependent on whether the interfacial free energies in the right- or left-hand boxes are lower, interaction will or will not occur (see also Eq. 1).

Table 1
Surface tension components and parameters (mJ m^{-2}) of liquids, often employed in contact angle measurements [86]

Liquid	γ_{lv}	γ_{lv}^{LW}	γ_{lv}^{AB}	$\gamma_{lv}^{\oplus}$	$\gamma_{lv}^{\ominus}$
Water	72.8	21.8	51.0	25.5	25.5
Glycerol	64	34	30	3.92	57.4
Ethylene glycol	48.0	29	19.0	1.92	47.0
Formamide	58	39	19	2.28	39.6
Dimethylsulfoxide	44	36	8	0.5	32.0
α-Bromonaphthalene	44.4	44.4	~0		
Diiodomethane	50.8	50.8	~0		
Hexadecane	27.5	27.5	0		

combined with in situ image analysis techniques, will be discussed in detail, including aspects of mass transport.

2. Physico-chemical approaches towards microbial adhesive interactions

Is 't not possible to understand in another tongue?
William Shakespeare: Hamlet

Microbial cell surfaces are both chemically and structurally more complex and heterogeneous than most inert substratum surfaces [65], which complicates a physico-chemical approach of microbial adhesive interactions. The simple concept of distance, for instance, remains meaningful for separation distances between inert surfaces up to several nanometers. Surface appendages on microbial cell surfaces can become as long as 1 μm, and consequently the concept of distance between a microorganism and any other surface already loses its meaning at fairly large separation distances.

Two physico-chemical approaches, initially considered distinctly different, are available to describe microbial adhesive interactions. In the thermodynamic approach [66,67], the interacting surfaces are assumed to physically contact each other under conditions of thermodynamic equilibrium, i.e. reversible adhesion. The thermodynamic approach is based on surface free energies of the interacting surfaces and does not include an explicit role for electrostatic interactions. Alternatively, the classical DLVO (Derjaguin, Landau, Verwey, Overbeek) approach describes the interaction energies between the interacting surfaces, based on Lifshitz-van der Waals and electrostatic interactions and their decay with separation distance [68,69]. Both approaches have proven merits for microbial adhesion, when certain collections of strains and species are considered, but have failed so far to yield a generalized description of all aspects of microbial adhesion valid for each and every strain [70].

Van Oss et al. [71] introduced a so-called extended DLVO theory by including short-range Lewis acid-base interactions in the above, classical DLVO approach. Inclusion of acid-base interactions in the classical DLVO approach probably [72] implies that 'hydrophobic attractive' [73] and 'hydrophilic repulsive' [74,75] forces can be accounted for in colloid and surface science in a more formal way now.

2.1. The thermodynamic approach

In the thermodynamic approach towards microbial adhesive interactions, the interfacial free energies between the interacting surfaces are compared, as schematically illustrated in Fig. 4. Accordingly, this comparison is expressed in the so-called free energy of adhesion

→

Fig. 5. Diagram of contact angle and surface tension data as can be used in various approaches to convert measured contact angles with liquids into surface free energies, i.e. Eqs. 3–5 eventually leading to the calculation of the free energy of adhesion, ΔG_{adh} (similar diagrams are valid for the calculation of $\Delta G_{(co)agg}$ or ΔG_{co-adh}). Note that the free energies of adhesion, as can be calculated according to the different approaches, are not necessarily equal.

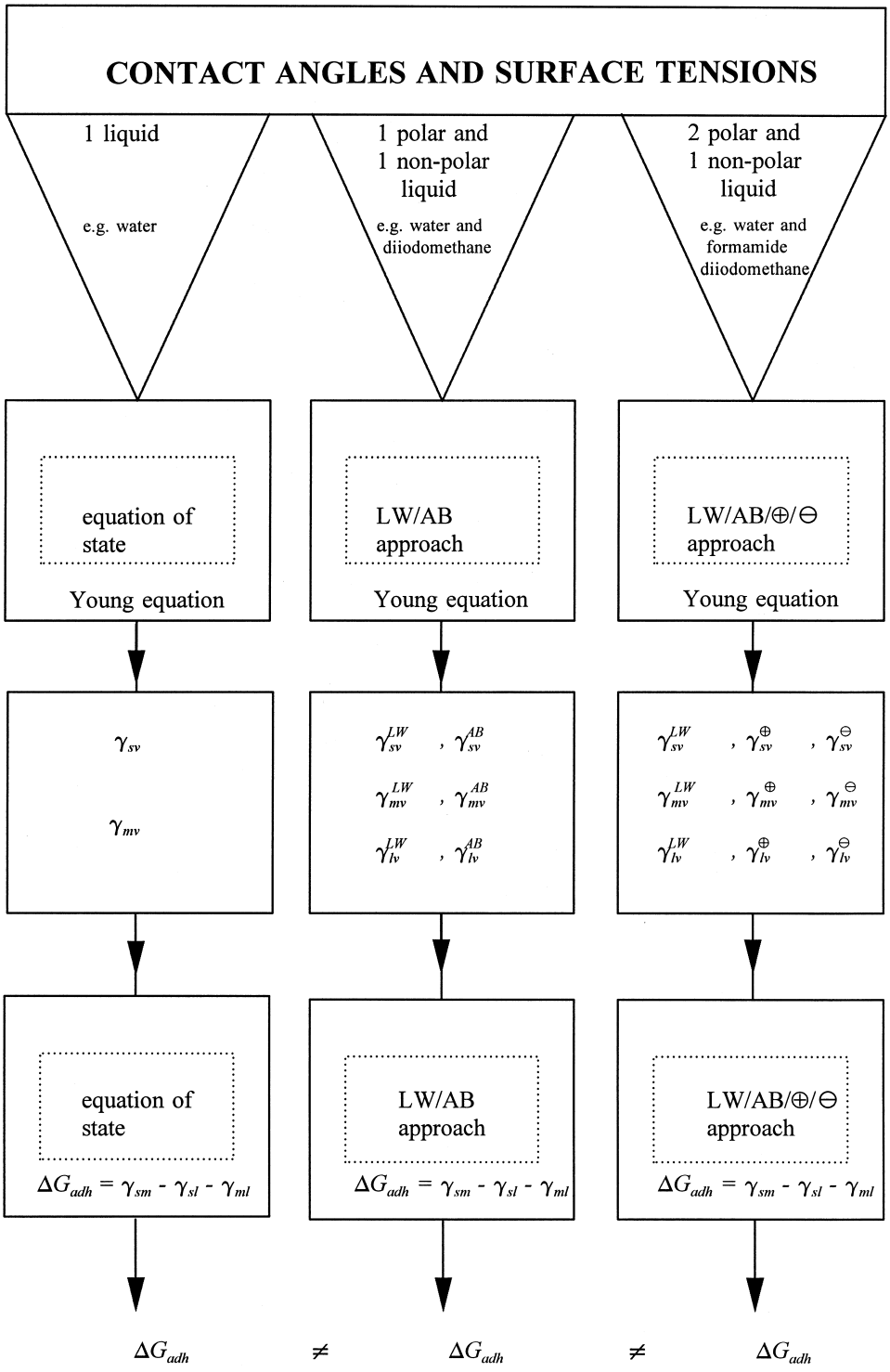
CONTACT ANGLES AND SURFACE TENSIONS
1 liquid
e.g. water
1 polar and 1 non-polar liquid
e.g. water and diiodomethane
2 polar and 1 non-polar liquid
e.g. water and formamide diiodomethane
equation of state
Young equation
LW/AB approach
Young equation
LW/AB/⊕/⊖ approach
Young equation
γ_{sv}
γ_{mv}
γ_{sv}^{LW} , γ_{sv}^{AB}
γ_{mv}^{LW} , γ_{mv}^{AB}
γ_{lv}^{LW} , γ_{lv}^{AB}
γ_{sv}^{LW} , $\gamma_{sv}^{\oplus}$, $\gamma_{sv}^{\ominus}$
γ_{mv}^{LW} , $\gamma_{mv}^{\oplus}$, $\gamma_{mv}^{\ominus}$
γ_{lv}^{LW} , $\gamma_{lv}^{\oplus}$, $\gamma_{lv}^{\ominus}$
equation of state
$\Delta G_{adh} = \gamma_{sm} - \gamma_{sl} - \gamma_{ml}$
LW/AB approach
$\Delta G_{adh} = \gamma_{sm} - \gamma_{sl} - \gamma_{ml}$
LW/AB/⊕/⊖ approach
$\Delta G_{adh} = \gamma_{sm} - \gamma_{sl} - \gamma_{ml}$
ΔG_{adh} ≠ ΔG_{adh} ≠ ΔG_{adh}

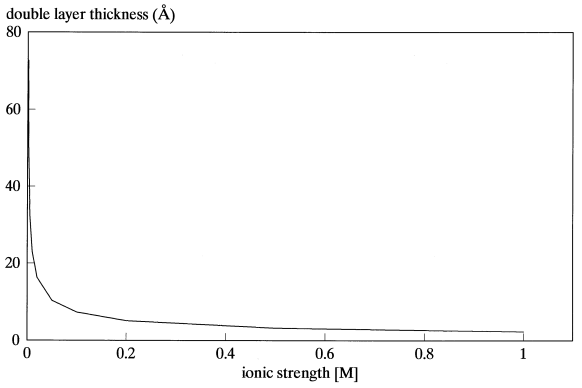

Fig. 6. The double layer thickness κ^{-1} as a function of the ionic strength of a potassium phosphate buffer at pH 7.0.

$$\Delta G_{adh} = \gamma_{sm} - \gamma_{sl} - \gamma_{ml} \quad (1)$$

in which γ_{sm}, γ_{sl}, and γ_{ml} are the solid-microorganism, solid-liquid, and microorganism-liquid interfacial free energies, respectively. At this point it is emphasized that Eq. 1 can also be set up to cover microbial (co)aggregation and co-adhesive interactions by replacing the solid by an identical microorganism or partner organism, in which case the free energy balance is preferably defined as $\Delta G_{(co)agg}$ or ΔG_{co-adh}, respectively. A free energy balance as expressed by Eq. 1 is important to predict from a physico-chemical perspective whether or not microbial interactions will occur. Like all systems in nature, the system of interacting surfaces depicted in Fig. 4 will also strive to obtain a state of minimal free energy. Therefore, microbial adhesion is favorable to occur from a free energy point of view, when ΔG_{adh} is negative ($\Delta G_{adh} < 0$), while adhesion is energetically unfavorable when $\Delta G_{adh} > 0$.

Unfortunately, it is impossible to experimentally determine the interfacial free energies occurring in Eq. 1 without the use of controversial theories [76], common to all being the input of contact angle data. Contact angles with liquids can be measured both on solid substrata and on microbial lawns [77] simply by putting μl-sized liquid droplets on the surface. Contact angles are related to the surface free energies in the contact angle equilibrium according to the equation of Young

$$\gamma_{lv} \cos\theta = \gamma_{sv} - \gamma_{sl} \quad (2)$$

in which the subscripts denote the respective surface free energy between the liquid (l), solid (s), or vapor (v). When contact angles on microbial lawns are measured, the subscript (s) should be replaced by (m).

Eq. 2 cannot be solved for the interfacial free energies γ_{sv} and γ_{sl} by measuring the contact angle θ and liquid surface tension γ_{lv} (see Table 1) without additional assumptions, which form the basis of serious controversy in colloid and surface science. In one of the first and still frequently used approaches [78], the existence of an equation of state is assumed relating

$$\gamma_{sl} = \frac{(\sqrt{\gamma_{sv}} - \sqrt{\gamma_{lv}})^2}{1 - 0.015\sqrt{\gamma_{sv}\gamma_{lv}}} \quad (3)$$

Combination of Eqs. 2 and 3 together with the experimental input data θ and γ_{lv} of only one liquid subsequently yields γ_{sv} from published computer tables [79]. The use of published computer tables 'mends' the difficulty (said by Neumann and coworkers to be of "purely mathematical origin") that may arise when the denominator of Eq. 3 becomes zero for large surface tension γ_{lv} 'by physical reasoning' [80] but to us, almost 25 years after the first publication on the equation of state, this 'physical reasoning' still is not clear. Next, the equation of state can be employed to calculate the interfacial free energies γ_{sm}, γ_{sl} and γ_{ml} occurring in Eq. 1 (see also the scheme in Fig. 5).

In another approach, surface free energies are separated in an apolar or Lifshitz-van der Waals (γ^{LW}) and a polar or acid-base (γ^{AB}) component [71,81–83]. These surface free energy components can be combined according to several combining rules [84], of which the geometric mean is most commonly applied

$$\gamma = {}_{sl}\left(\sqrt{\gamma_{sv}^{LW}} - \sqrt{\gamma_{lv}^{LW}}\right)^2 + \left(\sqrt{\gamma_{sv}^{AB}} - \sqrt{\gamma_{lv}^{AB}}\right)^2 \quad (4)$$

Once the liquid-vapor surface free energy compo-

nents in Eq. 4 are known, contact angle data with at least two liquids and combination of Eq. 2 and Eq. 4 yield γ_{sv}, while assuming that spreading pressures [85] are negligible, i.e. $\gamma_s = \gamma_{sv}$. Subsequently, the geometric mean equation can be employed to calculate the interfacial free energies occurring in Eq. 1.

A further separation of surface free energies, involving splitting the acid-base component into an electron-donating $\gamma^{\ominus}$ and an electron-accepting $\gamma^{\oplus}$ parameter, yields

$$\gamma_{sl} = \left(\sqrt{\gamma_{sv}^{LW}} - \sqrt{\gamma_{lv}^{LW}}\right)^2 + 2 \left(\sqrt{\gamma_{sv}^{\oplus}\gamma_{sv}^{\ominus}} + \sqrt{\gamma_{lv}^{\oplus}\gamma_{lv}^{\ominus}} - \sqrt{\gamma_{sv}^{\ominus}\gamma_{lv}^{\oplus}} - \sqrt{\gamma_{sv}^{\oplus}\gamma_{lv}^{\ominus}}\right) \quad (5)$$

By an analogous procedure, as described above for the use of the geometric mean equation to derive the interfacial free energy components occurring in Eq. 4, Eq. 5 can also be combined with the Young equation, Eq. 2, to yield γ_{sv}. It is emphasized that approximation of the surface free energy components γ^{LW} and γ^{AB} with its $\gamma^{\ominus}$ and $\gamma^{\oplus}$ parameters requires contact angle measurements with at least three different liquids, such as water, formamide (or glycerol) and methylene iodide (or α-bromonaphthalene). Hereafter, the interfacial free energies in Eq. 1 can be evaluated using the expression in Eq. 5.

Evaluation of ΔG_{adh} (Eq. 1) is relatively easy on the basis of the equation of state, but becomes increasingly complicated when surface free energy components γ^{LW} and γ^{AB} and parameters $\gamma^{\ominus}$ and $\gamma^{\oplus}$ are included. First, ΔG_{adh} can be separated into two components according to

$$\Delta G_{adh} = \Delta G_{adh}^{LW} + \Delta G_{adh}^{AB} \quad (6)$$

Evaluation of ΔG_{adh}^{LW} is similar for the application of Eqs. 4 or 5 and yields

$$\Delta G_{adh}^{LW} = -2\left(\sqrt{\gamma_{mv}^{LW}} - \sqrt{\gamma_{lv}^{LW}}\right)\left(\sqrt{\gamma_{sv}^{LW}} - \sqrt{\gamma_{lv}^{LW}}\right) \quad (7)$$

Table 2
The Lifshitz-van der Waals $G^{LW}(d)$ and electrostatic $G^{EL}(d)$ interaction energies for a sphere with radius a opposed to a semi-infinite plate ('microbial adhesion to a substratum surface') and for two interacting spherical particles with radii a_1 and a_2 ('microbial (co-)aggregation') as a function of the separation distance d

Configuration	Interaction energies	
	Lifshitz-van der Waals[a]	Electrostatic[b]
Sphere-plate	$-\frac{A}{6}\left[\frac{a}{d} + \frac{a}{d+2a} + \ln\left(\frac{d}{d+2a}\right)\right]$	$\pi\varepsilon a(\zeta_1^2 + \zeta_2^2)\left[\frac{2\zeta_1\zeta_2}{\zeta_1^2+\zeta_2^2}\ln\frac{1+\exp(-\kappa d)}{1-\exp(-\kappa d)} + \ln\{1-\exp(-2\kappa d)\}\right]$
Sphere-sphere	$\frac{-Aa_1a_2}{6d(a_1+a_2)}$	$\frac{\pi\varepsilon a_1a_2(\zeta_1^2+\zeta_2^2)}{(a_1+a_2)}\left[\frac{2\zeta_1\zeta_2}{\zeta_1^2+\zeta_2^2}\ln\frac{1+\exp(-\kappa d)}{1-\exp(-\kappa d)} + \ln\{1-\exp(-2\kappa d)\}\right]$

[a] A denotes the Hamaker constant.

[b] ε denotes the permittivity of the medium, ζ the zeta potential and κ^{-1} is the double layer thickness. κ^{-1} can be calculated from $\kappa = \left[\frac{e^2}{\varepsilon k T}\cdot\sum_i z_i\cdot n_i\right]^{1/2}$ $[m^{-1}]$in which e denotes the electron charge, k the Boltzmann constant, T the absolute temperature, z_i is the valency of the ions present and n_i is the number of ions per unit volume. The variation of the double layer thickness κ^{-1} with ionic strength for a potassium phosphate buffer (pH 7.0) is shown in Fig. 6. For a symmetrical 1-1 electrolyte this equation reduces to $\kappa = 0.328\times10^{10}\ (z_i^2\cdot M_i)^{1/2}$ $[m^{-1}]$, where M_i is molarity [mol l^{-1}] of the ions.

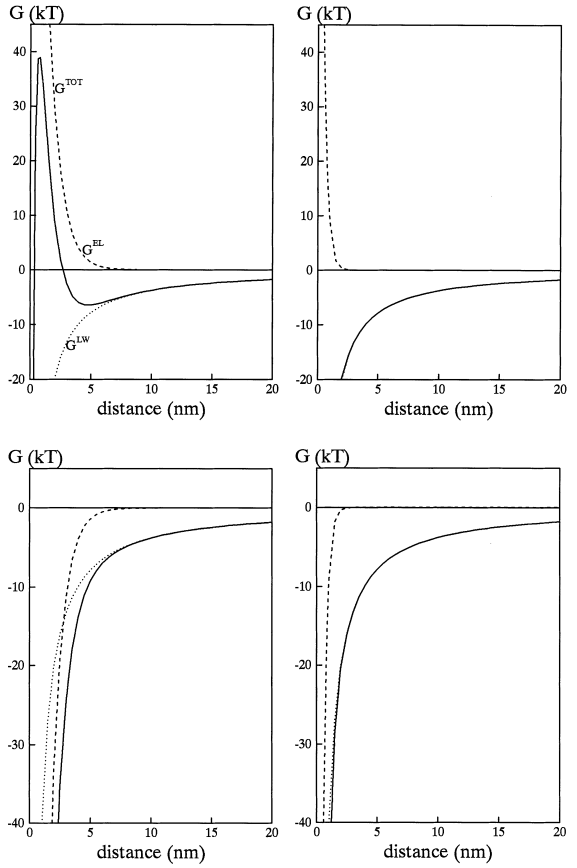

Fig. 7. Interaction energies, according to the classical DLVO theory, as a function of their separation distance. The interaction energies have been calculated for a Hamaker constant of 0.49 kT; particle radius of 500 nm; absolute zeta potentials of 15 mV with equal signs for the top panel and opposite signs for the bottom panel; the left panel is for a low ionic strength solution ($\kappa^{-1} = 9.6$ Å), while the right panel is for a high ionic strength solution ($\kappa^{-1} = 3.0$ Å).

The ΔG^{LW}_{adh} values in microbial interactions are nearly always negative, indicating that the Lifshitz-van der Waals forces are predominantly attractive and more or less favorable conditions for interactions must be inferred from ΔG^{AB}_{adh}, i.e. the acid-base interactions which can be positive or negative. The fully evaluated expression for ΔG^{AB}_{adh} differs when Eqs. 4 or 5 are applied and reads for the application of Eq. 4

$$\Delta G^{AB}_{adh} = -2\left(\sqrt{\gamma^{AB}_{mv}} - \sqrt{\gamma^{AB}_{lv}}\right)\left(\sqrt{\gamma^{AB}_{sv}} - \sqrt{\gamma^{AB}_{lv}}\right) \quad (8)$$

while for the application of Eq. 5

$$\Delta G^{AB}_{adh} = +2\left[\left(\sqrt{\gamma^{\oplus}_{mv}} - \sqrt{\gamma^{\oplus}_{sv}}\right)\left(\sqrt{\gamma^{\ominus}_{mv}} - \sqrt{\gamma^{\ominus}_{sv}}\right) - \left(\sqrt{\gamma^{\oplus}_{mv}} - \sqrt{\gamma^{\oplus}_{lv}}\right)\left(\sqrt{\gamma^{\ominus}_{mv}} - \sqrt{\gamma^{\ominus}_{lv}}\right) - \left(\sqrt{\gamma^{\oplus}_{sv}} - \sqrt{\gamma^{\oplus}_{lv}}\right)\left(\sqrt{\gamma^{\ominus}_{sv}} - \sqrt{\gamma^{\ominus}_{lv}}\right)\right] \quad (9)$$

Table 1 provides reference data for surface tension components of liquids that are often employed in contact angle measurements and that are applicable in any of the approaches outlined above and summarized in Fig. 5.

2.2. The classical DLVO approach

In the classical DLVO approach, microbial adhesion is described as a balance between attractive Lifshitz-van der Waals and repulsive or attractive electrostatic forces. The inclusion of electrostatic interactions here requires that the zeta potentials of the interacting surfaces are measured too, in addition to measuring contact angles. Accordingly, the interaction energy between two interacting surfaces can be separated as

$$G^{TOT}(d) = G^{LW}(d) + G^{EL}(d) \quad (10)$$

in which G^{TOT}, G^{LW}, and G^{EL} denote the total, the Lifshitz-van der Waals and the electrostatic interaction energy, respectively. The decay with distance (d) of these interaction energies depends on the geometry of the interacting bodies and is summarized in Table 2 for the configuration of a sphere opposed to a semi-infinite flat plate (e.g. microbial adhesion to a substratum surface) and for two interacting, spherical particles (e.g. microbial (co)aggregation). Fig. 7

illustrates the decay with distance of the Lifshitz-van der Waals and electrostatic interaction energies between a spherical particle, i.e. a microorganism and a semi-infinite flat plate for situations of repulsive and attractive electrostatic interactions and different ionic strengths. The Lifshitz-van der Waals attraction is not influenced by ionic strength, but both the range and the magnitude of the electrostatic interactions decrease with increasing ionic strength due to shielding of surface charges. In fact, for high ionic strengths, electrostatic interactions have lost their influence. Dependent on the ionic strength, a so-called secondary minimum exists of a few kT, in which microorganisms are said to become reversibly captured, prior to primary minimum adhesion requiring closer approach. For interaction energies, the use of a kT energy scale is generally preferred, as 1 kT represents the thermal or Brownian motion energy of an organism, which provides a reference value for adhesion.

2.3. The extended DLVO approach

The extended DLVO theory developed by Van Oss et al. [71] and recently related to the origin of hydrophobic interactions in microbial adhesion [64] considers the four fundamental, non-covalent interactions: Lifshitz-van der Waals, electrostatic, Lewis acid-base and Brownian motion forces. The acid-base interactions are based on electron-donating and electron-accepting interactions between polar moieties in aqueous solutions and possibly include in the classical DLVO theory ill-understood phenomena such as the effects of structured water at interfaces and disjoining pressures [87], hydrophobic attraction [73,88] and hydrophilic repulsion [74] between surfaces as measured by force balance instruments [75]. The polar or acid-base interfacial free energy balance ΔG^{AB}_{adh} is incorporated in the extended DLVO approach by attributing a decay function to

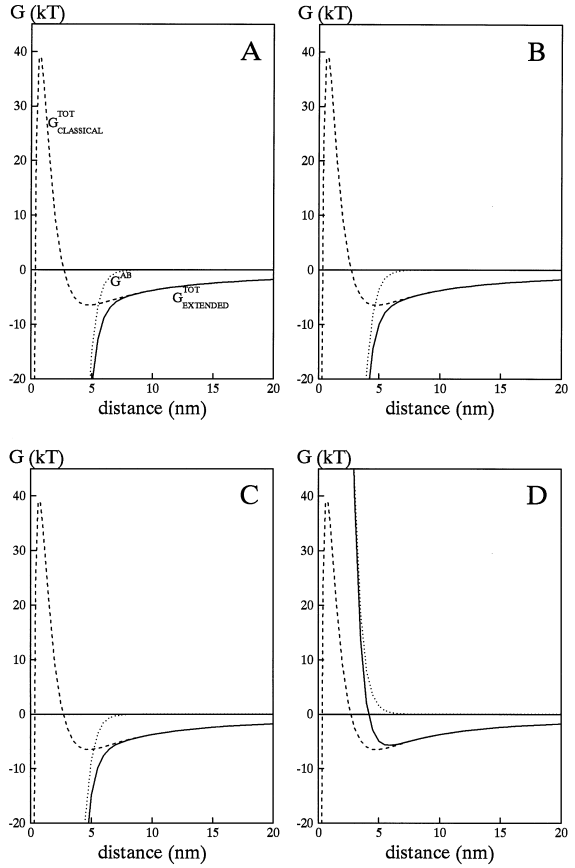

Fig. 8. A comparison of the interaction energies, according to the classical and the extended DLVO theory, between a spherical particle (microorganism) and a solid substratum as a function of the separation distance. The parameters for the calculation of the classical DLVO interaction energies are chosen to correspond with those occurring under most physiological conditions, i.e. with the presence of a secondary interaction minimum (see Fig. 7), while the acid-base interaction is calculated using:

Figure	γ_s^-	γ_s^+	γ_m^-	γ_m^+
7A	0	0	0	0
7B	15	0	15	0
7C	15	0	0	15
7D	50	2	20	2

All surface free energy parameters in mJ m^{-2}.

Table 3
The Lewis acid-base $G^{AB}(d)$ interaction energies for a sphere with radius a opposed to a semi-infinite plate and for two interacting spherical particles as a function of the separation distance d

Configuration	Lewis acid-base[a]
Sphere-plate	$2\pi a\lambda\Delta G^{AB}_{adh}\exp[(d_0-d)/\lambda]$
Sphere-sphere	$\pi a\lambda\Delta G^{AB}_{adh}\exp[(d_0-d)/\lambda]$

[a] d_0 is the distance of closest approach between two surfaces (1.57 Å; [63]), while λ denotes the correlation length of molecules in a liquid medium, and repeatedly equals 0.6 nm for hydrophilic repulsion. For situations in which hydrophobic attraction occurs, λ may become as high as 13 nm [59].

this balance. The decay with distance of the acid-base interaction energy occurring in the extended DLVO approach is assumed to describe the distance dependence of the boundary layer ordering, while the Lifshitz-van der Waals and electrostatic interaction energies are similar in the extended and classical DLVO approach. The decay with distance of the acid-base interaction energies for the sphere-plate and sphere-sphere configurations are summarized in Table 3. Fig. 8 illustrates the decay with distance of the sum of the Lifshitz-van der Waals and electrostatic interaction energies, and the acid-base interaction energy between a spherical particle (microorganism) and a semi-infinite flat plate for situations of repulsive electrostatic interactions in low ionic strength buffer between apolar, monopolar, and bipolar surfaces. As can be seen in Fig. 8, the influence of the acid-base interactions is enormous compared with electrostatic and Lifshitz-van der Waals interactions. However, the acid-base interactions are also relatively short-ranged, and a close approach between the interacting surfaces (less than 5 nm) is required before these forces can become operative.

The extended DLVO approach as developed by Van Oss and co-workers can be considered a combination of the thermodynamic and classical DLVO approaches, as the Hamaker constants A appearing in Table 2 can be obtained from the Lifshitz-van der Waals interaction energy ΔG_{adh}^{LW} as calculated from contact angle measurements according to

$$A = -12\,\pi\,d_0^2\,\Delta\,G_{adh}^{LW} \tag{11}$$

In fact, Eq. 11 is the expression for the Lifshitz-van der Waals interaction energy between two flat plates at closest approach (the minimum separation distance d_0 between two surfaces can be approximated as 1.57 Å [63] although larger estimates are also in use [5,89]. The application of the expression for two flat plates, while actually sphere-plate ('microbial adhesion to a substratum surface') or sphere-sphere ('microbial coaggregation') configurations are involved, is justified at closest approach, as the radii of curvature of the particles considered are very large compared to the distance of close approach d_0. The assumption underlying Eq. 11, that ΔG_{adh}^{LW} derived from contact angle measurements is the correct interaction energy to be used for Hamaker constants, is not ubiquitously accepted, but at present it represents the only way by which variations in microbial cell surface properties can be expressed in the Hamaker constants for their interaction with surfaces. Others [90] prefer not to do this and simply accept, for the time being, one average value for the Hamaker constant, valid for microbial adhesive interactions, regardless of the strains involved, which can be obtained from a macroscopic approach based on bulk materials properties, i.e. the frequency dependence of the complex dielectric constant over the en-

Table 4
Hamaker constants for the adhesive interaction between microorganisms and substratum or microbial cell surfaces[a] in aqueous suspensions as derived from contact angle measurements and macroscopic approaches

Microorganism	Substratum or microbial cell surfaces	A [kT][b]	Derived from	References
Listeria monocytogenes	glass	0.14	contact angles	[92]
	polystyrene	0.14		
	Teflon	0.015		
'Oral streptococci'	glass	1.73	contact angles	[62]
	polymethylmethacrylate	1.61		
	Teflon	0.15		
'Bacteria'	glass	1.54	macroscopic approach	[90,93]
	polystyrene	0.79		
	Teflon	0.035		
Streptococcus thermophilus	hexadecane	0.42	contact angles	[94]
Actinomyces naeslundii T14V-J1	*Streptococcus oralis* J22	1.05	contact angles	[95]
	Streptococcus sanguis PK1889	0.89		

[a]For exact comparison, the Hamaker constant for the interaction between two polystyrene surfaces in water from contact angles equals 1.25 kT, while from macroscopic approaches values of the Hamaker constant between 0.88 and 1.33 kT are reported [96].
[b]1 kT = 4×10^{-21} J = 4×10^{-14} erg.

Table 5
Characteristic features of currently employed methods to measure single strain microbial adhesion to inert substrata (see text for references)

Method		Mass transport		Enumeration		Measures	
name	pictogram	controlled	theory available	direct	in situ observation	adhesion	retention
MATH		N	N	N	N	Y	N
slide		N	N	N/Y	N	N	Y
beads		N	N	N	N	N	Y
packed-bed		Y	Y	N	N	Y	Y
stagnation point flow	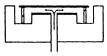	Y	Y	Y	Y	Y	Y
parallel plate	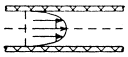	Y	Y	Y	Y	Y	Y
rotating disc	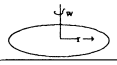	Y	Y	N	N	Y	Y

tire electromagnetic spectrum from the far UV to the soft X-ray region [91]. Table 4 compares values for Hamaker constants in aqueous solutions for a variety of microbial adhesive interactions, derived from contact angle measurements and a macroscopic approach. As can be seen, the order of magnitude of variously derived Hamaker constants is the same, but only the contact angle approach offers the possibility of distinguishing between microbial strains.

3. Methods to study microbial adhesive interactions

The balance between repulsive and attractive interactions in microbial adhesion is often a delicate one and can easily be disturbed by experimental conditions, such as slight rinsing, dipping or the occurrence of other hydrodynamic forces. These conditions are still frequently neglected in the design of methods to study microbial adhesion, despite the fact that the lack of their control may yield results that become uninterpretable and impedes comparison of results from different laboratories. Therefore, methods to study microbial adhesive interactions will be summarized and critically evaluated below, as subdivided in different categories.

3.1. Microbial adhesion to substratum surfaces

Microbial adhesion to inert substratum surfaces is studied at different levels of complexity in a wide variety of experimental systems. The choice for a particular system is sometimes related to the prevailing conditions in the natural environment of the adhesion process under study, e.g. a bioreactor, the marine environment or selected parts of the human body, such as the urinary tract, the oro-pharyngeal region or the oral cavity. More often, the choice for a particular system is dictated by cost aspects, ease of operation or the scientific background of the researchers. Table 5 summarizes the most frequently used experimental systems to study microbial adhesion to substratum surfaces.

3.1.1. MATH

In the MATH ('microbial adhesion to hydrocar-

bons') assay a suspension of microorganisms is (repeatedly) vortexed together with a small amount of hydrocarbon in order to create microdroplets of the hydrocarbon phase to serve as a hydrophobic substratum for microbial adhesion. After vortexing, the aqueous and the hydrocarbon phases are allowed to separate and the turbidity of the aqueous phase is measured as an indication of the number of microorganisms bound to the hydrocarbon phase [97]. In the kinetic mode [98] of MATH, the turbidity of the aqueous suspension is plotted versus the vortexing time to yield an initial removal rate R_0 of microorganisms by the hydrocarbon phase. It has been argued that MATH in its kinetic mode is preferable for quantitative studies [94,99–101]. The size and number of microdroplets created depend amongst others on the duration of vortexing, the power input, dimensions of the test tube and the ratio between the aqueous and hydrocarbon phase volumes. Thus, unpredictable hydrodynamic and mass transport conditions exist during the assay. Furthermore, the kinetic energy of the microorganisms is increased by vortexing beyond their thermal energy of 1 kT to levels that are not realistic any more compared to the situation in common, natural environments, with a likely influence upon adhesion. Another drawback of MATH is that only microbial adhesion to hydrophobic hydrocarbon surfaces can be studied, although recently other organic solvents have been used as well [102], in which case the assay is named MATS ('microbial adhesion to solvents'). In MATH or MATS, it is difficult to apply conditioning films to the substratum surface prior to adhesion.

3.1.2. Slide methods

This category is meant to include all assays in which a microbial suspension remains stationary with respect to an exposed substratum surface (a 'slide') or is agitated under poorly controlled conditions. After exposure, substrata are most often rinsed and adhering microorganisms enumerated. For enumeration, widely different procedures can be employed ranging from measuring the chemical oxygen demand of microorganisms [103] to fluorescent labelling [104]. During rinsing, adhering microorganisms are exposed to extremely large removal forces. It can be calculated, for instance, that the removal forces involved in passing an adhering microorganism through a liquid-air interface ('dipping') are approximately 10^{-7} N [105,106], whereas for 'slight' rinsing with an aqueous fluid flow, removal forces of around 10^{-9} to 10^{-10} N are estimated [107]. The exact value of these, often unintentionally exerted removal forces depends of course on the details of the experimental conditions, but even within this limitation it can be stated that the order of magnitude of these removal forces is the same as reported for the interaction forces between microorganisms and a substratum surface [108]. Thus, in these types of experiments, retention of adhering microorganisms is measured rather than adhesion, which is more than a semantic distinction because it may form the basis for conflicting results arising from different laboratories. Thus, these methods are disqualified for fundamental studies of microbial adhesion to surfaces. Application of a conditioning film is possible, taking into account the same problems for applying the conditioning film as described above for microbial adhesion.

3.1.3. Bead methods

Bead methods are essentially the same as slide methods, described above, but are distinguished by having a large substratum area relative to the suspension volume. Usually, beads of a particular material, for instance hydroxyapatite with or without an adsorbed salivary conditioning film [109,110], are agitated and washed after incubation with or without agitation and the number of adhering microorganisms is determined indirectly by radioactive labelling or spectrophotometrically. Consequently, the method suffers from many of the combined drawbacks of the MATH and slide methods.

3.1.4. Packed-bed systems

In microbial adhesion to packed beds, a suspension of microorganisms is passed through a column, packed with a well defined granular material such as washed sand, glass beads or fibers [111]. The microbial concentration of the effluent is determined in time (often called 'break-through' curves) with devices based on the Coulter-counter principle or spectrophotometrically [112]. When the porosity of the bed is known and the granular material can be approximated as spherical particles, mass transport equations are available [112] and the system can be used to model transport of microorganisms through

soil [113] or industrial bioreactors [114]. As a drawback, packed-bed systems lack the possibility of observing microbial deposition and the spatial arrangement of adhering organisms in situ.

3.1.5. Flow devices

Flow devices are designed to study microbial adhesion to substratum surfaces under carefully controlled hydrodynamic and mass transport conditions and experimental parameters such as the prevailing shear rate, fluid flow velocity, Reynolds and Péclet numbers as well as the theoretical mass transport can be calculated. Flow systems are generally characterized by a small substratum area compared to the suspension volume and consequently, the microbial concentration remains virtually constant up to a maximum surface coverage is attained. Several types of flow devices have been introduced to measure microbial adhesion to a variety of transparent and non-transparent substrata, some of which allow direct in situ observation of adhesion, such as stagnation point flow collectors [115], radial [116] and parallel plate flow chambers [117,118], whereas other types, such as rotating disk systems [119], do not allow direct observation of the adhesion process. An important advantage of parallel plate flow chambers is that deposition experiments can also be carried out on non-transparent metals when the system is equipped with the proper microscopic technique [48,120]. Conditioning films can be applied to the substratum surfaces with all flow devices under the same carefully controlled hydrodynamic and mass transport conditions as for microbial adhesion. In addition, in situ observation techniques combined with image analysis options provide the possibility of studying detachment of adhering microorganisms during the experiment and the spatial arrangement of the adhering microorganisms in those devices where a uniform shear exists over a sufficiently large portion of the substratum surface.

3.2. Coaggregation between microbial pairs

Basically, two types of methods to measure microbial coaggregation can be distinguished, based either on measuring the size of coaggregates (steady state assessment) or on determining the kinetics of the coaggregation process. In this section the most frequently used methods to measure microbial coaggregation are critically evaluated as summarized in Table 6.

Table 6
Characteristic features of currently employed methods to study coaggregation of microbial pairs (see text for references)

Method		Mass transport		Measures	
name	pictogram	controlled	theory available	aggregate size	kinetics of aggregation
visual scoring in a test tube	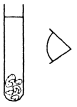	N	N	Y	N
steady state turbidometric	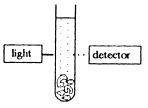	N	N	Y	N
kinetic turbidometric	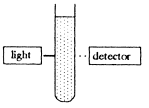	Y	Y	N	Y
microscopic observations	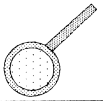	N	N	Y	N

3.2.1. Visual scoring in a test tube

Equal volumes of a dense microbial suspension of two microbial strains are mixed on a vortex apparatus or otherwise agitated and the extent of coaggregation is scored on a semi-quantitative scale ranging from 0 to 4; 0 when the mixed suspension remains evenly turbid and 4 as the maximum coaggregation score, when large microbial coaggregates are formed that sediment seconds after mixing [57,121]. This semi-quantitative assay has little control of hydrodynamic conditions and mass transport and must therefore be considered only suitable as a screening method for potential coaggregating microbial pairs or inhibitory compounds.

3.2.2. Steady-state turbidometric methods

In the so-called steady-state turbidometric methods [122–124], equal volumes of dense microbial suspensions are mixed on a vortex prior to the actual measurement, most often to speed up the kinetics of the process. In the assay as used by Handley et al. [122], suspensions are transferred to a UV spectrophotometer cuvette immediately after mixing and the turbidity is measured after 1 and 24 h as a coaggregation measure. Other investigators [123,124] use slow speed centrifugation to separate coaggregates from free cells after which the turbidity of the supernatant is determined. Obviously, there is no adequate control of hydrodynamic and mass transport conditions during the coaggregation part of an experiment in these assays, while furthermore ongoing sedimentation during measurements in the second phase of the experiment influences the results. Hence, it is doubtful whether the assay probes steady-state coaggregation or its kinetics.

3.2.3. Kinetic turbidometric methods

After adding equal volumes of microbial suspensions together in a cuvette, the resulting change in absorbance can also be recorded continuously as a function of time. Provided both volumes are carefully homogenized and the coaggregating microorganisms do not (auto-)aggregate, mass transport, i.e. the collision rate between organisms, depends solely on Brownian motion ('perikinetic aggregation'), which is small for microorganisms. Therefore,

Table 7
Characteristic features of currently employed methods to study co-adhesion of microbial pairs (see text for references)

Method		Mass transport		Enumeration		Measures	
name	pictogram	controlled	theory available	direct	in situ	adhesion	retention
co-adhesion MATH		N	N	N	N	Y	N
slide		N	N	N	N	N	Y

to speed up the coaggregation process, dense microbial suspensions are frequently employed, making sedimentation and auto-aggregation effects hard to avoid [125,126].

3.2.4. Microscopic observations

In microscopic observation methods, microbial suspensions are mixed on a microscope slide after which the coaggregation process is arrested by the addition of glutaraldehyde to allow direct observation of the coaggregates formed [126]. These methods are hampered by the limited microscopical depth of focus allowing observation of only the initial stages of coaggregation.

3.3. Co-adhesion between microbial pairs

Co-adhesion is the least studied of all microbial adhesive interactions and only few methods to measure co-adhesion have been described, as can be seen in Table 7.

3.3.1. Co-adhesion MATH

This variant of MATH was developed by Ellen et al. [34] as a direct extension of the MATH assay. In co-adhesion MATH experiments, microorganisms of one strain are allowed to adhere to hydrocarbon droplets after which these hydrocarbon droplets are used in a second MATH assay involving the partner strain. Subsequently, the phases are allowed to separate and the number of microorganisms co-adhering with the organisms adhering to the hydrocarbon droplets is related to the decrease in absorbance of the suspension. Unfortunately, the hydrodynamic and mass transport conditions are poorly defined, making the method unsuitable for kinetic studies, conditioning films are virtually impossible to apply and only microbial pairs can be studied of which only one binds to the hydrocarbon phase.

3.3.2. Slide methods

In slide methods to study co-adhesion, a continuous layer of a so-called base microbial strain is prepared on a solid support, which can either be tissue culture plates, (bovine) enamel chips [36], nitrocellulose membranes [35] or microtiter plates [127]. Subsequently, the solid supports are incubated with a suspension of a second, (radioactively) labelled strain and agitated. Next, this suspension is removed, the solid support is washed and the number of co-adhering microorganisms is calculated from the amount of label associated with the solid support. Both adhering and co-adhering microorganisms are repeatedly subjected to passaging through liquid-air interfaces during the washing steps and as a result, unpredictable numbers of co-adhering microorganisms are removed. Furthermore, the use of radioactivity requires special equipment and is environmentally demanding.

3.4. Conclusions

The best developed methods to study microbial adhesive interactions involve microbial adhesion to inert substrata. Methods to study microbial coaggregation can at best be called phenomenological, while no adequate method is available for the study of microbial co-adhesion. Within the collection of methods used to study microbial adhesion to inert substrata, flow chamber systems with in situ observation and image analysis options are considered superior, because mass transport is carefully controlled and generally fast as it is independent of diffusion only [128], liquid-air interface passages are effectively avoided, conditioning films can be easily applied and antimicrobials or detergents can be introduced during the experiment, while, moreover, in situ observation provides the possibility of quantifying nearly every conceivable parameter involved in the deposition process, including the kinetics of adsorption and desorption, as well as the spatial arrangements of the adhering microorganisms [29,31,118,129–131].

With a view to extending the use of a parallel plate flow chamber with in situ observation and image analysis options to the study of microbial co-adhesion, the parallel plate flow chamber system will now be extensively described.

4. The use of a parallel plate flow chamber system to study initial adhesion of single microbial strains to solid substrata

What Shall I do About You Know What
A.A. Milne: The House at Pooh Corner

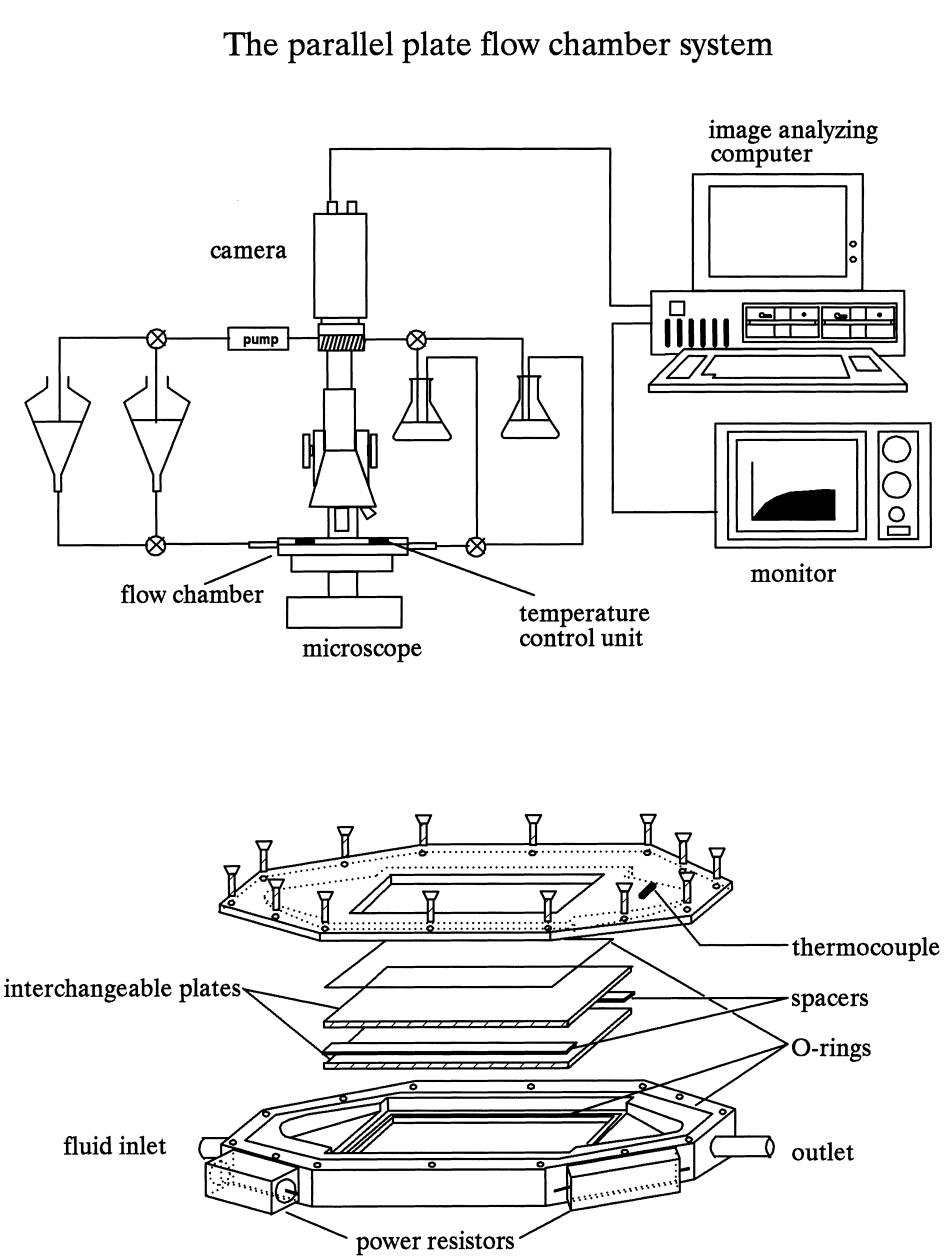

Fig. 9. Schematic overview of the parallel plate flow chamber system and detailed view of the chamber itself.

4.1. The parallel plate flow chamber system

Fig. 9 shows the construction of the parallel plate flow chamber (external dimensions 16×8×1.5 cm, length×width×height) [30,118,132]. The chamber consists of a nickel-coated brass bottom part and a poly(methylmethacrylate) top part (a metal top plate is used when a sterilizable chamber is needed) which encloses two plates with dimensions of 7.6×5.0×0.2 cm separated from each other by two Teflon spacers. The effective chamber dimensions are 7.6×3.8×0.06 cm, although the height

of the chamber can be varied by the thickness of the spacers. It has to be noted that the width-to-height ratio should be larger than five in order to exclude side-wall effects.

A reasonable stiffness of the top and bottom plates is required for maintaining a constant channel depth and plan parallellity during the flow experiment, whereas the application of phase contrast microscopy requires transparent bottom and top plates. Non-transparent, reflective substrata can be used as a bottom plate when an ordinary metallurgical microscope, based on incident reflected light, is available [48]. The establishment of a laminar flow between two plates is enhanced by the design of the chamber, i.e. the width and height of the inlet and outlet regions are made gradually changing to the chamber dimensions [133]. The chamber itself can be heated, if necessary, by four 33-Ω power resistors, mounted on the sides of the bottom part, connected in parallel to each other to a power supply (10 V). Feedback is provided by a Pt100 thermocouple, assembled in the top part in the downstream compartment of the flow chamber.

The entire flow chamber is placed on the stage of a phase contrast microscope (Olympus BH-2) equipped with a 40× objective with an ultra-long working distance (Olympus ULWD-CD Plan 40 PL) (Fig. 9). A CCD camera (CCD-MX High Technology, Eindhoven, The Netherlands) is mounted on the phase contrast microscope and is coupled to an image analyzer (TEA, Image-Manager, Difa, Breda, The Netherlands), installed in a personal computer. With this set-up, direct observation of the deposition process in situ is possible without any additional shear forces acting on the deposited bacteria. Thus the spatial arrangement of deposited bacteria with respect to each other is fully preserved. A pulse-free flow can be created by hydrostatic pressure and the suspension recirculated by a roller pump. By means of a valve system it is possible to connect flasks which contain e.g. buffer, reconstituted human whole saliva or bacterial suspension with the flow chamber without passing a liquid-air interface over the adsorbed conditioning film and/or adhering organisms [134].

4.2. The image analysis system and image handling

Enumeration of the total number of adhering bacteria as well as the determination of the deposition and desorption rates is usually done on the bottom plate of the flow chamber [130]. Sometimes experiments are done on the top plate to exclude sedimentation contributions to the mass transport [135]. During a deposition experiment, images are grabbed as rapidly as possible. An image is built up out of 512×512 pixels, with each pixel representing one byte, i.e. 256 gray values ranging from 0 (black) to 255 (white). The magnification of the system is such that the total field of view is approximately 0.017 mm^2 and the area of one microorganism equals approximately six pixels (depending of course on the microorganism under study). In order to distinguish between adherent microorganisms and in focus moving ones, two or more successively (approximately 1-s time interval) grabbed images are added or multiplied [129]. Because the gray value of the background is substantially higher than the gray value of the microorganisms, this procedure yields higher gray values for moving microorganisms than for adhering ones.

In order to eliminate artifacts caused by dust or dirt on the lenses and camera, an added or multiplied out-of-focus image is subtracted from the images, yielding a uniformly gray background. Furthermore, to amplify the gray value difference between microorganisms and background, a Laplace or analogous filter procedure is carried out. Finally the image is 'thresholded', in which all pixels with gray values below a certain, adjustable 'threshold' are made white (i.e. gray value 255) and the background is made black. At this point these black and white images and the times at which they were taken are written to a hard disk for later analysis. In its simplest form, this analysis yields the number of adherent microorganisms per unit area at time t, $n(t)$. Also, a more sophisticated image analysis was developed in which the times of arrival and departure of each microorganism can be determined [130]. This makes it possible to calculate the 'on' or adsorption rate of microbial deposition and the 'off' or desorption rate, together with the residence time during which a desorbing organism has been adhering on a substratum surface.

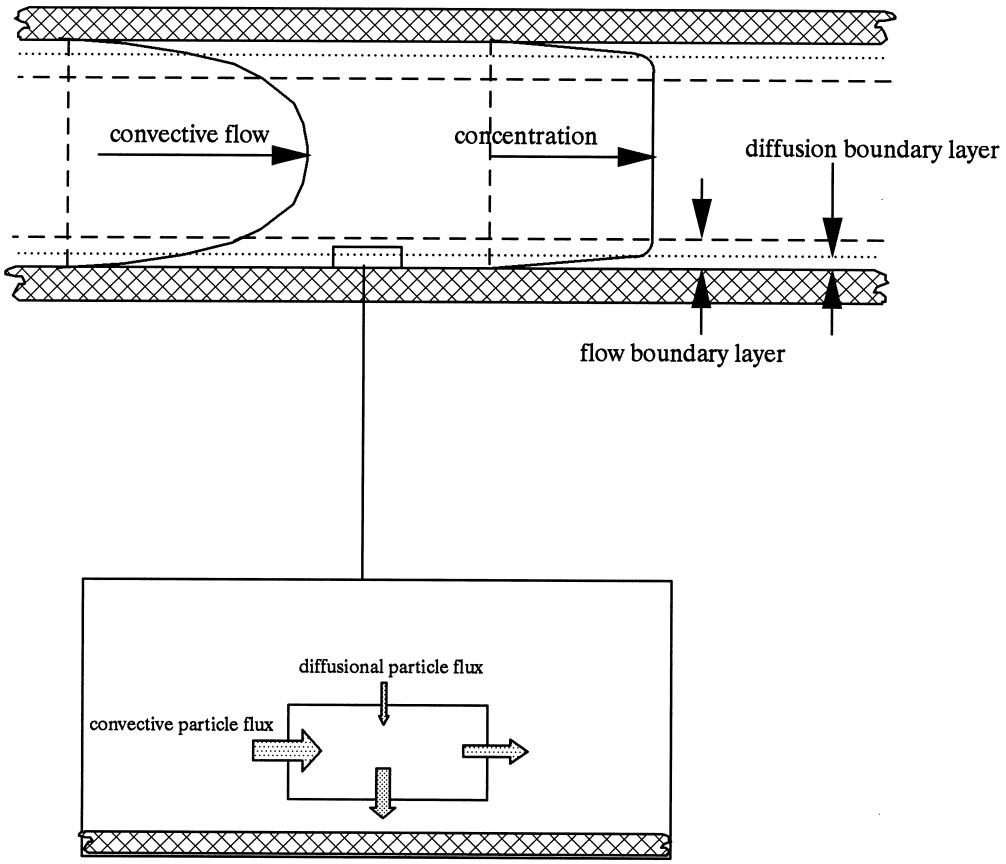

Fig. 10. Schematic overview of different aspects of mass transport in a parallel plate flow chamber, including the velocity profile across the chamber and the concentration distribution. Close to the surface, there is convective mass transport parallel to the surface, but only diffusional mass transport driven by concentration differences accros the diffusion boundary layer contributes to the mass transport towards the substratum surface.

4.3. *Hydrodynamic aspects of the parallel plate flow chamber design*

A fully developed, laminar flow between two parallel plates obeys the Poiseuille law and adopts a parabolic flow profile (see also Fig. 10) which depends on the volumetric flow rate Q, the half depth of the chamber b, the width of the chamber w, and the height above the bottom plate of the chamber z

$$v(z) = \frac{3}{2}\cdot\frac{Q}{2b\cdot w}\cdot\frac{z}{b}\left(2-\frac{z}{b}\right) \tag{12}$$

There are several criteria to be met before such a well defined flow actually develops. A first criterion for laminar flow to occur is that the Reynolds number [136,137]

$$Re = \rho\cdot\frac{Q}{(w+2b)\cdot\mu} < 2000 \tag{13}$$

in which ρ denotes the fluid density and μ the absolute viscosity.

However, this is not the only criterion because the chamber must be sufficiently long for laminar flow to develop and all effects from the inlet have disappeared. The establishment length for laminar flow through a rectangular cross-section can be calculated from

$$Le = constant.2b.Re \quad (14)$$

Proportionality constants in the literature range from 0.013 [137] to 0.044 [136]. From the Reynolds criterion, the maximal volumetric flow rate that can be allowed in our flow chamber is calculated to be approximately 100 $cm^3\ s^{-1}$ requiring an establishment length of between 2 and 6 cm.

The wall shear rate due to the parabolic flow profile is

$$\sigma = \frac{d\,v}{dz}|_{z=0} = \frac{3}{2}\frac{Q}{b^2 \cdot w} \quad (15)$$

There are two different types of forces working on an adhering organism as a result of the fluid flow. One is the 'Saffman' lift force

$$F_l = 81.2\ \mu\ a^2 \left(\frac{\sigma\ \rho}{\mu}\right)^{1/2} \cdot v\ (a) \quad (16a)$$

while the other is the viscous 'Stokes' drag force on an adhering spherical microorganism [89]

$$F_d = 1.7009\ (6\ \pi\ \mu\ a\ v(a)\ ) \quad (16b)$$

in which $v(a)$ is the fluid flow velocity at the center of the adhering organism. $v(a)$ can be obtained directly from Eq. 12.

The fluid flow forces in aqueous systems are extremely small and for our parallel plate flow chamber configuration at the limit for laminar flow (100 $cm^3\ s^{-1}$), it can be calculated that a micron-sized microorganism would experience a lift force of 10^{-10} N due to wall shear and of 10^{-10} N due to viscous drag. For most relevant conditions, however, flow rates are a thousand-fold lower and these fluid flow forces reduce to 10^{-15} N and 10^{-13} N, respectively. In this respect it is noted that viscous drag forces generally cause rolling of adhering particles [138,139], with a major chance upon re-adhesion, but the lift forces work perpendicular to the surface and particles once lifted off the surface have an extremely small chance of re-adhering within due time. However, fluid flow is not capable of detaching adhering microorganisms from substratum surfaces in significant numbers, which reportedly requires 10^{-10}–10^{-11} N [108].

4.4. Deposition kinetics and adhesion in a stationary end-point

The kinetics of microbial deposition can be markedly different from that of inert particles, amongst other reasons due to the presence of structural surface features such as fibrils and fimbriae, cell surface heterogeneities or biosurfactant release [131,135,140]. Due to the use of real-time automated image analysis, the data density in time will always be sufficiently high to allow calculation of an initial deposition rate describing the initial rate of arrival of microorganisms at the surface per unit time and area

$$j_0 = \frac{dn(t)}{dt}|_{t=0} \quad (17)$$

in which $n(t)$ denotes the number of adhering microorganisms at time t.

Mass transport of particles in controlled flow devices is amenable to theoretical predictions. The mass transport in the parallel plate flow chamber can be calculated by solving the convective-diffusion equation, which describes mass transport in terms of convection, diffusion and the interaction forces operating (see also Fig. 10). Often, however, an exact analytical solution of the convective-diffusion equation is too difficult to obtain and approximate solutions are chosen. In the Smoluchowski-Levich approximation, the attractive Lifshitz-van der Waals forces between a particle and a substratum surface are thought to be counterbalanced by the hydrodynamic drag which a particle experiences when approaching a substratum surface [141], while electrostatic interactions are neglected. Accordingly, a theoretical deposition rate can be calculated, which for the parallel plate flow configuration reads [142,143]

$$j_0^* = \frac{D_\infty \cdot c}{0.89 \cdot a_h}\left(\frac{2}{9}\frac{b \cdot Pe}{x}\right)^{1/3} \quad (18a)$$

where x is the longitudinal distance from the entrance of the flow chamber and in which Pe is the Péclet number, denoting the ratio between convective and diffusional mass transport, given for the parallel plate configuration as

$$Pe = \frac{3}{4}\frac{Q \cdot a_h^3}{b^3 \cdot w \cdot D_\infty} \quad (18b)$$

The microbial diffusion coefficient D_∞ can be calculated from the Einstein relation

$$D_\infty = \frac{kT}{6\,\pi\,\mu\,a_h} \quad (18c)$$

but should preferentially be measured experimentally, as the hydrodynamic radius of microorganisms may vary with ionic strength and pH [144,145]. However, microbial diffusion coefficients are usually small (approximately 10^{-13} m^2 s^{-1}), especially as compared to e.g. proteins (order of magnitude 10^{-11}–10^{-10} m^2 s^{-1}). Consequently, as a rule of thumb, a microorganism diffuses once its own diameter per minute.

Although the assumptions outlined in the Smoluchowski-Levich approach are seldom completely met, j_0^* is a convenient starting value for comparison of experimental j_0 values. The ratio j_0/j_0^* is sometimes referred to as the deposition efficiency α_d and denotes the fraction of microorganisms arriving at a surface that actually manage to adhere successfully [142,145,146].

The number of adherent microorganisms in a stationary end-point of the adhesion process n_∞ (as we consider it not unambiguously proven that microbial adhesion is a reversible process, we prefer to use the expression 'stationary end-point' rather than 'equilibrium') can either be counted directly when experiments run for long enough times to reach a stationary end-point of the process, or calculated from the time dependence of the number of adhering microorganisms using model equations. Because adherent microorganisms prevent adhesion of other depositing organisms in a certain area, the so-called 'blocked area' A_1 [146,147], the adsorption rate decreases during the course of an experiment

$$j_{ads}(t) = j_0(1-A_1 \cdot n(t)) \quad (19)$$

For inert particles, the blocked areas are mainly determined by the repulsive interactions between adherent particles. For adherent microorganisms larger blocked areas may arise, for instance due to biosurfactant production by an adherent organism [37,148,149], rendering unfavorable adhesion conditions over a larger area than geometrically blocked. Oppositely, when cooperative effects prevail creating favorable adhesion conditions around an already adhering microorganism [150,151], smaller blocked areas may be found. In most analytical approaches, blocked areas are taken to be constant over time, but this is not necessarily true.

To describe the kinetics of microbial deposition fully, a desorption rate has to be introduced as well

$$j_{des}(t) = \beta \cdot n(t) \quad (20)$$

In Eq. 20, desorption is assumed to be independent of the residence time during which an organism is adhering to the substratum surface and adhesion is assumed to acquire its final strength upon initial contact between the organism and the substratum surface [152]. From Eqs. 19 and 20 the deposition rate $j(t)$ can be calculated as

$$j(t) = j_{ads}(t) - j_{des}(t) \quad (21)$$

and accordingly

$$n(t) = \int_0^t j(t)dt = n_\infty \left(1 - e^{-(j_0 \cdot A_1 + \beta)\cdot t}\right) \quad (22)$$

Usually j_0, n_∞ and $(j_0 \cdot A_1 + \beta)$ can be directly obtained from the measured time dependence of the number of adhering microorganisms $n(t)$, while separate estimates of β can be derived from the measured $j_{des}(t)$ and for A_1 from the measured $j_{ads}(t)$. Optimization of the calculated parameters can be done by iterative procedures [130].

The approach just outlined and leading to Eq. 22 assumes that desorption does not depend on the residence time of an adhering organism, i.e. 'bond aging' does not occur. This is seldom true, as we even observed bond aging for the adhesion of inert polystyrene particles to glass [153], possibly due to progressive removal of interfacial water or rotation of an adhering particle to make the most favorable heterogeneity on its surface contact the substratum. Aging of the bond between adhering microorganisms and substratum surfaces has been documented [154,155] with a possible role for the collapse of surface appendages, biosurfactant release and the metabolic activity of the organisms.

Using the analysis method as described allows direct determination of the residence time-dependent desorption rate coefficient $\beta(t-\tau)$. It has been pro-

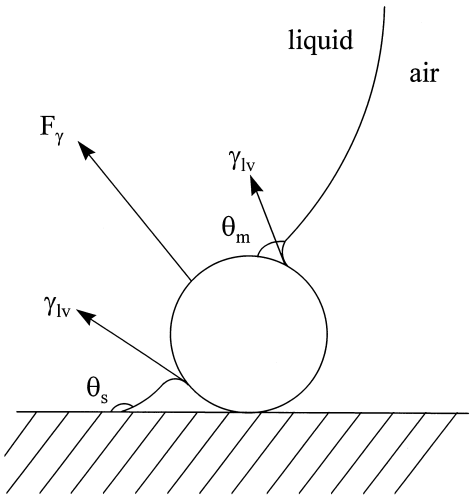

Fig. 11. Schematic presentation of the surface tension forces acting on a microorganism adhering on a substratum surface. The resulting detachment force F_γ depends on the surface tension, the hydrophobicity of the microorganism and the substratum surface as well as on the degree of immersion. As the interface gradually passes, the degree of immersion of the microorganisms varies and thus the direction and circumference over which the surface tension forces act. For an adhering microorganism that is pushed into a liquid from a substratum surface, the maximum surface tension force developed is

$$F_{\gamma,\max} = 2\,\pi\,a\,\gamma_{lv}\sin^2\left(\frac{\theta_m}{2}\right)\cos\theta_s$$

while when the microorganism is pulled out of the liquid

$$F_{\gamma,\max} = -2\,\pi\,a\,\gamma_{lv}\sin^2\left(90 + \frac{\theta_m}{2}\right)\cos\theta_s$$

posed [146] that $\beta(t-\tau)$ should be an exponential function of residence time $(t-\tau)$

$$\beta(t-\tau) = \beta_\infty - (\beta_\infty - \beta_0)\cdot e^{-\delta(t-\tau)} \qquad (23)$$

As $\beta(t-\tau)$ can be directly determined, provided sophisticated image analysis software comparing consecutive images is available, β_0, β_∞ and δ can be easily calculated from Eq. 23 and j_0 can be readily obtained from the measured time dependence $n(t)$ employing iterative procedures. When $\beta_0 < \beta_\infty$, the bond (adhesion) strength weakens during aging, while when $\beta_0 > \beta_\infty$, the bond strengthens during aging.

The analysis outlined so far deals solely with adhesion. When, however, surface-associated growth of adhering microorganisms occurs (as often happens, because nutrients have a tendency to accumulate at interfaces [23]), an additional term appears in Eq. 21 [156]

$$j(t) = j_{ads}(t) - j_{des}(t) + j_{growth}(t) \qquad (24)$$

in which $j_{growth}(t)$ equals the number of microorganisms adhering per unit area and time due to surface-associated growth. Habash et al. [157] recently measured the adhesion and growth terms in Eq. 24 separately for *Pseudomonas aeruginosa* on silicone rubber. As this review is aimed at initial adhesion phenomena, no attempts will be made to develop expressions for $n(t)$ on the basis of Eq. 24.

4.5. Analysis of surface tension forces on adhering microorganisms

At first glance, it appears that the use of flow chamber devices and the control of hydrodynamic conditions offer only advantages for the study of microbial adhesion to solid substrata. This is un-

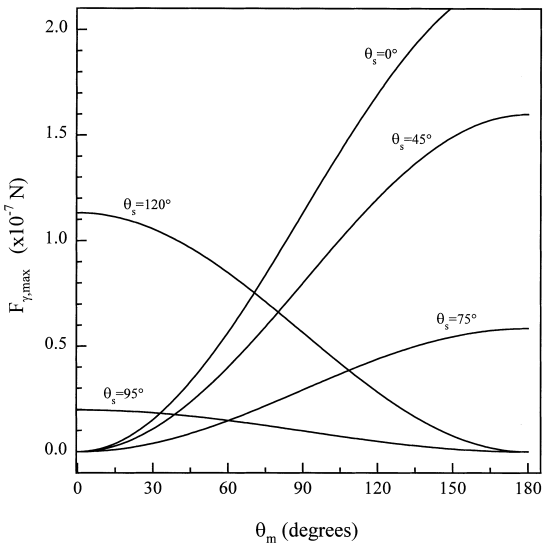

Fig. 12. The maximum detachment force $F_{\gamma,\max}$ originating from a passing aqueous liquid-air interface acting on micrometer-sized microorganisms with different hydrophobicities by their contact angles θ_m and adhering from an aqueous suspension to substrata with different wettabilities by their contact angles θ_s (graph: courtesy of ing. J. Noordmans).

doubtedly true for fundamental research, but not from an applied point of view. Very often, as in trickling filters [4], on rocks and ship hulls [13,158], on monumental buildings [159], on teeth [43], voice prostheses [160–162] and contact lenses [163,164], adhering microorganisms are subject to fluctuating shear forces that can become extremely high [165] when a liquid-air interface passes over the adhering organisms. Such events must be mimicked in a flow chamber in order to allow extrapolation of laboratory results to the in vivo situation. It has already been made clear from Eqs. 15 and 16 that a meaningful range of fluctuating shear cannot be obtained by increasing the flow rate through the flow chamber. Hence it is suggested that at the end of an adhesion experiment under controlled flow in a flow device, air bubbles are passed through the device, as happens in many in vivo situations. Thus an excessively high detachment force is exerted on the adhering organisms and one actually probes the adhesion forces.

Leenaars and O'Brien [105,106] have analyzed in detail the surface tension forces on an adhering microorganism on a substratum surface, as schematically depicted in Fig. 11.

Fig. 12 shows the detachment force $F_{\gamma,\max}$ as a function of the hydrophobicity by water contact angles of microorganisms adhering to substrata with different wettability. Microorganisms are always fully wettable, i.e. have a 0-° water contact angle, immediately after removal from an aqueous phase [67,77], although microbial plateau contact angles with water as high as 90° have been reported after drying [93,166]. Hence, it can be concluded from Fig. 12 that the passage of a liquid-air interface over adhering microorganisms is accompanied by detachment forces $F_{\gamma,\max}$ ranging up to 2×10^{-7} N, dependent upon the degree of immersion and the substratum wettability. Thus these forces are much higher than those originating from fluid flow, i.e. Eq. 16, and mimic the excessively high shear forces occasionally occurring in vivo. Also these detachment forces F_{γ} are often unintentionally exerted by 'slight rinsing' and 'dipping' in several of the methods summarized in Tables 5–7, justifying the source of our statement that most methods currently employed to study microbial adhesion in fact measure the capacity of adhering organisms to withstand a certain detachment force, i.e. microbial retention rather than adhesion. Rijnaarts et al. [128] attributed deviating deposition behavior of seven out of 22 strain-surface combinations to the tendencies of the strains to detach after the passage of a liquid-air interface in their experiments.

4.6. Analysis of the spatial arrangement of adhering microorganisms

Blocked areas cannot only be derived from the deposition kinetics and stationary end-point adhesion but also from the spatial arrangement of adhering microorganisms [31,131]. The final arrangement of microorganisms adhering on solid substrata is de-

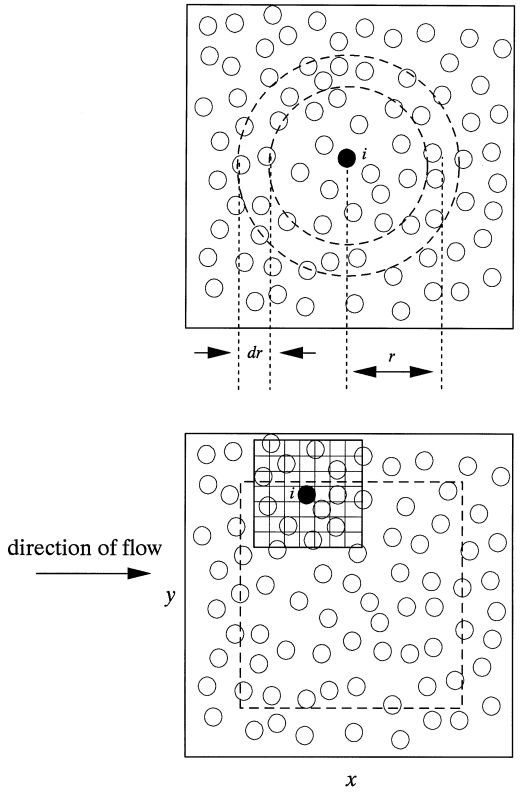

Fig. 13. Radial pair distribution functions $g(r)$ can be calculated from the local densities of adhering particles in a shell with thickness dr and radius r around a center particle (i) (top). Local pair distribution functions $g(x,y)$ can be calculated from a division of the field of view into squares $\Delta x\Delta y$ around a center particle (i) at position (x,y) (bottom). Each adhering particle is taken once as a center particle (filled particle).

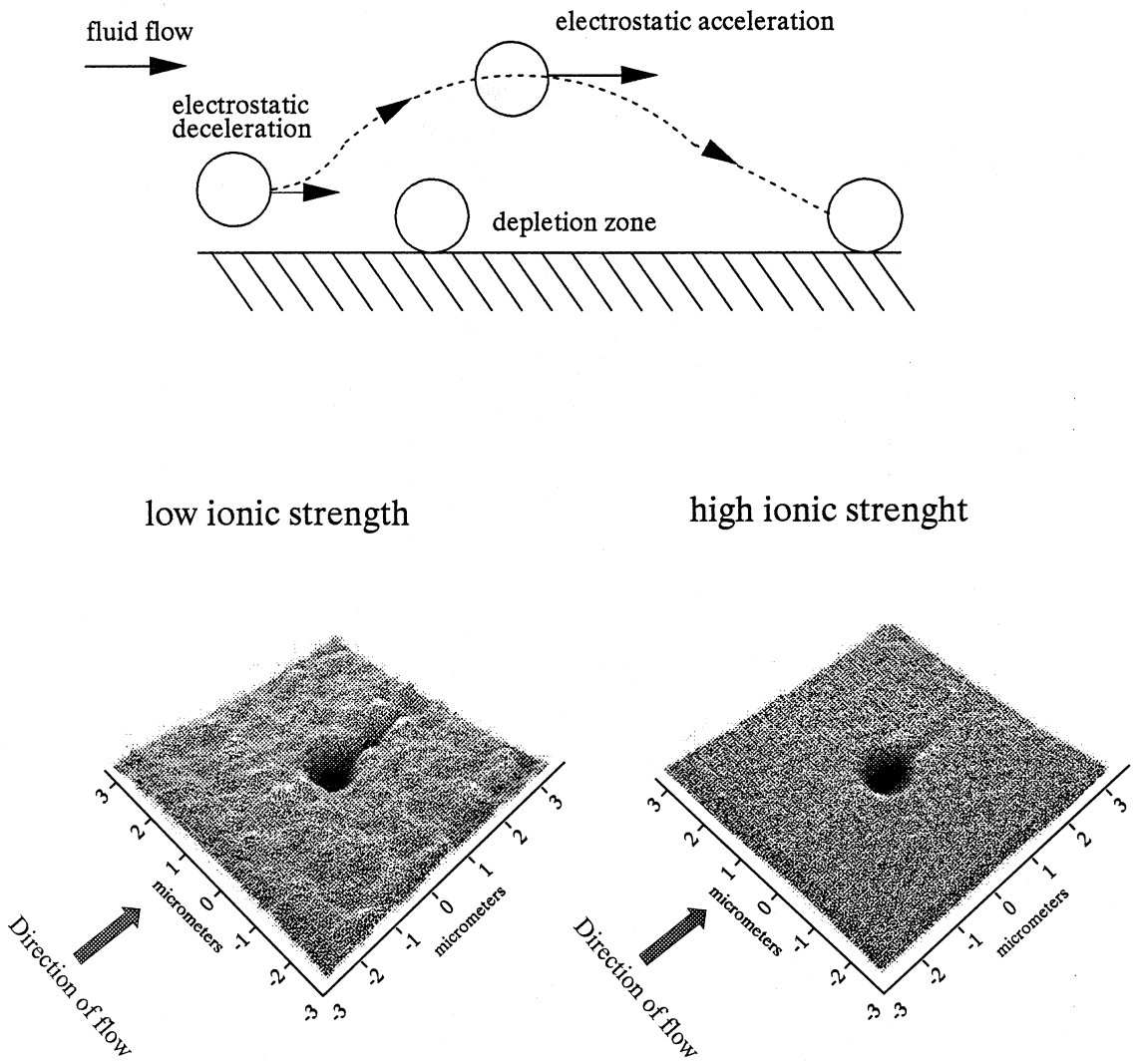

Fig. 14. The influence of fluid flow on the spatial arrangement of adhering microorganisms, expressed as a local pair distribution function $g(x,y)$ of *Streptococcus salivarius* HB-C12 adhering on glass at a wall shear rate of 10 s^{-1}. Left: In a low ionic strength suspension with strong electrostatic interactions present differences in up- and downstream microbial deposition occur due to electrostatic acceleration. Right: In a high ionic strength suspension, electrostatic interactions and acceleration are virtually negligible and the local pair distribution function $g(x,y)$ becomes rotationally symmetrical.

termined by the lateral interactions between adhering organisms which is a field that has hitherto not been extensively studied but has great relevance to the gliding behavior [167] and motility [168] of organisms on substratum surfaces. With in situ observation and image analysis techniques it is possible to determine the positions of all adhering microorganisms and subsequently these data can be employed to calculate so-called radial pair distribution functions. A radial pair distribution function reveals the density $\rho(r, dr)$ of adhering microorganisms in a circular shell around a given microorganism relative to the overall density ρ and is denoted $g(r)$ (see Fig. 13). In the presence of fluid flow, however, asymmetrical arrangements of microorganisms on a substratum surface often develop, because upon approach of a

flowing organism towards an adhering one, the two equally charged organisms repel each other and deceleration of the flowing microorganisms results, which increases the likelihood of upstream deposition. Alternatively, when the flowing microorganism has passed the adhering organism, electrostatic repulsion creates acceleration and decreases the likelihood of downstream deposition (see Fig. 14). Such spatial arrangements of adhering microorganisms that are not rotationally symmetric cannot be described by the radial distribution function $g(r)$, but require analysis by local distribution functions $g(x,y)$ (see also Fig. 14), in which upstream and downstream deposition are distinguished from the recorded times of arrival of adhering microorganisms.

4.7. Conclusions

Controlled flow devices, like the parallel plate flow chamber combined with in situ observation and image analysis methodology, offer the possibility of measuring every conceivable aspect of initial microbial adhesion to solid substrata in a quantitative way. Moreover, whereas at present adhesion data from different laboratories cannot be compared on an absolute scale, the use of controlled flow devices will make it possible to obtain data that can be compared on a wide-spread scale and hopefully delete expressions such as 'gentle rinsing to remove non-adherent or loosely adherent microorganisms' [169] from future literature.

5. The use of a parallel plate flow chamber system to study co-adhesion of microbial pairs

gIn the absence of an adequate, quantitative method to study microbial co-adhesion, we have extended the use of the parallel plate flow chamber system to study co-adhesion of microbial pairs. The measurement of microbial co-adhesion in the parallel plate flow chamber starts with the adhesion of strain 1 organisms, sometimes called the primer strain, to a substratum surface, with or without a conditioning film. Primer strain organisms are usually allowed to adhere up to 1.4×10^6 cm^{-2} (2% surface coverage) after which the actual co-adhesion phase starts by flowing a strain 2 suspension through the flow chamber.

5.1. Mass transport aspects of co-adhesion kinetics

Co-adhesion kinetics between the microbial pairs in a parallel plate flow chamber can be quantified by comparing the number of planktonic organisms of strain 2 that deposit in a shell around the center of already adhering, sessile organisms of strain 1, and to other parts of the substratum. Based on this analysis, the total initial deposition rate j_0, i.e. the number of organisms initially adhering per unit time and area of strain 2, can be written as the sum of the local initial deposition rate $j_{0,1}$ within the shells im-

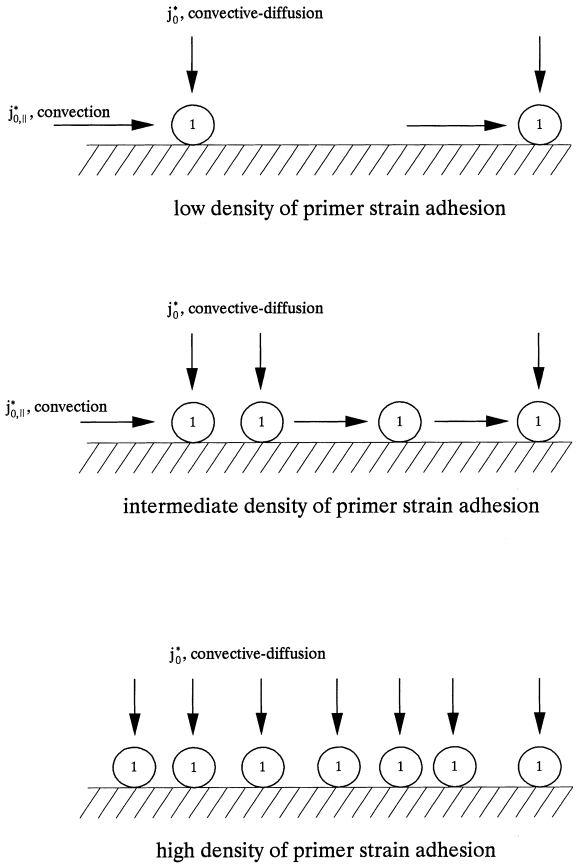

Fig. 15. Schematic presentation of co-adhesion mass transport in a parallel-plate flow chamber, illustrating the reduction of convective mass transport parallel to the substratum upon increase of the density of primer strain adhesion.

mediately around adhering primer organisms and the non-local initial deposition rate outside these shells on the bare substratum $j_{0,nl}$. For a co-adhering, oral microbial pair the ratio between local and non-local initial deposition rate, χ, can become up to 19 times unity with local initial deposition rates of streptococci to adhering actinomycetes exceeding the Smoluchowski-Levich limit by a factor of 10 [170]. For a non-co-adhering pair χ is equal to or smaller than unity [35].

In addition to convective diffusion, co-adhesion kinetics is also controlled by convective mass transport parallel to the substratum surface, yielding frequent collisions between flowing planktonic organisms and sessile primer strains. As the interaction between coaggregating or co-adhering pairs is a perfect sink interaction [170], those collisions have an extremely high efficiency and almost inevitably result in co-adhesion.

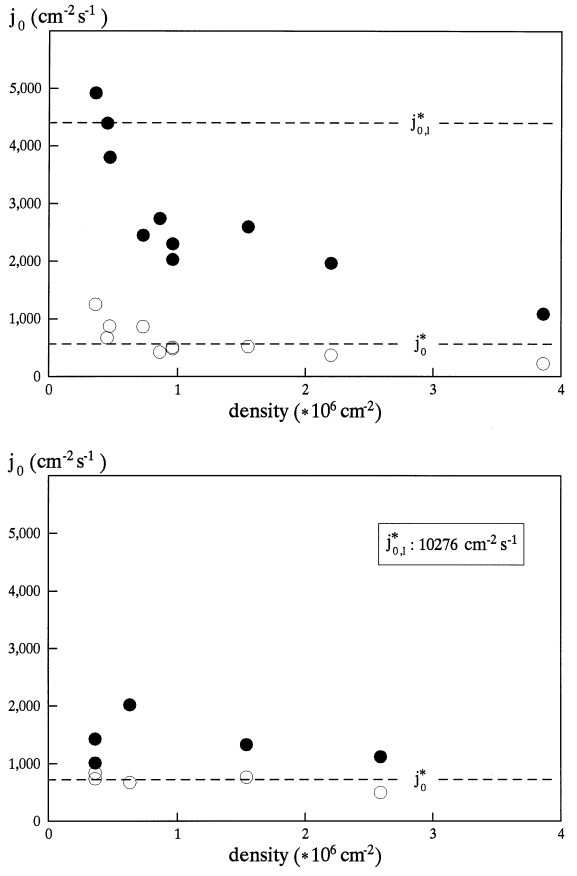

Fig. 16. The local (●) and non-local (○) deposition rates of *S. oralis* J22 to glass as a function of the seeding density of adhering *A. naeslundii* 5951 under different flow velocities (top: 10 s^{-1}; bottom: 25 s^{-1}). In addition, the theoretical local initial deposition rates $j^*_{0,l}$ based on Eq. 25 and theoretical initial deposition rates j^*_0 based on the Smoluchowski-Levich approach for convective diffusion are shown.

In Fig. 15 it is illustrated that the convective-diffusion component of co-adhesion mass transport j^*_0 is not dependent upon the seeding density of a primer strain. However, the convective co-adhesion mass transport component $j^*_{0,\|}$ depends strongly on the density of primer strain adhesion and can be approximated [170] for low densities ($<2\%$ surface coverage) as

$$j^*_{0,l} = j^*_0 + j^*_{0,\|} \tag{25}$$

in which j is the Smoluchowski-Levich mass transport and

$$j^*_{0,\|} = \frac{6Qc}{4w(2b^3)a_h^2\,\delta_d}(10ba_h^4 - 7a_h^5) \tag{26}$$

For intermediate seeding densities, an analytical expression is not yet available, due to the complicated mass transport downstream of an adhering primer strain after co-adhesion. After co-adhesion, a certain downstream suspension volume will be devoid of microorganisms and can only be replenished by slow diffusion processes, during which the suspension volume will have been displaced further downstream by the flow. Obviously, for high seeding densities, co-adhesion mass transport towards adhering primer strain organisms is equal to the convective diffusion to a substratum surface.

Fig. 16 gives an example of the dependence of the local initial deposition rate of streptococcus towards adhering *Actinomyces naeslundii* 5951 on glass under different flow conditions. Note that for low seeding densities, much higher local initial deposition rates are found at the low shear rate than at the high shear rate, presumably because at a high fluid flow the co-adhesion interaction time between the organisms has become too short. It can be calculated that for $\sigma = 10$ s^{-1}, it takes a streptococcus 0.1 s to pass an adhering actinomycetes, while for $\sigma = 25$ s^{-1} the passing time decreases to 0.04 s.

5.2. Analysis of co-adhesion in a stationary end-point

Co-adhesion in a stationary end-point was quantified by means of radial pair distribution functions analogous to the single strain analysis outlined in Fig. 13, revealing in this case the relative prevalence of strain 2 microorganisms adhering in the immediate vicinity of the adhering primer strain as compared to the average density of adhering strain 2 organisms over the entire substratum surface. Local densities of adhering strain 2 organisms were determined in shells with thickness dr (0.16 μm) at distances r from the center of the adhering primer strain organisms. This procedure was performed for each adhering primer organism. The local density of (co-)adhering strain 2 organisms in these shells was normalized with respect to the average density of strain 2 adhesion yielding the distribution function $g_{21}(r)$. When strain 2 organisms are randomly distributed over the entire substratum surface, $g_{21}(r)$ equals unity. However, if there is preferential (co-)adhesion around adhering primer organisms, then $g_{21}(r) > 1$ for regions between $0.5 < r < 1.5$ μm. Such regions must of course be compensated for by regions where $g_{21}(r) < 1$.

5.3. Conclusions

Among the few methods available at present to study microbial co-adhesion, the use of the parallel plate flow chamber with in situ observation and image analysis methodology offers the possibility of quantitatively evaluating the co-adhesion process, provided one strain is employed as a so-called primer strain. The evaluation of co-adhesion involving more than two strains or of co-adhesion processes without designating one of the strains as a primer strain is beyond reach at the present, but may become feasible in due time.

6. Mechanisms of microbial adhesion to substrata

Pooh looked at his two paws. He knew that one of them was the right, and he knew that when you had decided which one of them was the right, then the other one was the left, but he never could remember how to begin.

A.A. Milne: The House at Pooh Corner

In this section, examples will be given describing different features of microbial adhesion to substrata, considered important for an understanding of the physico-chemical aspects of the adhesion mechanism. Examples taken from different fields of application will be included, but it is emphasized that no attempt towards a complete bibliography on this point was made.

6.1. Microbial adhesion to substrata and the thermodynamic approach

Numerous studies have been done [66,76,149] to demonstrate that the thermodynamic approach towards microbial adhesion, i.e. Eq. 1, has any value for predicting actual microbial adhesion to substrata. In this respect, the question must first be asked whether or not it is correct to apply thermodynamics to the process of microbial adhesion. Principally, thermodynamics may only be applied to processes in an equilibrium state with equal 'on' and 'off' rates, implying a reversible process. Norde and Lyklema [171] concluded that adhesion of *Arthrobacter* spp., *Escherichia coli, Micrococcus luteus* and *Pseudomonas* spp. to polystyrene [172] and microbial adhesion in general [171] has the nature of a weak, secondary minimum interaction with interaction energies of a few kT. Consequently, these authors conclude that

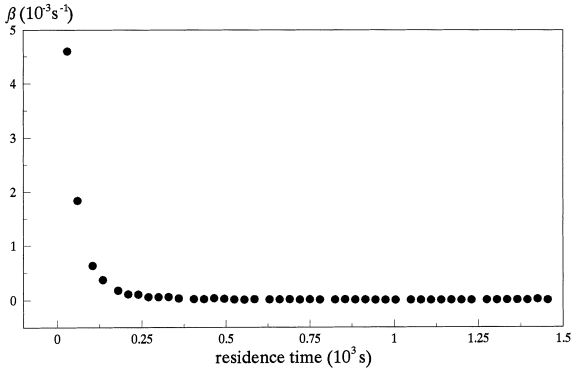

Fig. 17. An example of the desorption rate coefficient $\beta(t-\tau)$ as a function of residence time for *Enterococcus faecalis* 1131 on FEP in urine and at a wall shear rate of 15 s^{-1}, demonstrating a decrease in reversibility as the residence time of the adhering microorganisms increases.

microbial adhesion is a reversible process, although they do not rule out that secondary minimum adhesion may develop by a two-step adhesion kinetics, as observed for *Streptococcus sanguis* strains [173,174], into a strong, irreversible primary minimum interaction. Development of a reversible secondary minimum adhesion into irreversible primary minimum adhesion is suggested to be easier in high ionic strength suspensions and when the microorganisms involved have surface appendages [91]. Meinders et al. [155,175], using direct image analysis, observed for a number of strains, substrata and conditions that microbial adhesion is initially a reversible process with high desorption rate coefficients β_0 of around 10^{-3} s^{-1} that decreased strongly within 2–4 min to low, but non-zero desorption rate coefficients β_f of between 10^{-4} and 10^{-6} s^{-1}, implying minor reversibility (see also Fig. 17). Comparison of the decreases in desorption rate coefficients over time for bacteria and inert polystyrene particles have demonstrated that both show strengthening of the bond over time [153,155], but bond strengthening for bacteria extends over longer periods of time than for polystyrene particles [155]. Also estuarine bacteria adhering to hydrophilic, hydroxyl-terminated and to hydrophobic, methyl-terminated self-assembled monolayers had residence times of less than 10 min, suggesting that establishment of firm adhesion occurred quickly on all surfaces [154].

Possibly, an analogous situation exists for microbial adhesion to substrata as for protein adsorption, in which protein segments adsorb reversibly but, through multiple binding segments, an entire protein molecule effectively adsorbs irreversibly. In consequence, microbial adhesion should then be regarded as a collection of reversibly adhering cell surface structures rather than as one irreversibly adhering entity. An interaction energy of -19 kT has been reported for adhesion *Streptococcus epidermidis* 9855 to heparinized polyvinylchloride tubing [176]. Despite the lingering discussion on the issue of reversibility, the thermodynamic approach towards microbial adhesion is often employed.

The probability of initially adhering *Pseudomonas fluorescens* and *P. aeruginosa* to desorb from substratum surfaces decreased with increasing substratum surface free energy [120]. The reversibility of oral streptococcal adhesion to substrata with different wettability after replacing a bacterial suspension by the suspending fluid appeared greater when $\Delta G_{adh} > 0$ than when $\Delta G_{adh} < 0$ with ΔG_{adh} calculated from Eqs. 7 and 8 [177,178]. Also, when the kinetics of adhesion was followed up to a stationary end-point, it was observed that at the strain level, oral streptococcal adhesion to different substrata showed strong relationships between adhering numbers and ΔG_{adh} [149,179]. These relationships could not be extended to include data for the adhesion of different strains to a given substratum. Similar observations were done by Barton et al. [180] on adhesion of *S. epidermidis, P. aeruginosa* and *E. coli* to orthopedic implant polymers using the same thermodynamic approach. Only when limiting the analysis to adhesion of one strain to different implant polymers did they find strong relationships between numbers of adhering bacteria and ΔG_{adh} in their system. Analysis of adhesion data for *Listeria monocytogenes* to polypropylene, rubber, glass and stainless steel on the basis of thermodynamics led Mafu et al. [92] to conclude that thermodynamic implications could not be correlated with *L. monocytogenes* adhesion. In contrast again, Wang et al. [181] did a surface thermodynamic analysis by the equation of state (Eq. 3) of adhesion data for an encapsulated, slime-producing *S. epidermidis* strain to blood-contacting biomedical materials and found that interfacial free energies are strong driving forces for adhesion. Convincing relationships between ΔG_{adh}, calculated from the equation of state as well, and the adhesion of hydrophilic *Candida albicans* and hydrophobic *Candida tropicalis* yeasts to 19 different denture base materials have been described by Minagi et al. [182]. Bellon-Fontaine et al. [76] noted that the degree of success with which the thermodynamic approach could predict the adhesion of *Streptococcus thermophilus* and *Leuconostoc mesenteroides* strains to substrata depended greatly on which equation was used to convert measured contact angles into surface free energies, i.e. Eqs. 3, 4 or 5.

Obviously, certain factors that differentiate microorganisms from inert particles are not included in the thermodynamic approach. Pratt-Terpstra et al. [148,149] distinguished between so-called interfacial free energy sensitive and insensitive oral streptococcal strains. Interfacial free energy sensitive strains could generally be classified as the evenly fibrillated

streptococci [183] and their adhesion to substrata differed greatly upon a minor change in substratum wettability, while bald and extremely hydrophilic organisms, like *S. salivarius* HB-C12 [184] or biosurfactant-releasing *Streptococcus mitis* BMS [185], were insensitive to changes in the wettability of the substrata to which they adhered. When microorganisms release biosurfactants, as many strains do [186], differences in substratum wettability can disappear upon adsorption of these biosurfactants [187,188] and such strains become classified as 'interfacial free energy insensitive'. Alternatively, the bald and extremely hydrophilic *S. salivarius* HB-C12 is envisaged to be 'interfacial free energy insensitive' because it is surrounded by a layer of interfacial water [189] that impedes direct contact with substratum surfaces, while also fibrils that could pierce the water layer to contact a substratum surface are lacking.

Finally, it is emphasized that a thorough evaluation of the merits of the thermodynamic approach beyond the level of measured contact angles for explaining microbial adhesion is not possible as long as colloid and surface science has not advanced to a state in which a well argumented choice can be made for the equation of state (Eq. 3), the Lifshitz-van der Waals/acid-base approach (Eq. 4) or its further extensions distinguishing electron-donating and electron-accepting parameters (Eq. 5).

6.2. Microbial adhesion and the DLVO approach

6.2.1. Microbial adhesion to hydrocarbons (MATH) and other solvents (MATS)

MATH experiments have been carried out most frequently to determine the microbial cell surface hydrophobicity, based on the simple rationale that the hydrocarbon interface and the interface of other hydrophobic ligands against an aqueous solution would be uncharged. Hydrophilic organisms would remain in the aqueous phase and hydrophobic organisms would adhere to the hydrophobic hydrocarbon phase. However, water contact angle measurements on microbial lawns have become more and more accepted for the measurement of the intrinsic microbial cell surface hydrophobicity [190,191], especially since it has been demonstrated that microbial adhesion to hydrocarbons is governed by a combination of all structural [192,193] and physico-chemical [94,99–101] cell surface properties involved in adhesion. Recently, it has been shown that hydrocarbon droplets in aqueous suspension are negatively charged [99,159], with zeta potentials as low as −60 mV in potassium phosphate buffers at pH 7. In the pH range between 2 and 4, most hydrocarbons have a zero zeta potential. In consequence, according to the classical DLVO theory, microorganisms that bear a negative charge experience electrostatic repulsion at neutral pH, which has to be overcome by attractive Lifshitz-van der Waals forces in order to adhere in MATH [194]. Furthermore, classical DLVO theory predicts that microorganisms below their isoelectric point, i.e. bearing a positive surface charge, should adhere better to hydrocarbons than suspended in aqueous solutions above their isoelectric point.

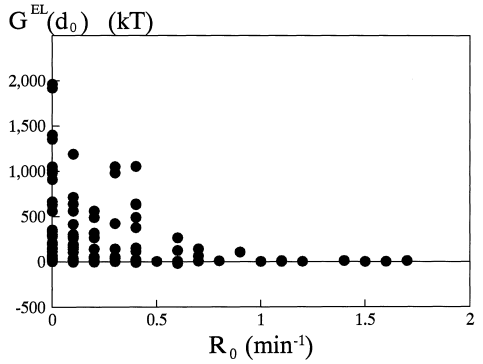

Fig. 18. The electrostatic interaction energy $G^{EL}(d_0)$ between hexadecane droplets and thermophilic dairy streptococci versus the microbial removal rate R_0 by hexadecane in a 10 mM potassium phosphate solution as in MATH (adapted from [94]) calculated for the minimal separation distance d_0 of 1.57 Å.

Fig. 18 presents the electrostatic interaction energy at closest approach (see Table 2) between hexadecane droplets and some thermophilic dairy streptococci as a function of their initial removal rates in the kinetic MATH assay [94]. Clearly from Fig. 18, microbial removal by hexadecane is fully impeded ($R_0 < 0.5$ min^{-1}) when the electrostatic repulsive interaction energy at closest approach exceeds 500–1000 kT. Significant removal rates ($R_0 > 1$ min^{-1}) only occur for situations in which the electrostatic interaction energies are small,

say repulsions of less than 100 kT. Consequently, it has been suggested that the removal rates as determined in MATH are indicative of the intrinsic cell surface hydrophobicity solely in case electrostatic interactions are absent. Similar results have been published for a collection of oral *S. mitis* strains [195].

Alternatively, Van Loosdrecht et al. [196] demonstrated for a collection of soil microorganisms that a threshold intrinsic microbial cell surface hydrophobicity (water contact angles above 30°) was required in order for cells to overcome the electrostatic repulsion and adhere to the hexadecane in MATH. Reid et al. [166] described such a threshold intrinsic microbial cell surface hydrophobicity for a collection of lactobacillus strains at a water contact angle of around 60°, which is a considerably higher threshold contact angle than reported by Van Loosdrecht et al. [196].

It is surprising that the most beautiful example of the complicated interplay of electrostatic and Lifshitz-van der Waals forces governing microbial adhesion [194] is provided by MATH experiments, considering at least its disadvantages as mentioned earlier. The hydrocarbon interface against an aqueous solution is chemically more homogeneous and microscopically smoother than any polymeric or metallic substratum. Possibly, this is why MATH experiments provide convincing evidence for classical DLVO interactions in microbial adhesion to substratum surfaces.

Although it has been known for a relatively long time that hydrocarbon droplets in aqueous suspensions carry a negative charge [99,101,197], electrostatic contributions in MATH are still frequently neglected which may complicate or even impede a proper interpretation of adhesion data. In a study by Takeuchi and Suzuki [198] it was noted that adhesion of *Thiobacillus thiooxidans* to elemental sulfur decreased in the presence of increasing potassium phosphate concentrations despite the fact that bacteria adhered better to hexadecane in MATH, without a consideration of electrostatic interactions. Kiely et al. [199] noticed that under conditions of physiological pH and low ionic strength *Brevibacterium linens* exhibited no affinity for an octyl ligand, despite favorable acid-base interactions but neglected electrostatic interactions.

Verification of the extended DLVO theory by a MATH-like assay was initiated recently by Bellon-Fontaine et al. [102], replacing the hydrocarbons by organic solvents, such as chloroform and diethylether, in which case the assay is called MATS. Microbial adhesion to chloroform and diethylether, with exclusively $\gamma^{\oplus}$ or $\gamma^{\ominus}$ parameters, respectively, was compared with the adhesion to a hydrocarbon with similar surface tension. Monopolar repulsion between diethylether ($\gamma^{\ominus} = 16.4$ mJ m^{-2}) and *Streptococcus thermophilus* B ($\gamma^{\oplus}_{mv} = 0.03$; $\gamma^{\ominus}_{mv} = 62.1$ mJ m^{-2} [102]) indeed hampered adhesion, while conversely, monopolar attraction stimulated adhesion of this strain to chloroform ($\gamma^{\oplus} = 3.8$ mJ m^{-2}), in line with predictions by the extended DLVO approach. Also lactobacilli adhered strongly to chloroform and not to hexadecane due to the ability of cell surface groups to exert acid-base interactions [200]. From the above it can be concluded that MATS seems a promising method to probe the electron-donating and -accepting properties of microbial cell surfaces using a non-contact angle-based method. Moreover, MATS may gain importance since it has been demonstrated [64] that the origin of microbial cell surface hydrophobicity is in the acid-base nature of the cell surface (as can be probed by water and formamide contact angles) and not so much in the ability of the cell surface to exert Lifshitz-van der Waals forces (as can be probed by apolar liquid contact angles like with α-bromonaphthalene and methylene iodide).

6.2.2. Bacterial adhesion to coal

Bacterial adhesion to coal is one of the novel methods recently explored to stimulate the separation of fine coal particles from the associated mineral matter [5]. *Mycobacterium phlei* is a hydrophobic bacterium (water contact angle 68°) with negative zeta potentials in 0.01 M sodium nitrate solutions ($2 \leq pH \leq 10$). By adhesion to fine coal particles, *M. phlei* bridges are formed yielding flocculation of the coal particles. A maximum flocculation efficiency by *M. phlei* bridging, corresponding to maximum adhesion of *M. phlei* to coal, occurred around pH 4. Interestingly, the total interaction energy according to the classical DLVO theory between a coal particle and *M. phlei* at an assumed minimal distance of approach of 6 Å ranges between 6×10^2 and

4×10^3 kT, with a distinct minimum around pH 4, where adhesion was maximal [5].

The above example is especially interesting, as it provides evidence in support of DLVO interactions in microbial adhesion to an inert, hydrophobic, real-life surface, i.e. coal, in addition to what has been concluded from microbial adhesion to hydrophobic hydrocarbon droplets in aqueous solution (MATH or MATS).

6.3. Microbial adhesion to substrata and electrostatic interactions

The charge properties of a substratum surface are difficult to vary independently without affecting other substratum surface properties as well. Morisaki et al. [201] developed an elegant way to circumvent this problem by studying adhesion of *Pseudomonas syringae* to electro-conductive glass plates in a parallel plate flow chamber in an external electric field applied perpendicular to the substratum surface. In electric fields up to 5 V cm^{-1}, bacterial deposition was enhanced when the substratum surface was the positive electrode and reduced when it was the negative electrode. By extrapolating the adhesion data to the (negative) electric field strength for which bacterial deposition was fully impeded, the microbial zeta potential was used to calculate the electrostatic force that could counterbalance the adhesive force. In this way, the adhesive force of *P. syringae* to glass was estimated at 5×10^{-11} N per cell, which seems reasonable [108].

In a slightly different experimental set-up, detachment of a *Bacillus* spp. from quartz was studied as stimulated by an external electric field of up to 27 V cm^{-1} applied parallel to the substratum surface [202]. The adhering cells appeared not to be removed at a specific strength of the electrostatic removal force but were removed over a wide range of force, about 10^{-14}–10^{-12} N per cell. Obviously, this is a removal force parallel to the substratum surface, which must not be mistaken for the adhesive force, acting perpendicular to the surface.

Van der Mei et al. [203] studied adhesion of six coagulase-negative staphylococcal strains (see Table 8) to positively and negatively charged acrylate surfaces with similar wettability in a parallel plate flow chamber without application of an external electric field. Initial deposition rates of all staphylococcal strains were high, up to 2.5 times the Smoluchowski-Levich solution j_0^* of the convective-diffusion equation (Eq. 18a), on the positively charged substratum ($\zeta=+2$ mV) and reduced to a fraction of the Smoluchowski-Levich solution on the negatively charged substratum ($\zeta=-13$ mV). Analogous to the analysis of Morisaki et al. [201] for an applied, external electric field, we extrapolated our adhesion data to a hypothetical substratum zeta potential ζ_s^* for which the initial deposition rate would be zero and electrostatic repulsion would counterbalance the Lifshitz-van der Waals attraction. Using these zeta potentials ζ_s^* and the microbial zeta potentials ζ_b (see Table 8), to calculate this electrostatic repulsion $G^{EL*}(d_0)$ and equating it with the Lifshitz-van der Waals interaction energy $G^{LW}(d_0)$ yields direct estimates for the Hamaker constants (see Table 8). Comparison of thus obtained Hamaker constants for *S. epidermidis* SL 58, NCTC 100835 and NCTC 100894 with the values summarized in Table 4 demonstrates that the estimates are realistic. Hamaker

Table 8
Water contact angles and zeta potentials of coagulase-negative staphylococci [203] together with the zeta potentials ζ_s^* of hypothetical acrylate substrata to which their initial deposition would be fully impeded by electrostatic repulsion. The interaction energy associated with this electrostatic repulsion $G^{EL}*(d_0)$ can be calculated from the equations in Table 2 and equated with the Lifshitz-van der Waals interaction energy to obtain estimates for the Hamaker constant A

Strain	θ_{H_2O} [degrees]	ζ_b [mV]	ζ_s* [mV]	$G^{EL}*(d_0)$ [J]	A [kT]
S. epidermidis SL 58	22	+4.5	+150	459	0.9
S. epidermidis NCTC 100835	27	−2.5	−140	238	0.4
S. epidermidis NCTC 100894	27	−5.0	−626	2129	4.0
S. hominis SL 33	37	−13.0	−493	4360	8.2
S. saprophyticus SAP1	20	−14.5	−547	5395	10.2
S. epidermidis NCTC 100892	19	−9.5	–[a]	–	–

[a]Data did not allow an extrapolation to a meaningful substratum zeta potential ζ_s^*.

constants for *Staphylococcus hominis* SL 33 and *Staphylococcus saprophyticus* SAP1 are rather high and either artefactual due to long extrapolations involved in obtaining ζ_s^* or related to the fact that these strains are encapsulated, thus emphasizing the role of capsules in staphylococcal adhesion [204,205].

More straightforward ways of demonstrating a role of electrostatic interactions in microbial adhesion are based on carrying out experiments as a function of ionic strength [11,184] or pH [175]. In all such studies, a critical ionic strength is revealed, above which electrostatic repulsion becomes negligible and microbial adhesion strongly increases, analogous to what is commonly found for adhesion of inert polystyrene particles [206].

Under low ionic strength conditions, electrostatic repulsion generally dominates. Strain-dependent relationships between oral streptococcal adhesion to restorative dental materials have been found with maximal adhesion to the restorative material having the least negative potential [207]. Adhesion of Gram-negative rhizobacteria to polystyrene and rice roots was virtually absent for strains with zeta potentials more negative than −25 mV and increased with zeta potentials of the strains becoming less negative [208], but adhesion of Gram-positive rhizobacteria was low regardless of their zeta potentials. In an analysis of the near-surface swimming behavior of negatively charged *E. coli*, larger numbers of irreversibly adhering bacteria were found at higher ionic strengths than at lower ionic strengths [209]. Even adhesion to a complicated biological surface like meat of *Pseudomonas fluorescence, Bacillus subtilis, E. coli, L. monocytogenes, Salmonella typhimurium, Serratia marcescens* and of staphylococcal strains related to increasing negative charge on the bacterial cell surface [8–10,12].

When analyzing microbial adhesion data in terms of electrostatic interactions, it should not be a priori assumed that the electrostatic interaction is repulsive, simply because the zeta potentials of the interacting surfaces are both negative. At a more microscopic level than the overall level of particulate microelectrophoresis, microbial cell surfaces may have positively charged domains mediating adhesion through local electrostatic attraction despite overall repulsion, as described e.g. for the interaction between *Treponema denticola* and human erythrocytes [210]. On a series of *E. coli*, Zita and Hermansson [211] found that the number of positively charged surface structures per cell surface was only a fraction of the number of negatively charged surfaces structures, but that nevertheless the presence of positive surface charges was more influential upon adhesion of the strains to activated sludge flocs than the presence of negative surface charges. At a macroscopic level, only two studies [140,212] report microbial strains with a positive surface charge over the entire pH

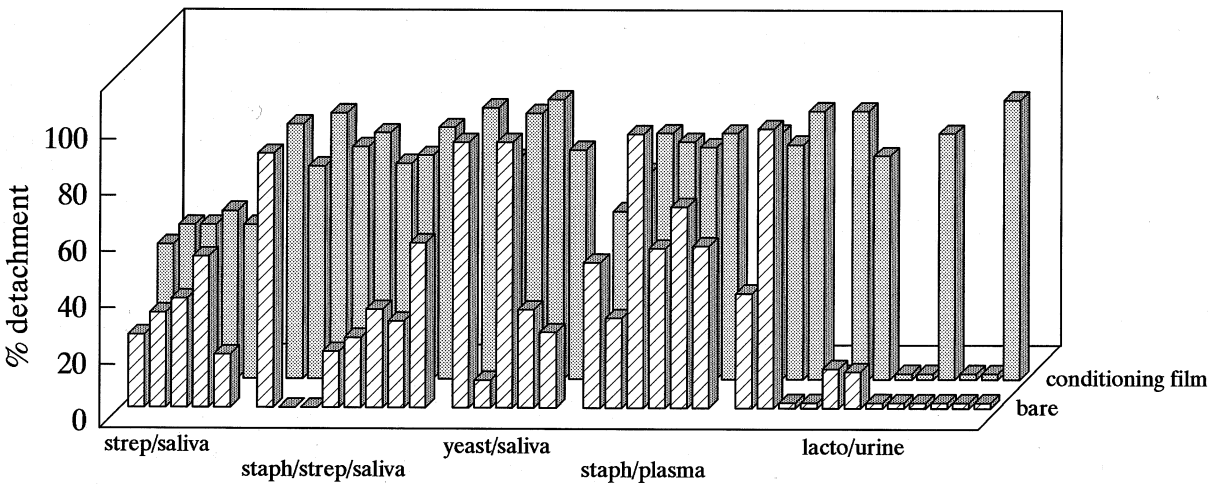

Fig. 19. The percentage microbial detachment stimulated by the passage of a liquid-air interface for adhesion in the presence and absence of a conditioning film. Data taken from [29,220–223].

range. Busscher et al. [140] described a *S. thermophilus* dairy strain with zeta potentials as positive as +20 mV in 10 mM potassium phosphate solutions. Consequently, the initial deposition rate of this strain to negatively charged glass was extremely high, approximately two times *j*, calculated from the Smoluchowski-Levich approach, Eq. 18a. Jucker et al. [212] isolated a *Stenotrophomonas maltophilia* strain from a catheter of a patient with a suspected urinary tract infection and measured zeta potentials of around +10 mV at physiological pH, suggested to originate from proteins located in the outer membrane. *S. maltophilia*, as did the positively charged *S. thermophilus* strain, strongly favored adhesion to negatively charged surfaces as compared with negatively charged bacteria, constituting the majority of microbial strains and species found in nature.

6.4. Microbial adhesion to conditioning films and detachment

The formation of conditioning films on substratum surfaces tends to mask the physico-chemical properties of the surfaces and equalize them [25,213,214]. Although the wettability and charge properties of many substratum surfaces converge upon adsorption of conditioning film components, microorganisms often seem to probe an influence of the underlying substratum surface through the conditioning film.

When, for instance, a conditioning film is an adsorbed, single-component protein layer, the conformation of the adsorbed proteins and spatial homogeneity of the film are governed by the substratum surface. This explains why adhesion of oral streptococci to protein-coated substrata with different wettabilities is either in line with the thermodynamic approach based on bare substratum surface properties for adsorbed bovine serum albumin [134] or fully opposite, for adsorbed salivary mucins [215]. Alternatively, when multicomponent conditioning films are involved, such as the salivary pellicle on teeth [19] or on the esophageal flange of voice prostheses [160–162], tear film constituents (lysozyme, albumin, immunoglobulins, mucins and lipids) on contact lenses [163] and adsorbed proteins from plasma on polyurethane or silicone rubber [216–218], selective protein adsorption stimulated by the physico-chemical properties of the substrata may pass the influence of the substratum surface through the conditioning film to the interface with adhering microorganisms. Herewith, the conditioning film and the microorganisms initially adhering to it adopt a role as a so-called linking film, attaching the biofilm to a substratum surface [219].

Fig. 19 summarizes the percentages of microorganisms detached from various substrata, when adhering in a parallel plate flow chamber with and without a conditioning film in between as stimulated by the high detachment force of passing a liquid-air interface. As a trend, it can be seen from this compilation that the detachment force exerted by the liquid-air interface detaches a higher percentage of microorganisms adhering to a conditioning film than when adhering directly to a substratum surface.

Christersson et al. [224] allowed oral microorganisms to adhere from human whole saliva to germanium surfaces in a parallel plate flow chamber to form a conditioning film on the substratum and the microbial cell surfaces and stimulated detachment by increasing the flow up to a factor of 32. Significant detachment was already seen at very low drag and lift forces of 10^{-12} and 10^{-16} N per cell, respectively. Possibly, these values are low due to the presence of a conditioning film on both interacting surfaces. Interestingly [224], similar results were found for experiments carried out at 22°C and 37°C.

Although in vitro evidence of a pertaining role of substratum surface properties on microbial adhesion despite the presence of conditioning films is not always convincing, in vivo studies in the oro-pharyngeal cavity are convincing in this respect and have demonstrated that

1. dental plaque formation over a time scale of at least 9 days on polymer strips glued to the front incisors of human volunteers [225,226] and on restorative dental materials in vivo [227] is far less on hydrophobic than on hydrophilic surfaces;
2. biofilm formation over a time scale of at least 4 weeks on partly hydrophobic and hydrophilic oesophageal flanges of voice prostheses, is far less on the hydrophobic than on the hydrophilic side [228].

It has been hypothesized that the fluctuating shear

conditions in the oro-pharyngeal cavity can become occasionally excessively high yielding cohesive failure in the linking film therewith detaching the entire biofilm on top of it. Likely, the cohesivity of the linking film may be relatively weak and governed by the substratum surface properties [219]. Taylor et al. [229] demonstrated that substrata exposed to oligotrophic, subtropic marine waters adsorbed the fewest conditioning film components when the dispersion and polar components of the substratum surface free energy were extreme. In addition, a maximal number of adhering marine bacteria was found on substrata for which the polar surface free energy component comprised about 30% of the total substratum surface free energy.

Generally, it can therefore be concluded that adhering microorganisms are more easily stimulated to detach when adhering to a conditioning film than when adhering directly to the substratum, providing evidence in support of the hypothesis that a conditioning film constitutes a weak link between a substratum surface and a biofilm.

6.5. Influence of microbial cell surface appendages

Microbial cell surfaces can be equipped with various kinds of appendages, such as fibrils, fimbriae or flagella, that can all play a role in microbial adhesion to surfaces [66]. Often the presence of these structural features is not expressed in microbial contact angles and zeta potentials, while they do assist adhesion. *S. mitis* BMS, for instance, having similar contact angles and zeta potentials as polystyrene particles, adhere much better to substratum surfaces than the relatively smooth polystyrene particles [206] due to the presence of fibrils up to 1 μm in length. Sjollema et al. [118,135] noted that oral streptococci depositing in a parallel plate flow chamber to glass had initial deposition rates that were much higher than calculated from the Smoluchowski-Levich approach (Eq. 18a) which was attributed to fibrillar surface appendages assisting adhesion.

Our knowledge of the physico-chemistry of the tips on microbial cell surface appendages involved in adhesion is extremely limited. As a direct consequence of the small diameter of surface appendages, however, it follows directly from the equations listed in Table 2 that a negatively charged tip experiences less electrostatic repulsion when approaching a negatively charge substratum surface than a micrometer-sized microorganism as a whole simply owing to its smaller dimensions. Thus, even negatively charged appendages can pierce the electrostatic energy barrier (see Fig. 7). Piercing the electrostatic energy barrier is also facilitated when the hydrophobicity of the tip is different from the one of the overall cell surface as illustrated in Fig. 20.

Handley [65,230] localized the charge and hydrophobicity on the cell surface of laterally tufted *Streptococcus sanguis* strain by adsorbing cationized ferritin or colloidal gold to the cell surfaces prior to negative staining. Cationized ferritin attached at pH 6.5 only to a short fibril component in the tufts, indicating the presence of negative charge. Alterna-

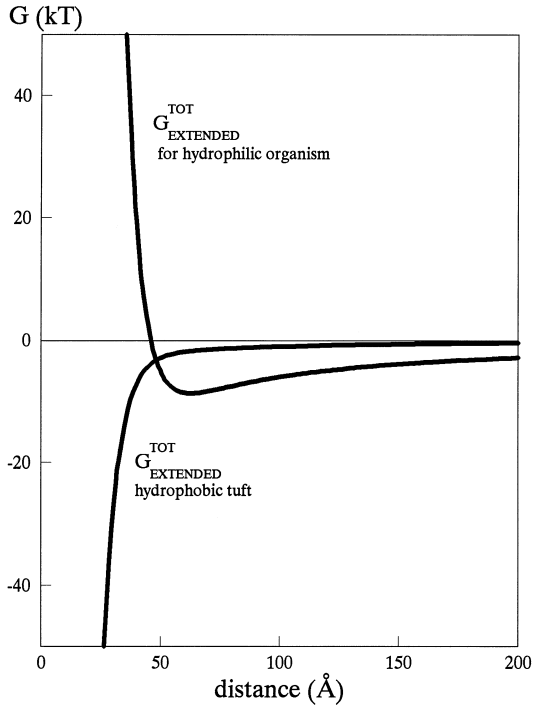

Fig. 20. Interaction energies, according to the extended DLVO theory, as a function of separation distance for a bald, hydrophilic microorganism and for hydrophobic, 200 nm wide, tufts opposed to a solid substratum surface under conditions of electrostatic repulsion. DLVO input data: $A = 0.78$ kT; $a = 500$ nm; $\zeta_m = -15$ mV; $\zeta_s = -15$ mV; $\kappa^{-1} = 9.6$ Å. Note that the potential energy barrier present for the organism as a whole has disappeared for the small, hydrophobic tuft and a local attraction results, i.e. the potential energy barrier is 'pierced'.

tively, colloidal gold attached independent of pH to the ends of a long fibril component, suggested to be hydrophobic. Interestingly, the negatively charged colloidal gold also attached to the short fibril component with an optimum at pH 3.4, confirming the presence of negative charge on these fibrils above pH 3.4. The localization of hydrophobicity at the ends of the long fibrils on laterally tufted *S. sanguis* strains also follows from water contact angles on microbial lawns [231], demonstrating higher water contact angles on a tufted strain (74°) than on a bald variant (31°), despite the fact that negative staining only revealed the tuft as a prominent crest on the equator of the bacteria.

It is obvious that application of thermodynamic approaches or the DLVO theory towards adhesion of microorganisms with structural surface features is impossible on the basis of overall cell surface properties, especially at close approach. By combining results from deposition experiments at various ionic strengths with DLVO predictions one can estimate the contribution of structural surface features to microbial adhesion [90,93]. For a variety of coryneform bacteria and pseudomonads, it was calculated that structural features on cell surfaces of these organisms had lengths up to 165 nm. One strain, with exceptionally long (several micrometers) polymers protruding from the dehydrated cell surface adhered up to 10 times better to Teflon and glass than 'smoother' strains [232] by piercing the potential energy barrier to establish adhesion. It was furthermore hypothesized [93] that *Rhodococcus* strains with an isoelectric point $\leq$2.8 had abundant cell surface polysaccharide-rich appendages containing negatively charged phosphates and carboxyl groups, inhibiting adhesion to both hydrophilic and hydrophobic surfaces. Coryneform bacteria with their isoelectric point around pH 3.0 were envisaged to have amphiphilic appendages facilitating adhesion to hydrophobic but not to hydrophilic surfaces. Bacteria with an isoelectric point above pH 3.2 appeared to be free of inhibiting polymeric appendages and were predicted to adhere to any substratum surface.

Although Rijnaarts et al. [93] postulated that the isoelectric point of bacteria is an indicator for the presence of polymeric cell surface appendages inhibiting adhesion, as a generally valid statement, examples are available to demonstrate that their conclusions only apply to their collection of coryneform bacteria and pseudomonads. Within a collection of eight isolates of *E. coli* from urinary tract infections, two isolates adhered to xylene in MATH, despite the fact that all isolates had isoelectric points around or below pH 2 [233]. Similarly, oral *S. mitis* BMS, possessing long fibrils and with an isoelectric point of pH 3.7, did not adhere in significant numbers to hydrophilic glass nor to hydrophobic polymers [148].

7. Mechanisms of microbial coaggregation

Coaggregation between microbial pairs has almost exclusively been studied in the oral field. Hence most examples on microbial coaggregation dealt with in this section originate from this domain, although there is increasing interest in developing degradative microbial communities through the formation of ordered microbial coaggregates [234]. Only recently have studies into oral microbial coaggregation taken a physicochemical approach, often complementary to biochemical and structural studies [122,235]. Hence, by comparison with the section on microbial adhesion to substrata, this section will be relatively small.

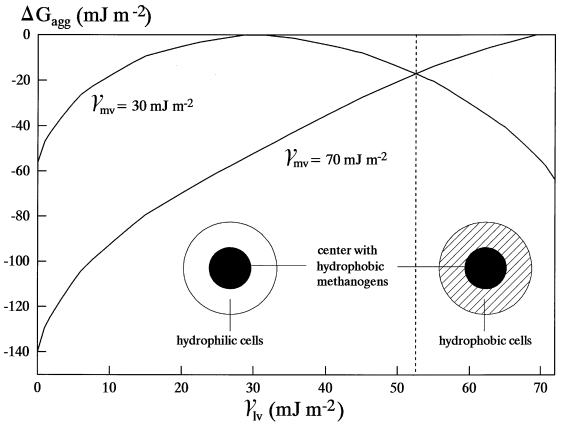

Fig. 21. Free energies of aggregation of two identical bacteria with a hydrophilic ($\gamma_{mv} = 70$ mJ m^{-2}) or a hydrophobic ($\gamma_{mv} = 30$ mJ m^{-2}) cell surface as a function of the surface tension of upflow anaerobic sludge bed reactor fluids. The surface tension of the reactor fluid is suggested to control the outer layer cells of the microbial granules formed (adapted from [234]).

7.1. Microbial (co)aggregation and the thermodynamic approach

Application of surface thermodynamics towards microbial coaggregation immediately raises the issue whether or not microbial coaggregation is thermodynamically reversible. Whereas for microbial adhesion to substrata a minor reversibility in the thermodynamic sense has been observed [155,175], reversibility of microbial coaggregative interactions has only been established by the addition of a particular carbohydrate or chelating agent such as EDTA to break up coaggregating microbial pairs [55].

Pending the above issue, Thaveesri et al. [234] applied surface thermodynamics using the equation of state (Eq. 3), to explain the formation of microbial granules and sludge bed stability in upflow anaerobic sludge bed reactors. Depending on the liquid surface tension γ_{lv}, either hydrophilic or hydrophobic microorganisms were predicted to form granules or aggregates and the formation of structured coaggregates was predicted to be controlled by the surface tension γ_{lv} of the reactor fluid, as schematically summarized in Fig. 21. As can be seen in Fig. 21, within the range of liquid surface tensions encountered in reactor systems, i.e. between 32 and 62 mJ m^{-2}, aggregation of hydrophilic organisms is favored in low surface tension reactor fluids, while aggregation of hydrophobic organisms is energetically more favorable in high surface tension reactor fluids, as based on the free energy of aggregation between identical bacteria defined in analogy to the free energy of adhesion ΔG_{adh}, as given by Eq. 1. Consequently, structurally different (co)aggregates are predicted to form in various reactor systems that have indeed been experimentally observed [234]. However, Daffonchio et al. [190] rightly criticized this model by pointing out that surface thermodynamics did not explain the adhesive interaction between the center hydrophobic methanogens and the outer layer hydrophobic or hydrophilic cells.

Prevotella intermedia and *Prevotella nigrescens* both form coaggregating pairs with *A. naeslundii*. In contrast to many other oral microbial pairs, the interaction between these microorganisms does not require calcium [236]. Table 9 lists the free energy of coaggregation, defined in analogy to Eq. 1 and calculated from the measurement of contact angles on microbial lawns employing the Lifshitz-van der Waals/acid-base approach (Eq. 5). The coaggregating pair, constituted by *P. intermedia* MuI WT with *A. naeslundii* T14V-J1, is the only pair with a significantly negative interfacial free energy of coaggregation, opposite to the non-coaggregating pairs having positive or slightly negative interfacial free energies of coaggregation. Thus, surface thermodynamics fully predicts the coaggregation of these pairs.

Table 9 also lists similarly calculated free energies of coaggregation for oral microbial pairs that do require calcium for their interaction. In contrast with pairs not requiring calcium for their coaggregation, surface thermodynamics predicts a coaggregation behavior for these strains that is at odds with experimental observations, i.e. pairs coaggregate despite a

Table 9
Lifshitz-van der Waals and acid-base Gibbs interfacial free energies (mJ m^{-2}) of interaction according to Van Oss et al. [71] between *A. naeslundii* T14V-J1 and various streptococcal [95] and *Prevotella*[a] strains either requiring or not requiring calcium for their coaggregation, as approximated from the measured contact angles

Microbial pair	ΔG_{coagg}^{LW}	ΔG_{coagg}^{AB}	$\Delta G_{coagg}^{LW}+\Delta G_{coagg}^{AB}$	Coaggregation score
Coaggregation not requiring calcium				
P. intermedia MuI 1 WT	−2.5	−5.8	−8.3	+
P. intermedia 1e	−1.7	−0.1	−1.8	−
P. intermedia 2b	−1.5	+7.2	+5.7	−
P. intermedia 4d	−1.2	+7.6	+6.4	−
P. intermedia 9d	−2.5	+2.1	−0.4	−
Calcium-mediated coaggregation				
S. oralis J22	−4.5	+5.1	+0.6	+
S. oralis 34	−3.9	+1.6	−2.3	+
S. sanguis PK1889	−4.0	−0.6	−4.6	−

[a]Data: courtesy of Dr. A. Cookson, Dr. P.S. Handley and Dr. A.E. Jacob, University of Manchester, UK.

positive interfacial free energy of coaggregation or do not in case of negative values (see Table 9).

Thus it becomes important from a surface thermodynamic point of view to distinguish between Ca-mediated and non-Ca-mediated microbial coaggregation. Non-Ca-mediated coaggregation follows surface thermodynamics in a relatively straightforward manner, but Ca-mediated coaggregation is governed by a different mechanism. Possibly, adsorption of calcium ions to microbial cell surface components interferes with the acid-base surface free energy parameters of the cell surface to decrease the electron donating surface free energy parameter $\gamma^{\ominus}$, thus rendering more hydrophobic cells [59] that coaggregate more readily. This suggestion is confirmed by preliminary MATH and MATS assays (see Fig. 22), demonstrating that addition of calcium ions does not affect adhesion of *A. naeslundii* 5951 to hexadecane lacking acid-base interactions (see also Table 1), while adhesion to chloroform is reduced due to masking of electron-donating groups on the microbial cell surface by adsorbed calcium ions.

The above examples illustrate the virtues of surface thermodynamics in explaining microbial coaggregative interactions, but simultaneously emphasize that great care has to be taken to avoid erroneous conclusions, especially when specific cation adsorption is involved.

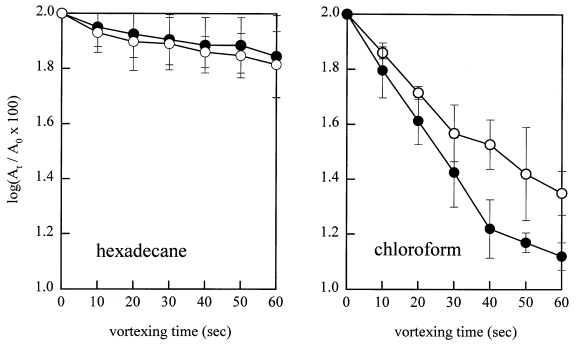

Fig. 22. Adhesion, expressed as log ($A_t/A_0 \times 100$) of *A. naeslundii* 5951 to hexadecane (MATH) and chloroform (MATS) as a function of the vortexting time. Experiments were performed in the absence (open symbols) and presence (closed symbols) of 10 mM $CaCl_2$ in a 10 mM potassium phosphate solution (pH 7.0). Bars are S.D. over four separate experiments.

7.2. Microbial (co)aggregation and the DLVO approach

Microbial coaggregation is mediated by the ever present attractive Lifshitz-van der Waals forces and attractive acid-base interactions between the interacting microorganisms, sometimes resulting from the addition of calcium ions. As nearly all microorganisms are negatively charged [212], these attractive interaction forces always have to overcome a certain electrostatic repulsion in order for coaggregation to occur. In this respect, the requirement of calcium ions for the coaggregation of oral streptococci with actinomycetes not only serves to enhance acid-base attraction, but also breaks down the electrostatic energy barrier between the organisms. Bos et al. [95] demonstrated that addition of calcium ions to oral microorganisms showing coaggregation made their zeta potentials slightly less negative by approximately 1.5 mV. Using the equations in Table 2, it can be calculated that this corresponds to a reduction of the electrostatic repulsive interaction energy by 4 kT at closest approach (1.57 Å). Obviously, from a physico-chemical point of view, it is a very critical colloid-chemical balance that determines whether or not coaggregation occurs.

The amount of physico-chemical data on the surface properties of coaggregating microbial pairs is limited, but seems to warrant the general statement that microbial pairs cannot coaggregate in the presence of strong electrostatic repulsion, although the absence of electrostatic repulsion is not always a sufficient condition for coaggregation.

7.3. Microbial cell surface appendages in microbial coaggregation

Several investigators have demonstrated the importance of microbial cell surface appendages in coaggregation [237–239], but due to lack of data on the tip physico-chemistry, a detailed mechanistic treatise from a physico-chemical point of view is still beyond reach. Some studies demonstrated that the molecules mediating coaggregation seem to be located at the distal portion of the appendages [237,238], like the adhesins mediating the coaggregation between *S. sanguis* and *A. israelii* [238].

Also, in calcium-mediated coaggregation, calcium

ions adsorb to the fimbriae involved [95,240]. Tentatively, cation-mediated coaggregation involves charge reversal of the tips by adsorption of positively charged ions. Handley et al. [122,241] compared the coaggregation of *Veillonella* strains with fibrillated and fimbriated *S. salivarius* isolates and found that fibrillar *S. salivarius* strains coaggregated better than did fimbriated strains. From a physico-chemical point of view, these findings may be related to the smaller diameters of fibrils, thus experiencing less electrostatic repulsion, as compared to fimbriae, although fimbriae are generally longer and more evenly distributed. Interestingly, *S. sanguis* strains with peritrichous fibrils formed visible coaggregates with *Actinomyces* strains, while *S. sanguis* strains with only tufts of fibrils lacked the ability to coaggregate [122].

In conclusion, it can be stated that fibrillar surface appendages assist coaggregative interactions between microorganisms provided they are present in sufficient numbers and randomly distributed.

7.4. Coaggregation between bacteria and yeasts

Yeasts are emerging more and more as life-threatening pathogens in hospitalized and immunodeficient patients, stimulated by the increase in invasive medical techniques, the need for immunosuppressive drugs, and the impact of AIDS [242]. Coaggregation between yeasts and bacteria has been suggested to be involved in biofilm formation on dentures [243–245], on nasogastric tubes [246] or on voice prostheses [161,162]. Proper methods to study coaggregation between bacteria and yeasts do not yet exist and those studies adapting coaggregation assays for bacteria to this end are hampered by the strong sedimentation of the yeasts [247]. Most of the coaggregating pairs studied include *C. albicans* together with oral streptococci [235] or actinomycetes [248] as partner strains. Both lectin-carbohydrate as well protein-protein binding have been suggested to be involved in yeast-bacteria coaggregation.

From a physico-chemical point of view, the coaggregative interaction between yeasts and bacteria cannot be any different from that between two bacterial pairs, although yeast cells are larger than bacterial cells. However, there is not enough physico-chemical information available to allow a conclusion or generalized statement to be made [247].

8. Mechanisms of microbial co-adhesion

The distinction between microbial coaggregation and co-adhesion has only been made recently in the literature, hence the number of papers dealing with microbial co-adhesion is limited and this section will be small, dealing only with examples of oral microbial co-adhesion. In fact, mechanistically co-adhesion differs from coaggregation solely by the presence of a solid substratum surface with or without a conditioning film to which one of the organisms under study is already adhering. Consequently, only the use of the parallel plate flow chamber is suitable to demonstrate influences of substratum surfaces and conditioning films.

8.1. Influence of substratum surfaces upon co-adhesion of oral microbial pairs

Adhesion of primer strain microorganisms to a substratum surface can affect their ability to interact with planktonic microorganisms. In a study on the combined effects of ionic strength and substratum hydrophobicity on co-adhesion of *A. naeslundii* T14V-J1 and *A. naeslundii* 5951 with *Streptococcus oralis* 34 in the parallel plate flow chamber, Bos et al. [249] described that the co-adhesion kinetics, i.e. the ratio χ between local and non-local initial deposition of streptococci, decreased with increasing ionic strength of the suspension. In the low ionic strength suspension, however, there was no influence of substratum hydrophobicity and co-adhesion kinetics were similar on hydrophilic and hydrophobic, silane-coated glass. In the high ionic strength suspension, the co-adhesion kinetics were approximately twice as high on hydrophilic glass as on hydrophobic glass. Surprisingly, co-adhesion of the pairs in a stationary end-point was not affected by ionic strength on hydrophilic glass and on hydrophobic glass for *A. naeslundii* 5951 with *S. oralis* 34, while for the pair *A. naeslundii* T14V-J1 with *S. oralis* 34 stationary end-point co-adhesion was similar on hydrophilic and hydrophobic glass in low ionic strength suspensions,

but on hydrophobic glass it decreased three-fold in the high ionic strength suspension.

Dynamic light scattering has demonstrated that appendages on microbial cell surfaces collapse on the cell surface when the organisms are suspended in high ionic strength suspensions [144], thus becoming less available for interactions with other surfaces. Alternatively, in low ionic strength suspensions, surface appendages tend to adapt a so-called stand-off configuration to increase the hydrodynamic radius of the organism and the chances of interaction with other surfaces. Bos et al. [249] hypothesized that in the high ionic strength suspensions fibrillar appendages on the primer strain actinomycete also collapse and, since they are known to be hydrophobic, adsorb to hydrophobic but not to hydrophilic substrata. Consequently, the lectins mediating coaggregation with streptococci are no longer available for co-adhesion under those conditions. Immobilization of cell surface appendages mediating coaggregation by adsorption to a substratum surface probably also explains why certain microbial pairs with the same coaggregation scores can behave differently in co-adhesion studies [250].

From a physico-chemical point of view, coaggregation and co-adhesion proceed for a major part by the same mechanisms [95]. The only possible difference for which experimental evidence exists is that through immobilization of cell surface appendages mediating coaggregation by adsorption to a substratum surface, co-adhesion may sometimes be reduced.

8.2. Oral microbial co-adhesion and salivary conditioning films

From a physico-chemical point of view, the presence of a conditioning film on a substratum surface does not alter the mechanisms governing co-adhesion between microbial pairs, although the film itself must constitute a link between the organisms that has to be strong enough to withstand the shear forces operative. Bos et al. [251] described that co-adhesion between actinomycetes and streptococci occurred equally well to glass with and without a salivary conditioning film. In addition, co-adhesion also occurred when the streptococci were suspended in reconstituted human whole saliva. In general, actinomycetes have strong interactions with substratum surfaces [252] and are little stimulated to detach, e.g. by the passage of a liquid-air interface, contrary to streptococci, desorbing in high numbers upon the exposure to high shear especially when adhering to a conditioning film (see also Fig. 19). Bos et al. [251] noted that the co-adhesive bond between actinomycetes and streptococci was not disrupted by the passage of a liquid-air interface and that adhering actinomycetes might therefore be considered strongholds for other microorganisms to adhere in the development of dental plaque.

Several authors [20,253], however, have pointed out that co-adhesion between oral microbial pairs in saliva occurs predominantly at room temperature and less around 37°C. Hence in the oral cavity, co-adhesion probably only contributes to dental plaque formation when the tooth surface temperatures are lowered to around 30°C, as during open mouth breathing, yielding convective (cold) air flow and subsequent evaporation [254,255]. From a physico-chemical point of view again, the strong dependence of the co-adhesion interaction on temperature emphasizes the critical nature of the interaction, in which a minor increase in thermal kinetic energy of the interacting microorganisms by only 0.06 kT at room temperature [253] can impede the interaction from occurring.

9. Synthesis

I tell thee everything I can: There is little to relate.
Lewis Carroll: Through the Looking Glass and What Alice Found There

9.1. Mechanisms of microbial adhesive interactions

9.1.1. Microbial adhesion to substrata

Microbial adhesive interactions are extremely complex and unlikely to be ever captured in one generally valid mechanism. Physico-chemistry nevertheless has yield a number of mechanisms to explain microbial adhesion to substrata with a rather broad validity, which are summarized by the following statements (see also Fig. 23).

- Initial microbial deposition can be impeded by electrostatic repulsion and increases with decreas-

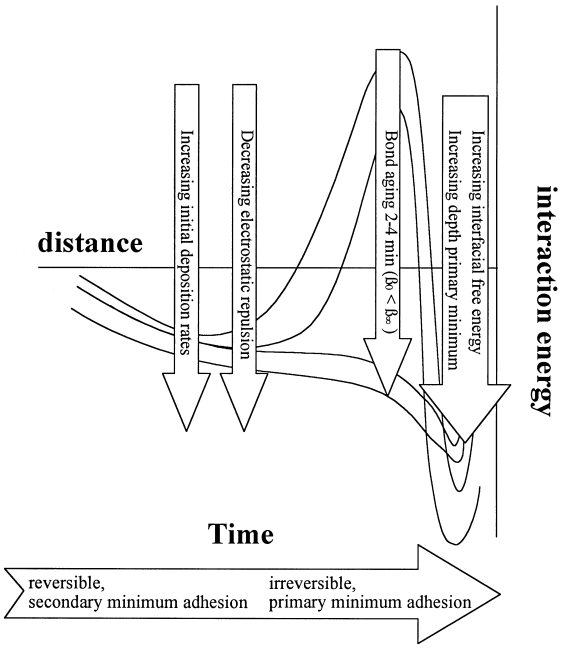

Fig. 23. Sequentially occurring physico-chemical mechanisms and their interaction energies in the adhesion of a microorganism to a substratum surface, including initial deposition governed mainly by electrostatic interactions, reversible secondary minimum adhesion and irreversible primary minimum adhesion, as related to interfacial free energy of adhesion. After initial deposition, a specific local attraction may develop strong enough to overcome the general macroscopic potential barrier.

ing electrostatic repulsion until a mass transport limited maximum under electrostatic attraction.

Initial microbial adhesion is reversible in the secondary interaction minimum and can develop over time into irreversible primary minimum interaction. The degree to which this happens depends on whether the organism under consideration has the means to pierce, or elsewise break down, the potential energy barrier.

The depth of the primary interaction minimum is related to the interfacial energy of adhesion, but the exact relationship depends on the length, physico-chemistry and homogeneity of the surface appendages on the organisms under consideration. Unfortunately, this statement is clouded by the controversies lingering in colloid and surface science about the conversion of measured contact angles into surface free energies.

9.1.2. Microbial coaggregation

Coaggregation of microbial pairs not requiring specific cations such as calcium proceeds in a relatively straightforward manner and is governed by attractive Lifshitz-van der Waals and acid-base interactions, in the absence of strong electrostatic repulsion. Calcium-mediated coaggregation, such as between several oral streptococcal strains and actinomycetes, is mechanistically more complicated, as illustrated in Fig. 24. The role of calcium ion adsorption is pivotal and on the one hand may serve to stimulate attractive acid-base interactions, but on the other hand may yield a reduction of the overall electrostatic repulsion between the organisms [256] or create conditions of local electrostatic attraction [257]. The model outlined in Fig. 24 also explains the lactose reversibility of calcium-mediated coaggregation, as lactose can associate with free calcium ions [258]. All available experimental evidence suggests, however, that from a physico-chemical point of view, microbial coaggregation must be considered an extremely critical colloid-chemical phenomenon, governed by a delicate free energy balance that can be very easily disturbed.

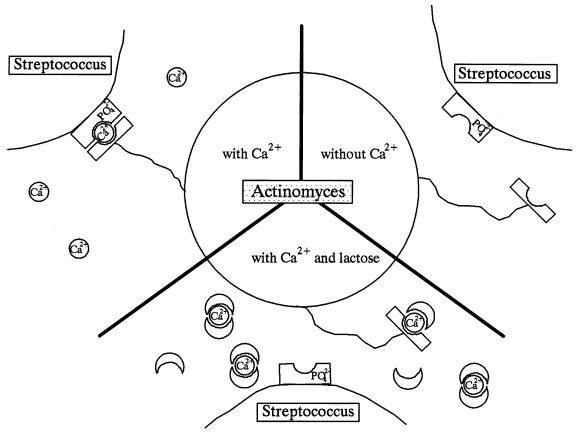

Fig. 24. Hypothetical model for the calcium-mediated coaggregation between actinomycetes and streptococci, illustrating the physico-chemical mechanisms important in their adhesive interaction. Calcium ions are assumed to be adsorbed to the tips of cell surface appendages on the actinomycetes to break down the local electrostatic repulsion between negatively charged phosphate groups on the interacting surfaces and stimulate acid-base attraction.

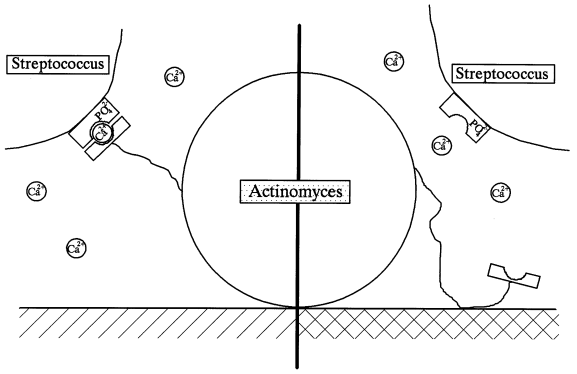

Fig. 25. Co-adhesion mechanisms between microbial pairs may become disturbed through immobilization of surface structures of primer organisms by adhesion to a substratum surface. The degree to which surface structures become unavailable for co-adhesion by immobilization depends on the affinity of the structures for the substratum surface.

9.1.3. Microbial co-adhesion

Mechanistically, co-adhesion between microbial pairs appears to proceed according to the same mechanisms as described for coaggregation. However, fibrillar structures on adhering primer strains may become immobilized by adhesion to a substratum surface, thus becoming unavailable for co-adhesion with planktonic organisms (see Fig. 25). Whether or not all cell surface structures will indeed interact with a substratum surface depends on a variety of aspects, including their length and physico-chemistry, the physico-chemical surface properties of the substratum, ionic strength and temperature.

Thus, despite the fact that the physico-chemical mechanisms of co-adhesion and coaggregation are similar, co-adhesion of coaggregating microbial pairs does not necessarily occur.

9.2. Concluding remarks: the future

At present, sufficient experimental evidence is available to state that several aspects of microbial adhesive interactions can be described by physico-chemical approaches. The degree of success of a physico-chemical approach frequently decreases as the complexity of cell surface appendages on the organisms under consideration increases. A ubiquitously valid physico-chemical model for microbial adhesive interactions calls for a microscopic physico-chemical cell surface characterization that is still beyond reach.

Through the use of atomic force microscopy [259], however, it is already possible to directly measure the decay with distance of the interaction force between particles and a substratum surface [260] and application towards microorganisms may only be a matter of time. Therewith, the interaction energies as a function of separation distance can be determined and compared with theoretical DLVO plots, as in Figs. 7 and 8, to shed light on the importance of overall versus microscopic approaches towards microbial adhesion. Atomic force microscopy has already been used to study the thickness and width of exopolymeric capsules and flagella of bacteria adhering to mica at a nanometer resolution [261].

Considerable progress has been made over the last decade with regard to the methodology to study initial microbial adhesion using image analysis computers and controlled flow devices, especially now that experiments with more than one strain have become possible, thus including microbial community aspects in initial adhesion studies [33,250]. The application of neural network image filters [262] and other sophisticated image filters [263] may stimulate this development. Advanced software is available to determine the speed, direction, angular velocity and acceleration of motile microorganisms on surfaces [264]. Also, confocal scanning laser microscopy [265] combined with the application of controlled flow devices enabled the quantitative study of biofilm formation [266]. It is a challenge for the future to develop models, based on these improved methodologies, that will allow prediction of biofilm features from the initial adhesion events. To this end, the use of these advanced in situ methodologies has to become more widespread, requiring multidisciplinary research teams to overcome the technical complexities involved.

> *So she went on, wondering more and more each step, as everything turned into a tree the moment she came up to it, and she quite expected the egg to do the same.*
>
> Lewis Carroll: Through the Looking Glass and What Alice Found There

Acknowledgements

The authors want to thank Dr. Pauline S. Handley for critical review of the manuscript and helpful comments. Furthermore, the authors are grateful to Mrs. Ellen van Drooge and Marjon Schakenraad for manuscript preparation.

References

[1] Lappin-Scott, H.M. and Costerton, J.W. (1989) Bacterial biofilms and surface fouling. Biofouling 1, 323–342.
[2] Bouwer, E.J. and Zehnder, A.J.B. (1993) Bioremediation of organic compounds – putting microbial metabolism to work. Trends Biotechnol. 11, 360–367.
[3] MacDonald, J.A. and Rittmann, B.E. (1993) Performance standards for in situ bioremediation. Environ. Sci. Technol. 27, 1975–1979.
[4] Diks, R.M.M. and Ottengraf, S.P.P. (1991) Verification studies of a simplified model for the removal of dichloromethane from waste gases using a biological trickling filter. Bioprocess Eng. 6, 93–100.
[5] Raichur, A.M., Misra, M., Bukka, K. and Smith, R.W. (1996) Flocculation and flotation of coal by adhesion of hydrophobic *Mycobacterium phlei*. Colloids Surfaces B Biointerfaces 8, 13–24.
[6] Lalande, M., Rene, F. and Tissier, J.P. (1989) Fouling and its control in heat exchangers in the dairy industry. Biofouling 1, 233–250.
[7] Notermans, S., Dormans, J.A.M.A. and Mead, G.C. (1991) Contribution of surface attachment to the establishment of microorganisms in food processing plants: A review. Biofouling 5, 21–36.
[8] Piette, J.P.G. and Idziak, E.S. (1989) New method to study bacterial adhesion to meat. Appl. Environ. Microbiol. 55, 1531–1536.
[9] Piette, J.P.G. and Idziak, E.S. (1991) Adhesion of meat spoilage bacteria to fat and tendon slices and to glass. Biofouling 5, 3–20.
[10] Piette, J.P.G. and Idziak, E.S. (1992) A model study of factors involved in adhesion of *Pseudomonas fluorescens* to meat. Appl. Environ. Microbiol. 58, 2783–2791.
[11] Bouttier, S., Han, K.G., Bellon-Fontaine, M.N. and Fourniat, J. (1994) Role of electrostatic interactions in the adhesion of *Pseudomonas fragi* and *Brochothrix thermospacta* to meat. Colloids Surfaces B Biointerfaces 2, 57–65.
[12] Dickson, J.S. and Koohmaraie, M. (1989) Cell surface charge characteristics and their relationship to bacterial attachment to meat surfaces. Appl. Environ. Microbiol. 55, 832–836.
[13] Cooksey, K.E. and Wigglesworth-Cooksey, B. (1995) Adhesion of bacteria and diatoms surfaces in the sea: a review. Aquat. Microb. Ecol. 9, 87–96.
[14] Dankert, J., Hogt, A.H. and Feijen, J. (1986) Biomedical polymers, bacterial adhesion, colonization and infection. CRC Crit. Rev. Biocompat. 2, 219–301.
[15] Marsh, P.D. and Martin, M.V. (1992) Oral Microbiology, 3rd edn. Chapman and Hall, London.
[16] Wolfaardt, G.M., Lawrence, J.R., Robarts, R.D., Caldwell, S.J. and Caldwell, D.E. (1994) Multicellular organization in a degradative biofilm community. Appl. Environ. Microbiol. 60, 434–446.
[17] Costerton, J.W., Cheng, K.-J., Geesey, G.G., Ladd, T.I., Nickel, J.C., Dasgupta, M. and Marrie, T.J. (1987) Bacterial biofilms in nature and disease. Annu. Rev. Microbiol. 41, 435–464.
[18] Reid, G., Bruce, A.W., McGroarty, J.A., Cheng, K.J. and Costerton, J.W. (1990) Is there a role for lactobacilli in prevention of urogenital and intestinal infections? Clin. Microbiol. Rev. 3, 335–344.
[19] Bloomquist, C.G., Reilly, B.E. and Liljemark, W.F. (1996) Adherence accumulation, and cell division of a natural adherent bacterial population. J. Bacteriol. 178, 1172–1177.
[20] Liljemark, W.F., Bloomquist, C.G., Bandt, C.L., Philstrom, B.L., Hinrichs, J.E. and Wolff, L.E. (1993) Comparison of the distribution of *Actinomyces* in dental plaque on inserted enamel on natural tooth surfaces in periodontal health and disease. Oral Microbiol. Immunol. 8, 5–15.
[21] Devoyod, J.J. and Poullain, F. (1988) The Leuconostocs characteristics. Their role in dairy technology. Lait 68, 249–280.
[22] Escher, A. and Characklis, W.G. (1990) Modeling the initial events in biofilm accumulation. In: Biofilms (Characklis, W.G. and Marshall, K.C., Eds.), pp. 445–486. John Wiley and Sons, New York.
[23] Van Loosdrecht, M.C.M., Lyklema, J., Norde, W. and Zehnder, A.J.B. (1990) Influences of interfaces on microbial activity. Microbiol. Rev. 54, 75–87.
[24] Gristina, A.G. (1987) Biomaterial-centered infection, microbial vs tissue integration. Science 237, 1588–1597.
[25] Schneider, R.P. and Marshall, K.C. (1994) Retention of the Gram-negative marine bacterium SW8 on surfaces – effects of microbial physiology, substratum nature and conditioning films. Colloids Surfaces B Biointerfaces 2, 387–396.
[26] Dufrêne, Y.F., Boonaert, C.P.J. and Rouxhet, P.G. (1996) Adhesion of *Azospirillum brasilense*, role of proteins at the cell-support interface. Colloids Surfaces B Biointerfaces 7, 113–128.
[27] Neu, T.R. and Marshall, K.C. (1990) Bacterial polymers: Physico-chemical aspects of their interactions at interfaces. J. Biomater. Appl. 5, 107–133.
[28] Bradshaw, D.J., Marsh, P.D., Watson, G.K. and Allison, C. (1997) Effect of conditioning films on oral microbial biofilm development. Biofouling 11, 217–226.
[29] Busscher, H.J., Doornbusch, G.I. and Van der Mei, H.C. (1992) Adhesion of mutans streptococci to glass with and without a salivary coating as studied in a parallel plate flow chamber. J. Dent. Res. 71, 491–500.
[30] Busscher, H.J. and Van der Mei, H.C. (1995) Use of flow chamber devices and image analysis methods to study microbial adhesion. In: Methods in Enzymology, Adhesion of Mi-

crobial Pathogens, Vol. 253 (Doyle, R.J. and Ofek, I., Eds.), pp. 455–477. Academic Press, San Diego, CA.
[31] Busscher, H.J., Noordmans, J., Meinders, J. and Van der Mei, H.C. (1991) Analysis of the spatial arrangement of microorganisms adhering to solid surfaces – methods of presenting results. Biofouling 4, 71–79.
[32] Dabros, T. (1989) Interparticle hydrodynamic interactions in deposition processes. Colloids Surfaces 39, 127–141.
[33] Bos, R., Van der Mei, H.C. and Busscher, H.J. (1995) A quantitative method to study co-adhesion of microorganisms in a parallel plate flow chamber. II: Analysis of the kinetics of co-adhesion. J. Microbiol. Methods 23, 169–182.
[34] Ellen, R.P., Veisman, H., Buivids, I.A. and Rosenberg, M. (1994) Kinetics of lactose-reversible coadhesion of *Actinomyces naeslundii* WVU 398A and *Streptococcus oralis* 34 on the surface of hexadecane droplets. Oral Microbiol. Immunol. 9, 364–371.
[35] Lamont, R.J. and Rosan, B. (1990) Adherence of mutans streptococci to other oral bacteria. Infect. Immun. 58, 1738–1743.
[36] Liljemark, W.F., Bloomquist, C.G., Coulter, M.C., Fenner, L.J., Skopek, R.J. and Schachtele, C.F. (1988) Utilization of a continuous streptococcal surface to measure interbacterial adherence in vitro and in vivo. J. Dent. Res. 67, 1455–1460.
[37] Rosenberg, E. (1986) Microbial surfactants. CRC Crit. Rev. Biotechnol. 3, 109–131.
[38] Velraeds, M.M.C., Van der Mei, H.C., Reid, G. and Busscher, H.J. (1996) Inhibition of initial adhesion of uropathogenic *Enterococcus faecalis* by biosurfactants from Lactobacillus isolates. Appl. Environ. Microbiol. 62, 1958–1963.
[39] Bradshaw, D.J., Homer, K.A., Marsh, P.D. and Beighton, D. (1994) Metabolic cooperation in oral microbial communities during growth on mucin. Microbiology 140, 3407–3412.
[40] Fletcher, M., Lessmann, J.M. and Loeb, G.I. (1991) Bacterial surface adhesives and biofilm matrix polymers of marine and freshwater bacteria. Biofouling 4, 129–140.
[41] Rittmann, B.E. (1989) Detachment from biofilms. In: Structure and Function of Biofilms (Characklis, W.G. and Wilderer, P.A., Eds.), pp. 49–58. John Wiley and Sons, Chichester.
[42] Boulangé-Petermann, L., Rault, J. and Bellon-Fontaine, M.N. (1997) Adhesion of *Streptococcus thermophilus* to stainless steel with different surface topography and roughness. Biofouling 11, 201–216.
[43] Quirynen, M. and Bollen, C.M. (1995) The influence of surface roughness and surface-free energy on supra- and subgingival plaque formation in man. A review of the literature. J. Clin. Periodontol. 22, 1–14.
[44] Busscher, H.J. and Van der Mei, H.C. (1997) Physico-chemical interactions in initial microbial adhesion and relevance for biofilm formation. Adv. Dent. Res. 11, 24–32.
[45] Reid, G., Van der Mei, H.C. and Busscher, H.J. (1998) Microbial biofilms and urinary tract infections, submitted. In: Urinary Tract Infections (Brumfitt, W., Hamilton-Miller, T. and Bailey, R.R., Eds.), pp. 111–118. Chapman and Hall, London.
[46] Taylor, J.H. and Holah, J.T. (1996) A comparitive evaluation with respect to the bacterial cleanability of a range of wall and floor surface materials used in the food industry. J. Appl. Bacteriol. 81, 262–266.
[47] Jansen, B. and Kohnen, W. (1995) Prevention of biofilm formation by polymer modification. J. Ind. Microbiol. 15, 391–396.
[48] Van Hoogmoed, C.G., Van der Mei, H.C. and Busscher, H.J. (1997) The influence of calcium on the initial adhesion of *S. thermophilus* to stainless steel under flow studied by metallurgical microscopy. Biofouling 11, 167–176.
[49] Korber, D.R., Choi, A., Wolfaardt, G.M., Ingham, S.C. and Caldwell, D.E. (1997) Substratum topography influences susceptibility of *Salmonella enteritidis* biofilms to trisodium phosphate. Appl. Environ. Microbiol. 63, 3352–3358.
[50] Kolenbrander, P.E. (1988) Intergeneric coaggregation among human oral bacteria and ecology of dental plaque. Annu. Rev. Microbiol. 42, 627–656.
[51] Reid, G., McGroarty, J.A., Angotti, R. and Cook, R.L. (1988) Lactobacillus inhibitor production against *Escherichia coli* and coaggregation ability with uropathogens. Can. J. Microbiol. 34, 344–351.
[52] Reid, G. and Bruce, A.W. (1995) The role of the urogenital flora in probiotics. In: Microbial Biofilms (Lappin-Scott, H.M. and Costerton, J.W., Eds.), pp. 274–281. Cambridge University Press, Cambridge.
[53] Buswell, C.M., Herlihy, Y.M., Marsh, P.D., Keevil, C.W. and Leach, S.A. (1997) Coaggregation amongst aquatic biofilm bacteria. J. Appl. Microbiol. 83, 477–484.
[54] Gibbons, R.J. and Nygaard, M. (1970) Interbacterial aggregation of plaque bacteria. Arch. Oral Biol. 15, 1397–1400.
[55] Kolenbrander, P.E. (1989) Surface recognition among oral bacteria, multigeneric coaggregations and their mediators. Crit. Rev. Microbiol. 17, 137–159.
[56] Jones, S.J. (1972) A special relationship between spherical and filamentous microorganisms in mature human dental plaque. Arch. Oral Biol. 17, 613–616.
[57] Cisar, J.O., Kolenbrander, P.E. and McIntire, F.C. (1979) Specificity of coaggregation reactions between human oral streptococci and strains of *Actinomyces viscosus* or *Actinomyces naeslundii*. Infect. Immun. 24, 742–752.
[58] Kolenbrander, P.E. and London, J. (1992) Ecological significance of coaggregation among oral bacteria. In: Advances in Microbial Ecology, Vol. 12. (Marshall, K.C., Ed.), pp. 183–217. Plenum Press, New York.
[59] Van Oss, C.J. (1994) Polar or Lewis acid-base interactions. In: Interfacial Forces in Aqueous Media, pp. 18–46. Marcel Dekker, New York.
[60] Van Oss, C.J. (1995) Hydrophobic, hydrophilic and other interactions in epitope-paratope binding. Mol. Immunol. 32, 199–211.
[61] Busscher, H.J., Cowan, M.M. and Van der Mei, H.C. (1992) On the relative importance of specific and non-specific approaches to oral microbial adhesion. FEMS Microbiol. Rev. 88, 199–210.
[62] Busscher, H.J. and Weerkamp, A.H. (1987) Specific and non-specific interactions in bacterial adhesion to solid substrata. FEMS Microbiol. Rev. 46, 165–173.

[63] Van Oss, C.J. (1990) Aspecific and specific intermolecular interactions in aqueous media. J. Mol. Recognit. 3, 128–136.
[64] Van Oss, C.J. (1995) Hydrophobicity of biosurfaces – origin, quantitative determination and interaction energies. Colloids Surfaces B Biointerfaces 5, 91–110.
[65] Handley, P.S. (1990) Structure, composition and function of surface structures on oral bacteria. Biofouling 2, 239–264.
[66] Absolom, D.R., Lamberti, F.V., Policova, Z., Zingg, W., Van Oss, C.J. and Neumann, A.W. (1983) Surface thermodynamics of bacterial adhesion. Appl. Environ. Microbiol. 46, 90–97.
[67] Busscher, H.J., Weerkamp, A.H., Van der Mei, H.C., Van Pelt, A.W.J., De Jong, H.P. and Arends, J. (1984) Measurement of the surface free energy of bacterial cell surfaces and its relevance for adhesion. Appl. Environ. Microbiol. 48, 980–983.
[68] Rutter, P.R. and Vincent, B. (1980) The adhesion of microorganisms to surfaces, physico-chemical aspects. In: Microbial Adhesion to Surfaces (Berkeley, R.C.W., Lynch, J.M., Melling, J., Rutter, P.R. and Vincent, B., Eds.), pp. 79–91. Ellis Horwood, London.
[69] Tadros, Th.F. (1980) Particle-surface adhesion. In: Microbial Adhesion to Surfaces (Berkeley, R.C.W., Lynch, J.M., Melling, J., Rutter, P.R. and Vincent, B., Eds.), pp. 93–113. Ellis Horwood, London.
[70] Van Loosdrecht, M.C.M., Lyklema, J., Norde, W. and Zehnder, A.J.B. (1989) Bacterial adhesion: A physicochemical approach. Microb. Ecol. 17, 1–15.
[71] Van Oss, C.J., Good, R.J. and Chaudhury, M.K. (1986) The role of van der Waals forces and hydrogen bonds in 'hydrophobic interactions' between biopolymers and low energy surfaces. J. Colloid Interface Sci. 111, 378–390.
[72] Van Oss, C.J., Good, R.J. and Chaudhury, M.K. (1988) Additive and nonadditive surface tension components and the interpretation of contact angles. Langmuir 4, 884–891.
[73] Wood, J. and Sharma, R. (1995) How long is the long-range hydrophobic attraction? Langmuir 11, 4797–4802.
[74] Elimelech, M. (1990) Indirect evidence for hydration forces in the deposition of polystyrene latex colloids on glass surfaces. J. Chem. Soc. Faraday Trans. 86, 1623–1624.
[75] Pashley, R.M. and Israelachvili, J.N. (1984) DLVO and hydration forces between mica surfaces in Mg^{2+}, Ca^{2+}, Sr^{2+} and Ba^{2+} chloride solutions. J. Colloid Interface Sci. 97, 446–455.
[76] Bellon-Fontaine, M.N., Mozes, N., Van der Mei, H.C., Sjollema, J., Cerf, O., Rouxhet, P.G. and Busscher, H.J. (1990) A comparison of thermodynamic approaches to predict the adhesion of dairy microorganisms to solid substrata. Cell Biophys. 17, 93–106.
[77] Van Oss, C.J. and Gillman, C.F. (1972) Phagocytosis as a surface phenomenon. I. Contact angles and phagocytosis of non-opsonized bacteria. J. Reticulocyte Soc. 12, 283–292.
[78] Neumann, A.W., Good, R.J., Hope, C.J. and Sejpal, M. (1974) An equation-of-state approach to determine surface tensions of low-energy solids from contact angles. J. Colloid Interface Sci. 49, 291–304.
[79] Neumann, A.W., Absolom, D.R., Francis, D.W. and Van Oss, C.J. (1980) Conversion tables of contact angles to surface tension. Sep. Purif. Methods 9, 69–163.
[80] Spelt, J.K., Li, D. and Neumann, A.W. (1992) The equation of state approach to interfacial tensions. In: Modern Approaches to Wettability – Theory and Application (Schrader, M.E. and Loeb, G.I., Eds.), pp. 101–142. Plenum Press, New York.
[81] Dann, J.R. (1970) Forces involved in the adhesive process. I. Critical surface tensions of polymeric solids as determined with polar liquids. J. Colloid Interface Sci. 32, 302–320.
[82] Dann, J.R. (1970) Forces involved in the adhesive process. II. Nondispersion forces at solid-liquid interfaces. J. Colloid Interface Sci. 32, 321–331.
[83] Owens, D.K. and Wendt, R.C. (1969) Estimation of the surface free energy of polymers. J. Appl. Polymer Sci. 13, 1741–1747.
[84] Wu, S. (1973) Polar and nonpolar interactions in adhesion. J. Adhes. 5, 39–55.
[85] Busscher, H.J., Van Pelt, A.W.J., De Jong, H.P. and Arends, J. (1983) Effect of spreading pressure on surface free energy determinations by means of contact angle measurements. J. Colloid Interface Sci. 95, 23–27.
[86] Good, R.J. and Van Oss, C.J. (1992) The modern theory of contact angles and the hydrogen bond components of surface energies. In: Modern Approaches to Wettability – Theory and Application (Schrader, M.E. and Loeb, G.I., Eds.), pp. 1–28. Plenum Press, New York.
[87] Derjaguin, B.V., Churaev, N.V. and Muller, V.M. (1987) The structure of boundary layers of liquids and the structural component of disjoining pressure. In: Surface Forces, pp. 231–291. Consultants Bureau, Plenum Press, New York.
[88] Ducker, W.A., Xu, Z. and Israelachvili, J.N. (1994) Measurements of hydrophobic and DLVO forces in bubble-surface interactions in aqueous solutions. Langmuir 10, 3279–3289.
[89] Ryan, J.N. and Elimelech, M. (1996) Colloid mobilization and transport in groundwater. Colloids Surfaces A Physicochem. Eng. Asp. 107, 1–56.
[90] Rijnaarts, H.H.M., Norde, W., Bouwer, E.J., Lyklema, J. and Zehnder, A.J.B. (1995) Reversibility and mechanisms of bacterial adhesion. Colloids Surfaces B Biointerfaces 4, 5–22.
[91] Nir, S. (1976) Van der Waals interactions between surfaces of biological interest. Prog. Surface Sci. 8, 1–58.
[92] Mafu, A.A., Roy, D., Goulet, J. and Savoie, L. (1991) Characterization of physicochemical forces involved in adhesion of *Listeria monocytogenes* to surfaces. Appl. Environ. Microbiol. 57, 1969–1973.
[93] Rijnaarts, H.H.M., Norde, W., Lyklema, J. and Zehnder, A.J.B. (1995) The isoelectric point of bacteria as an indicator for the presence of cell surface polymers that inhibit adhesion. Colloids Surfaces B Biointerfaces 4, 191–197.
[94] Van der Mei, H.C., De Vries, J. and Busscher, H.J. (1993) Hydrophobic and electrostatic cell surface properties of thermophilic dairy streptococci. Appl. Environ. Microbiol. 59, 4305–4312.
[95] Bos, R., Van der Mei, H.C., De Vries, J. and Busscher, H.J. (1996) The role of physico-chemical and structural surface properties in co-adhesion of microbial pairs in a parallel plate flow chamber. Colloids Surfaces B Biointerfaces 7, 101–112.
[96] Visser, J. (1973) The Adhesion of Colloidal Particles to a

Planar Surface in Aqueous Solutions, pp. 1–108. Thesis, Council for National Academic Awards, London.
[97] Rosenberg, M., Rosenberg, E., Judes, H. and Weiss, E. (1983) Bacterial adherence to hydrocarbons and to surfaces in the oral cavity. FEMS Microbiol. Lett. 20, 1–5.
[98] Lichtenberg, D., Rosenberg, M., Scharfman, M. and Ofek, I. (1985) A kinetic approach to bacterial adherence to hydrocarbons. FEMS Microbiol. Lett. 4, 141–146.
[99] Busscher, H.J., Van de Belt-Gritter, B. and Van der Mei, H.C. (1995) Implications of microbial adhesion to hydrocarbons for evaluating cell surface hydrophobicity 1. Zeta potentials of hydrocarbon droplets. Colloids Surfaces B Biointerfaces 5, 111–116.
[100] Geertsema-Doornbusch, G.I., Van der Mei, H.C. and Busscher, H.J. (1993) Microbial cell surface hydrophobicity – The involvement of electrostatic interactions in microbial adhesion to hydrocarbons (MATH). J. Microbiol. Methods 18, 61–68.
[101] Van der Mei, H.C., Van de Belt-Gritter, B. and Busscher, H.J. (1995) Implications of microbial adhesion to hydrocarbons for evaluating cell surface hydrophobicity 2. Adhesion mechanisms. Colloids Surfaces B Biointerfaces 5, 116–126.
[102] Bellon-Fontaine, M.N., Rault, J. and Van Oss, C.J. (1996) Microbial adhesion to solvents, a novel method to determine the electron-donor/electron acceptor or Lewis acid-base properties of microbial cells. Colloids Surfaces B Biointerfaces 7, 47–53.
[103] Liu, Y. (1995) Adhesion kinetics of nitrifying bacteria on various thermoplastic supports. Colloids Surfaces B Biointerfaces 5, 213–219.
[104] Wirtanen, G., Alanko, T. and Mattila-Sandholm, T. (1996) Evaluation of epifluoresence image analysis of biofilm growth on stainless steel surfaces. Colloids Surfaces B Biointerfaces 5, 319–326.
[105] Leenaars, A.F.M. (1988) A new approach to the removal of sub-micron particles from solid (silicon) substrates. In: Particles on Surfaces, Detection, Adhesion and Removal, Vol. 1 (Mittal, K.L., Ed.), pp. 361–372. Plenum Press, New York.
[106] Leenaars, A.F.M. and O'Brien, S.B.G. (1989) Particle removal from silicon substrates using surface tension forces. Philips J. Res. 44, 183–209.
[107] Visser, J. (1976) Adhesion of colloidal particles. In: Surface and Colloid Science, Vol. 8 (Marijevic, E., Ed.), pp. 3–84. John Wiley and Sons, New York.
[108] Rutter, P.R. and Vincent, B. (1988) Attachment mechanisms in the surface growth of microorganisms. In: Physiological Models in Microbiology (Bazin, M.J. and Prosser, J.I., Eds.), pp. 87–107. CRC Press, Boca Raton, FL.
[109] Clark, W.B., Bammann, L.L. and Gibbons, R.J. (1978) Comparative estimates of bacterial affinities and adsorption sites on hydroxyapatite surfaces. Infect. Immun. 19, 846–853.
[110] Wassall, M.A., Embery, G. and Bagg, J. (1995) The role of hydrophobicity in *Streptococcus sanguis* and *Streptococcus salivarius* adhesion to salivary fraction-coated hydroxyapatite. Colloids Surfaces B Biointerfaces 5, 143–152.
[111] Lytle, M.S., Adams, J.C., Dickman, D.G. and Bressler, W.R. (1989) Use of nutrient response techniques to assess the effectiveness of chlorination of rapid sand filter gravel. Appl. Environ. Microbiol. 55, 29–32.
[112] Elimelech, M. (1995) Experimental techniques in particle deposition kinetics. In: Particle Deposition and Aggregation. Measurement, Modelling and Simulation (Elimelech, M., Gregory, J., Jia, X. and Williams, R., Eds.), pp. 290–309. Hartnolls, Bodmin.
[113] Cunningham, A.B., Brouwer, E.J. and Characklis, W.G. (1990) Biofilms in porous media. In: Biofilms (Characklis, W.G. and Marshall, K.C., Eds.), pp. 697–732. John Wiley and Sons, New York.
[114] Bryers, J.D. (1990) Biofilms in biotechnology. In: Biofilms (Characklis, W.G. and Marshall, K.C., Eds.), pp. 733–773. John Wiley and Sons, New York.
[115] Dabros, T. and Van de Ven, T.G.M. (1987) Deposition of latex particles on glass surfaces in an impinging jet. Phys. Chem. Hydrodyn. 8, 161–172.
[116] Dickinson, R.B., Nagel, J.A., McDevitt, D., Foster, T.J., Proctor, R.A. and Cooper, S.L. (1995) Quantitative comparison of clumping factor- and coagulase-mediated *Staphylococcus aureus* adhesion to surface-bound fibrinogen under flow. Infect. Immun. 63, 3143–3150.
[117] Christersson, C.E., Fornalik, M.S., Baier, R.E. and Glantz, P.O. (1987) In vitro attachment of oral microorganisms to solid surfaces: Evaluation of a controlled flow method. Scand. J. Dent. Res. 95, 151–158.
[118] Sjollema, J., Busscher, H.J. and Weerkamp, A.H. (1989) Real-time enumeration of adhering microorganisms in a parallel plate flow cell using automated image analysis. J. Microbiol. Methods 9, 73–78.
[119] Abbott, A., Berkeley, R.C.W. and Rutter, P.R. (1980) Sucrose and the deposition of *Streptococcus mutans* at solid liquid interfaces. In: Microbial Adhesion to Surfaces (Berkeley, R.C.W., Lynch, J.M., Melling, J., Rutter, P.R. and Vincent, B., Eds.), pp. 117–142. Ellis Horwood, Chichester.
[120] Mueller, R.F., Characklis, W.G., Jones, W.L. and Sears, J.T. (1992) Characterization of initial events in bacterial surface colonization by two *Pseudomonas* species using image analysis. Biotechnol. Bioeng. 39, 1161–1170.
[121] Li, J. and Ellen, R.P. (1990) Coaggregation of *Porphyromonas (Bacteroides) gingivalis* other species of bacteroides and *Actinomyces viscosus*, methodological evaluation. J. Microbiol. Methods 12, 91–96.
[122] Handley, P.S., Harty, D.W.S., Wyatt, J.E., Brown, C.R., Doran, J.P. and Gibbs, A.C.C. (1987) A comparison of the adhesion, coaggregation and cell-surface hydrophobicity properties of fibrillar and fimbriate strains of *Streptococcus salivarius*. J. Gen. Microbiol. 133, 3207–3217.
[123] Kagermeier, A.S., London, J. and Kolenbrander, P.E. (1984) Evidence for the participation of N-acetylated amino sugars in the coaggregation between *Cytophaga* species strain DR2001 and *Actinomyces israelii* PK16. Infect. Immun. 44, 299–305.
[124] Mizuno, J., Cisar, J.O., Vatter, A.E., Fennessey, P.V. and McIntire, F.C. (1983) A factor from *Actinomyces viscosus* T14V that specifically aggregates *Streptococcus sanguis* H1. Infect. Immun. 40, 1204–1213.

[125] Ericson, T., Pruitt, K. and Wedel, H. (1975) The reaction of salivary substances with bacteria. J. Oral Pathol. 4, 307–323.
[126] Koop, H.M., Valentijn-Benz, M., Nieuw Amerongen, A.V., Roukema, P.A. and De Graaff, J. (1989) Aggregation of 27 oral bacteria by human whole saliva. Influence of culture medium, calcium, and bacterial cell concentration, and interference by autoaggregation. Antonie van Leeuwenhoek 55, 277–290.
[127] Ligtenberg, A.J.M. (1992) Intervention of Saliva in the Colonization Process of Oral Bacteria. Ph.D. Thesis, Free University of Amsterdam, Amsterdam.
[128] Rijnaarts, H.H.M., Norde, W., Bouwer, E.J., Lyklema, J. and Zehnder, A.J.B. (1993) Bacterial adhesion under static and dynamic conditions. Appl. Environ. Microbiol. 59, 3255–3265.
[129] Meinders, J.M., Noordmans, J. and Busscher, H.J. (1992) Simultaneous monitoring of the adsorption and desorption of colloidal particles during deposition in a parallel plate flow chamber. J. Colloid Interface Sci. 152, 265–280.
[130] Meinders, J.M., Van der Mei, H.C. and Busscher, H.J. (1992) In situ enumeration of bacterial adhesion in a parallel plate flow chamber – elimination of in focus flowing bacteria from the analysis. J. Microbiol. Methods 16, 119–124.
[131] Sjollema, J. and Busscher, H.J. (1990) Deposition of polystyrene particles in a parallel plate flow cell. 2. Pair distribution functions between deposited particles. Colloids Surfaces 47, 337–352.
[132] Van Kooten, T.G., Schakenraad, J.M., Van der Mei, H.C. and Busscher, H.J. (1992) Development and use of a parallel-plate flow chamber for studying cellular adhesion to solid surfaces. J. Biomed. Mater. Res. 26, 725–738.
[133] McQueen, A. and Bailey, J.E. (1989) Influence of serum level, cell line, flow type, and viscosity on flow-induced lysis of suspended mammalian cells. Biotechnol. Lett. 11, 531–536.
[134] Pratt-Terpstra, I.H., Weerkamp, A.H. and Busscher, H.J. (1987) Adhesion of oral streptococci from a flowing suspension to uncoated and albumin-coated surfaces. J. Gen. Microbiol. 133, 3199–3206.
[135] Sjollema, J., Busscher, H.J. and Weerkamp, A.H. (1988) Deposition of oral streptococci and polystyrene latices onto glass in a parallel plate flow cell. Biofouling 1, 101–112.
[136] Bowen, B.D. (1985) Streaming potential in the hydrodynamic entrance region of cylindrical and rectangular capillaries. J. Colloid Interface Sci. 106, 367–376.
[137] Van Wagenen, R.J. and Andrade, J.D. (1980) Flat plate streaming potential investigations, hydrodynamics and electrokinetic equivalency. J. Colloid Interface Sci. 76, 305–314.
[138] Busnaina, A., Taylor, J. and Kashkoush, I. (1993) Measurement of the adhesion and removal forces of submicron particles on silicon substrates. J. Adher. Sci. Technol. 7, 441–455.
[139] Krishnan, S., Busnaina, A.A., Rimai, D.S. and Demejo, L.P. (1994) The adhesion-induced deformation and the removal of submicron particles. J. Adher. Sci. Technol. 8, 1357–1370.
[140] Busscher, H.J., Bellon-Fontaine, M.N., Mozes, N., Van der Mei, H.C., Sjollema, J., Cerf, O. and Rouxhet, P.G. (1990) Deposition of *Leuconostoc mesenteroides* and *Streptococcus thermophilus* to solid substrata in a parallel plate flow cell. Biofouling 2, 55–63.
[141] Brenner, H. (1961) The slow motion of a sphere through a viscous fluid towards a plane surface. Chem. Eng. Sci. 16, 242–251.
[142] Adamczyk, Z. and Van de Ven, T.G.M. (1981) Deposition of particles under external forces in laminar flow through parallel plate and cilindrical channels. J. Colloid Interface Sci. 80, 340–356.
[143] Bowen, B.D., Levine, S. and Epstein, N. (1976) Fine particles deposition in laminar flow through parallel plate and cylindrical channels. J. Colloid Interface Sci. 54, 375–390.
[144] Van der Mei, H.C., Meinders, J.M. and Busscher, H.J. (1994) The influence of ionic strength and pH on diffusion of microorganisms with different surface features. Microbiology 140, 3413–3419.
[145] Xia, Z., Woo, L. and Van de Ven, T.G.M. (1989) Microrheological aspects of adhesion of *Escherichia coli* on glass. Biorheology 23, 359–375.
[146] Dabros, T. and Van de Ven, T.G.M. (1982) Kinetics of coating by colloidal particles. J. Colloid Interface Sci. 89, 232–244.
[147] Schaaf, P. and Talbot, J. (1989) Surface exclusion effects in adsorption processes. J. Chem. Phys. 91, 4401–4409.
[148] Pratt-Terpstra, I.H., Weerkamp, A.H. and Busscher, H.J. (1988) On a relation between interfacial free energy-dependent and non-interfacial free energy-dependent adherence of oral streptococci to solid substrata. Curr. Microbiol. 16, 311–313.
[149] Pratt-Terpstra, I.H., Weerkamp, A.H. and Busscher, H.J. (1989) Microbial factors in a thermodynamic approach of oral streptococcal adhesion to solid substrata. J. Colloid Interface Sci. 129, 568–574.
[150] Nesbitt, W.E., Doyle, R.J., Taylor, K.G., Staat, R.H. and Arnold, R.R. (1982) Positive cooperativity in the binding of *Streptococcus sanguis* to hydroxylapatite. Infect. Immun. 35, 157–165.
[151] Van der Mei, H.C., Cox, S.D., Geertsema-Doornbusch, G.I., Doyle, R.J. and Busscher, H.J. (1993) A critical appraisal of positive cooperativity in oral streptococcal adhesion, Scatchard analyses of adhesion data versus analyses of the spatial arrangement of adhering bacteria. J. Gen. Microbiol. 139, 937–948.
[152] Dabros, T. and Van de Ven, T.G.M. (1983) On the effects of blocking and particle detachment on coating kinetics. J. Colloid Interface Sci. 93, 576–579.
[153] Meinders, J.M. and Busscher, H.J. (1993) Influence of interparticle interactions on blocked areas and desorption during particle deposition to glass in a parallel plate flow chamber. Langmuir 11, 327–333.
[154] Wiencek, K.M. and Fletcher, M. (1995) Bacterial adhesion to hydroxyl- and methyl-terminated alkanethiol self-assembled monolayers. J. Bacteriol. 177, 1959–1966.
[155] Meinders, J.M., Van der Mei, H.C. and Busscher, H.J. (1995) Deposition efficiency and reversibility of bacterial adhesion under flow. J. Colloid Interface Sci. 176, 329–341.
[156] Bryers, J.D. and Characklis, W.G. (1992) Biofilm accumulation and activity, a process analysis approach. In: Biofilms –

Science and Technology, NATO ASI Series E, Applied Sciences, Vol. 223 (Melo, L.F., Bott, T.R., Fletcher, M. and Capdeville, B., Eds.), pp. 221–237. Kluwer Academic, Dordrecht.

[157] Habash, M., Van der Mei, H.C., Reid, G. and Busscher, H.J. (1997) Adhesion of *Pseudomonas aeruginosa* to silicone rubber in the absence and presence of nutrient broth. Microbiology 143, 2569–2574.

[158] Doig, F., Lollar, B.S. and Ferris, F.G. (1995) Microbial communities in deep Canadian shield ground waters – An in situ biofilm experiment. Geomicrobiol. J. 13, 91–102.

[159] Urzi, C., Lisi, S., Criseo, G. and Pernice, A. (1991) Adhesion to and degradation of marble by *Micrococcus* strain isolated from it. Geomicrobiol. J. 9, 81–90.

[160] Mahieu, H.F., Van Saene, H.K.F., Rosingh, H.J. and Schutte, H.K. (1986) *Candida* vegetations on silicone voice protheses. Arch. Otolaryngol. 112, 321–325.

[161] Neu, T.R., De Boer, C.E., Verkerke, G.J., Schutte, H.K., Rakhorst, G., Van der Mei, H.C. and Busscher, H.J. (1994) Biofilm development in time on a silicone voice prosthesis – a case study. Microb. Ecol. Health Dis. 7, 27–33.

[162] Neu, T.R., Dijk, F., Verkerke, G.J., Van der Mei, H.C. and Busscher, H.J. (1992) Scanning electron microscopy study of biofilms on silicone voice prostheses. Cells Mater. 2, 261–269.

[163] Liesegang, T.J. (1997) Contactlens-related microbial keratitis. Part II: Pathophysiology. Cornea 16, 265–273.

[164] Elder, M.J., Stapleton, F., Evans, E. and Dart, J.K. (1995) Biofilm-related infections in ophthalmology. Eye 9, 102–109.

[165] Pitt, W.G., McBride, M.O., Barton, A.J. and Sagers, R.D. (1993) Air-water interface displaces adsorbed bacteria. Biomaterials 14, 605–608.

[166] Reid, G., Cuperus, P.L., Bruce, A.W., Van der Mei, H.C., Tomeczek, L., Khoury, A.H. and Busscher, H.J. (1992) Comparison of contact angles and adhesion to hexadecane of urogenital, dairy, and poultry lactobacilli, effect of serial culture passages. Appl. Environ. Microbiol. 58, 1549–1553.

[167] Burchard, R.P., Rittschoft, D. and Bonaventura, J. (1990) Adhesion and motility of gliding bacteria on substrata with different surface free energies. Appl. Environ. Microbiol. 56, 2529–2534.

[168] Liu, Z. and Papadopoulos, K. (1995) Unidirectional motility of *Escherichia coli* in restrictive capillaries. Appl. Environ. Microbiol. 61, 3567–3572.

[169] Morra, M. and Cassinelli, C. (1996) *Staphylococcus epidermidis* adhesion to films deposited from hydroxyethylmethacrylate plasma. J. Biomed. Mater. Res. 31, 149–155.

[170] Bos, R., Van der Mei, H.C. and Busscher, H.J. (1996) Particle deposition to protruding local sinks adhering on a collector surface. Langmuir 12, 3241–3244.

[171] Norde, W. and Lyklema, J. (1989) Protein adsorption and bacterial adhesion to solid surfaces: A colloid-chemical approach. Colloids Surfaces 38, 1–13.

[172] Lyklema, J., Norde, W., Van Loosdrecht, M.C.M. and Zehnder, A.J.B. (1989) Adhesion of bacteria to polystyrene surfaces. Colloids Surfaces 39, 175–187.

[173] Busscher, H.J., Uyen, M.H.W.J.C., Van Pelt, A.W.J., Weerkamp, A.H. and Arends, J. (1986) Kinetics of adhesion of the oral bacterium *S. sanguis* CH3 to polymers with different surface free energies. Appl. Environ. Microbiol. 51, 910–914.

[174] Cowan, M.M., Taylor, K.G. and Doyle, R.J. (1986) Kinetic analysis of *Streptococcus sanguis* adhesion to artificial pellicle. J. Dent. Res. 65, 1278–1283.

[175] Meinders, J.M., Van der Mei, H.C. and Busscher, H.J. (1994) Physicochemical aspects of deposition of *Streptococcus thermophilus* B to hydrophobic and hydrophilic substrata in a parallel plate flow chamber. J. Colloid Interface Sci. 164, 355–363.

[176] Nomura, S., Lundberg, F., Stollenwerk, M., Nakamura, K. and Ljungh, A. (1997) Adhesion of staphylococci to polymers with and without immobilized heparin in cerebrospinal fluid. J. Biomed. Mater. Res. 38, 35–42.

[177] Busscher, H.J., Uyen, M.H.W.J.C., Weerkamp, A.H., Postma, W.J. and Arends, J. (1986) Reversibility of adhesion of oral streptococci to solids. FEMS Microbiol. Lett. 35, 303–306.

[178] Van Pelt, A.W.J., Weerkamp, A.H., Uyen, H.M., Busscher, H.J., De Jong, H.P. and Arends, J. (1985) Adhesion of *Streptococcus sanguis* to polymers with different surface free energies. Appl. Environ. Microbiol. 49, 1270–1275.

[179] Uyen, H.M., Busscher, H.J., Weerkamp, A.H. and Arends, J. (1985) Surface free energies of oral streptococci and their adhesion to solids. FEMS Microbiol. Lett. 30, 103–106.

[180] Barton, A.J., Sagers, R.D. and Pitt, W.G. (1996) Bacterial adhesion to orthopedic implant polymers. J. Biomed. Mater. Res. 30, 403–410.

[181] Wang, I., Anderson, J.M., Jacobs, M.R. and Marchant, R.E. (1995) Adhesion of *Staphylococcus epidermidis* to biomedical polymers: Contributions of surface thermodynamics and thermodynamic shear conditions. J. Biomed. Mater. Res. 29, 485–493.

[182] Minagi, S., Miyake, Y., Inagaki, K., Tsuru, H. and Suginaka, H. (1985) Hydrophobic interaction in *Candida albicans* and *Candida tropicalis* adherence to various denture base resin materials. Infect. Immun. 47, 11–14.

[183] Van der Mei, H.C., Léonard, A.J., Weerkamp, A.H., Rouxhet, P.G. and Busscher, H.J. (1988) Surface properties of *Streptococcus salivarius* HB and non-fibrillar mutants, zeta potential and elemental composition using X-ray photoelectron spectroscopy. J. Bacteriol. 170, 2462–2466.

[184] Sjollema, J., Van der Mei, H.C., Uyen, H.M.W. and Busscher, H.J. (1990) The influence of collector and bacterial cell surface properties on the deposition of oral streptococci in a parallel plate flow cell. J. Adher. Sci. Technol. 4, 765–777.

[185] Van der Vegt, W., Van der Mei, H.C., Noordmans, J. and Busscher, H.J. (1991) Assessment of bacterial biosurfactant production through axisymmetric drop shape analysis by profile. Appl. Microbiol. Biotechnol. 35, 766–770.

[186] Desai, J.D. and Desai, A.J. (1993) Production of biosurfactants. In: Biosurfactants – Production, Properties, Application (Kosaric, N., Ed.), pp. 65–97. Marcel Dekker, New York.

[187] Neu, T.R. (1996) Significance of bacterial surface-active com-

pounds in interaction of bacterial with interfaces. Microbiol. Rev. 6, 151–166.
[188] Neu, T.R. and Marshall, K.C. (1991) Microbial 'footprints' – a new approach to adhesive polymers. Biofouling 3, 101–112.
[189] Etzler, F.M. and Fagundus, D.M. (1987) The extent of vicinal water. Implications from the density of water in silica pores. J. Colloid Interface Sci. 115, 513–519.
[190] Daffonchio, D., Thaveesri, J. and Verstraete, W. (1995) Contact angle measurement and cell hydrophobicity of granular sludge from upflow an aerobic sludge bed reactors. Appl. Environ. Microbiol. 61, 3676–3680.
[191] Kasahara, Y., Morisaki, H. and Hattori, T. (1993) Hydrophobicity of the cells of fast-and-slow growing bacteria isolated from a grassland soil. J. Gen. Appl. Microbiol. 39, 381–388.
[192] Oyston, P.C.F. and Handley, P.S. (1990) Surface structures, haemagglutination and cell surface hydrophobicity of *Bacteroides fragilis* strains. J. Gen. Microbiol. 136, 941–948.
[193] Van der Mei, H.C., Weerkamp, A.H. and Busscher, H.J. (1987) Physico-chemical surface characteristics and adhesive properties of *Streptococcus salivarius* strains with defined cell surface structures. FEMS Microbiol. Lett. 40, 15–19.
[194] Mozes, N., Marchal, F., Hermesse, M.P., Van Haecht, J.L., Reuliaux, L., Leonard, A.J. and Rouxhet, P.G. (1987) Immobilization of microorganisms by a support, interplay of electrostatic and non-electrostatic interactions. Biotechnol. Bioeng. 30, 439–450.
[195] Van der Mei, H.C. and Busscher, H.J. (1996) Detection by physio-chemical techniques of an amphiphilic surface component on *Streptococcus mitis* strains involved in non-electrostatic binding to surfaces. Eur. J. Oral Sci. 104, 48–55.
[196] Van Loosdrecht, M.C.M., Lyklema, J., Norde, W., Schraa, G. and Zehnder, A.J.B. (1987) The role of bacterial cell wall hydrophobicity in adhesion. Appl. Environ. Microbiol. 53, 1893–1897.
[197] Medrzycka, K.B. (1991) The effect of particle concentration on zeta potential in extremely dilute solutions. Colloid Polymer Sci. 269, 85–90.
[198] Takeuchi, T.L. and Suzuki, I. (1997) Cell surface hydrophobicity and sulfur adhesion of *Thiobacillus thiooxidans*. Appl. Environ. Microbiol. 63, 2058–2061.
[199] Kiely, L.J., Olson, N.F. and Mortensen, G. (1997) The physicochemical surface characteristics of *Brevibacterium linens*. Colloids Surfaces B Biointerfaces 9, 297–304.
[200] Pelletier, C., Bouley, C., Cayuela, C., Bouttier, S., Bourlioux, P. and Bellon-Fontaine, M.N. (1997) Cell surface characteristics of *Lactobacillus casei* subsp. *casei, Lactobacillus paracasei* subsp. *paracasei*, and *Lactobacillus rhamnosus* strains. Appl. Environ. Microbiol. 63, 1725–1731.
[201] Morisaki, H., Nakagawa, K. and Shiraishi, H. (1996) Measurement of attachment force of microbial cells. Colloids Surfaces B Biointerfaces 6, 347–352.
[202] Morisaki, H. (1991) Measurement of the force necessary for removal of bacterial cells from a quartz plate. J. Gen. Microbiol. 137, 2649–2655.
[203] Van der Mei, H.C., Brokke, P., Dankert, J., Feijen, J. and Busscher, H.J. (1992) Influence of electrostatic interactions on the deposition efficiencies of coagulase-negative staphylococci to collector surfaces in a parallel plate flow chamber. J. Disp. Sci. Technol. Biocoll. Biosurf. 13, 447–458.
[204] Hancock, I.C. (1989) Encapsulation of coagulase-negative staphylococci. Int. J. Med. Microbiol. 272, 11–18.
[205] Muller, E., Takeda, S., Hiro, H., Goldmann, D. and Pier, G.B. (1993) Occurrence of capsular polysaccharide/adhesin among clinical isolates of coagulase-negative staphylococci. J. Infect. Dis. 168, 1211–1218.
[206] Uyen, H.M., Van der Mei, H.C., Weerkamp, A.H. and Busscher, H.J. (1988) Comparison between the adhesion to solid substrata of *Streptococcus mitis* and that of polystyrene particles. Appl. Environ. Microbiol. 54, 837–838.
[207] Satou, J., Fukunaga, A., Satou, N., Sintani, H. and Okuda, K. (1988) Streptococcal adherence on various dental materials. J. Dent. Res. 67, 588–591.
[208] Achouak, W., Thomas, F. and Heulin, T. (1994) Physicochemical surface properties of rhizobacteria and their adhesion to rice roots. Colloids Surfaces B Biointerfaces 3, 131–137.
[209] Vigeant, M.A.S. and Ford, R.M. (1997) Interactions between motile *Escherichia coli* and glass in media with various ionic strengths, as observed with a three-dimensional tracking microscope. Appl. Environ. Microbiol. 63, 3474–3479.
[210] Cowan, M.M., Mikx, F.H.M. and Busscher, H.J. (1994) Electrophoretic mobility and hemagglutination of *Treponema denticola* ATCC33520. Colloids Surfaces B Biointerfaces 2, 407–410.
[211] Zita, A. and Hermansson, M. (1997) Effects of bacterial cell surface structures and hydrophobicity on attachment to activated sludge flocs. Appl. Environ. Microbiol. 63, 1168–1170.
[212] Jucker, B.A., Harms, H. and Zehnder, A.J.B. (1996) Adhesion of the positively charged bacterium *Stenotrophomona (Xanthomonas) maltophilia* 70401 to glass and Teflon. J. Bacteriol. 178, 5472–5479.
[213] Van Dijk, L.J., Goldsweer, R. and Busscher, H.J. (1988) Interfacial free energy as a driving force for pellicle formation in the oral cavity: An in vivo study in beagle dogs. Biofouling 1, 19–25.
[214] Dickinson, R.B., Nagel, J.A., Proctor, R.A. and Cooper, S.L. (1997) Quantitative comparison of shear-dependent *Staphylococcus aureus* adhesion to three polyurethane ionomer analogs with distinct surface properties. J. Biomed. Mater. Res. 36, 152–162.
[215] Pratt-Terpstra, I.H. and Busscher, H.J. (1991) Adsorption of salivary mucins onto enamel and artificial solid substrata and its influence on oral streptococcal adhesion. Biofouling 3, 199–207.
[216] Elam, J.H. and Nygren, H. (1992) Adsorption of coagulation proteins from whole blood on to polymer materials: Relation to platelet activation. Biomaterials 13, 3–8.
[217] Fabrizius-Homan, D.J. and Cooper, S.L. (1991) A comparison of the adsorption of three adhesive proteins to biomaterials surfaces. J. Biomater. Sci. Polymer Edn. 3, 27–48.
[218] Ziats, N.P., Pankowsky, D.A., Tierney, B.P., Ratnoff, O.D. and Anderson, J.M. (1990) Adsorption of Hageman factor

(factor XII) and other human plasma proteins to biomedical polymers. J. Lab. Clin. Med. 116, 687–696.
[219] Busscher, H.J., Bos, R. and Van der Mei, H.C. (1995) Initial microbial adhesion is a determinant for the strength of biofilm adhesion. FEMS Microbiol. Lett. 128, 229–234.
[220] Busscher, H.J., Geertsema-Doornbusch, G.I. and Van der Mei, H.C. (1997) Adhesion to silicone rubber of yeasts and bacteria isolated from voice prostheses – influence of salivary conditioning films. J. Biomed. Mater. Res. 34, 201–210.
[221] Landa, A.S., Van der Mei, H.C. and Busscher, H.J. (1996) A comparison of the detachment of an adhering oral streptococcal strain stimulated by mouthrinses and a prebrushing rinse. Biofouling 9, 327–339.
[222] Millsap, K.W., Reid, G., Van der Mei, H.C. and Busscher, H.J. (1996) Adhesion of *Lactobacillus* species in urine and phosphate buffer to silicone rubber and glass under flow. Biomaterials 18, 87–91.
[223] Van Raamsdonk, M., Van der Mei, H.C., Geertsema-Doornbusch, G.I., De Soet, J.J., Busscher, H.J. and De Graaff, J. (1995) Physicochemical aspects of microbial adhesion - influence of antibody adsorption on the deposition of *Streptococcus sobrinus* in a parallel plate flow chamber. Colloids Surfaces B Biointerfaces 4, 401–410.
[224] Christersson, C.E., Glantz, P.O. and Baier, R.E. (1988) Role of temperature and shear force on microbial detachment. Scand. J. Dent. Res. 96, 91–98.
[225] Quirynen, M., Marechal, M., Busscher, H.J., Weerkamp, A.H., Arends, J., Darius, P.L. and Van Steenberghe, D. (1989) The influence of surface free energy on planimetric plaque growth in man. J. Dent. Res. 68, 796–799.
[226] Quirynen, M., Van der Mei, H.C., Bollen, C.M.L., Geertsema-Doornbusch, G.I., Busscher, H.J. and Van Steenberghe, D. (1994) Clinical relevance of the influence of surface free energy and roughness on the supragingival and subgingival plaque formation in man. Colloids Surfaces B Biointerfaces 2, 25–31.
[227] Glantz, P.O. (1971) The adhesiveness of teeth. J. Colloid Interface Sci. 37, 281–290.
[228] Everaert, E.P.J.M., Mahieu, H.F., Wong Chung, R.P., Verkerke, G.J., Van der Mei, H.C. and Busscher, H.J. (1997) A new method for in vivo evaluation of biofilms on surface modified silicone rubber voice prostheses. Eur. Arch. Oto-Rhino-Laryngol. 254, 261–263.
[229] Taylor, G.T., Zheng, D., Lee, M., Troy, P.J., Gyananath, G. and Sharma, S.K. (1997) Influence of surface properties on accumulation of conditioning films and marine bacteria on substrata exposed to oligotrophic waters. Biofouling 11, 31–57.
[230] Handley, P.S. (1991) Negative staining. In: Microbial Cell Surface Analysis – Structural and Physicochemical Methods (Mozes, N., Handley, P.S., Busscher, H.J. and Rouxhet, P.G., Eds.), pp. 63–86. VCH Publishers, New York.
[231] Busscher, H.J., Handley, P.S., Rouxhet, P.G., Hesketh, L.M. and Van der Mei, H.C. (1991) The relationship between structural and physico-chemical surface properties of tufted *Streptococcus sanguis* strains. In: Microbial Cell Surface Analysis – Structural and Physicochemical Methods (Mozes, N., Handley, P.S., Busscher, H.J. and Rouxhet, P.G., Eds.), pp. 317–338. VCH Publishers, New York.
[232] Bendinger, B., Rijnaarts, H.H.M., Altendorf, K. and Zehnder, A.J.B. (1993) Physicochemical cell surface and adhesive properties of coryneform bacteria related to the presence and chain length of mycolic acids. Appl. Environ. Microbiol. 59, 3973–3977.
[233] Harkes, G., Van der Mei, H.C., Rouxhet, P.G., Dankert, J., Busscher, H.J. and Feijen, J. (1992) Physico-chemical characterization of *Escherichia coli* – A comparison with Gram-positive bacteria. Cell Biophys. 20, 17–32.
[234] Thaveesri, J., Daffonchio, D., Liessens, B., Vandermeren, P. and Verstraete, W. (1995) Granulation and sludge bed stability in upflow anaerobic sludge bed reactors in relation to surface thermodynamics. Appl. Environ. Microbiol. 61, 3681–3686.
[235] Jenkinson, H.F., Lala, H.C. and Shepherd, M.G. (1990) Coaggregation of *Streptococcus sanguis* and other streptococci with *Candida albicans*. Infect. Immun. 58, 1429–1436.
[236] Cookson, A.L., Handley, P.S., Jacob, A.E., Watson, G.K. and Allison, C. (1995) Coaggregation between *Prevotella nigrescens* and *Prevotella intermedia* with *Actinomyces naeslundii* strains. FEMS Microbiol. Lett. 132, 291–296.
[237] Weerkamp, A.H., Handley, P.S., Baars, A. and Slot, J.W. (1986) Negative staining and immunoelectron microscopy of adhesion-deficient mutants of *Streptococcus salivarius* reveal that the adhesive protein antigens are separate classes of cell surface fibrils. J. Bacteriol. 165, 746–755.
[238] Weiss, E.I., London, J., Kolenbrander, P.E., Hand, A.R. and Siraganian, R. (1988) Localization and enumeration of fimbria-associated adhesins of *Bacteroides loescheii*. J. Bacteriol. 170, 1123–1128.
[239] Willcox, M.D. and Drucker, D.B. (1989) Surface structures, coaggregation and adherence phenomena of *Streptococcus oralis* and related species. Microbios 59, 19–29.
[240] Yellohi Roa, M.K., Somasundaran, P., Schilling, K.M., Carson, R. and Ananthapadmanabhan, K.P. (1995) Electrokinetic properties of *Streptococcus sanguis* and *Actinomyces naeslundii*. Colloids Surfaces B Biointerfaces 4, 87–95.
[241] Handley, P.S., Carter, P.L., Wyatt, J.E. and Hesketh, L.M. (1985) Surface structures (peritrichous fibrils and tufts of fibrils) found on *Streptococcus sanguis* strains may be related to their ability to coaggregate with other oral genera. Infect. Immun. 47, 217–227.
[242] Hazen, K.C. (1995) New and emerging yeast pathogens. Clin. Microbiol. Rev. 8, 462–478.
[243] Fouche, M.H., Slabbert, J.C.G. and Coogan, M.M. (1986) Microorganisms isolated from patients with denture stomatitis. J. Dent. Assoc. South Afr. 41, 313–316.
[244] Theilade, E. and Budtz-Jorgensen, E. (1988) Predominant cultiviable microflora of plaque on removable dentures in patients with denture-induced stomatitis. Oral Microbiol. Immunol. 3, 8–13.
[245] Verran, J. and Motteram, K.L. (1987) The effect of adherent oral streptococci on the subsequent adherence of *Candida albicans* to acrylic in vitro. J. Dent. 15, 73–76.
[246] Marrie, T.J., Sung, J.Y. and Costerton, J.W. (1990) Bacterial

biofilm formation on nasogastric tubes. J. Gastroenterol. Hepatol. 5, 505–508.
[247] Millsap, K.W., Van der Mei, H.C., Bos, R. and Busscher, H.J. (1998) Adhesive interactions between medically important yeasts and bacteria. FEMS Microbiol. Rev. 21, 321–336.
[248] Grimaudo, N.J., Nesbitt, W.E. and Clark, W.B. (1996) Coaggregation of *Candida albicans* with oral *Actinomyces* species. Oral Microbiol. Immunol. 11, 59–61.
[249] Bos, R., Van der Mei, H.C. and Busscher, H.J. (1996) Influence of ionic strength and substratum hydrophobicity on the co-adhesion of oral microbial pairs. Microbiology 142, 2355–2361.
[250] Bos, R., Van der Mei, H.C., Meinders, J.M. and Busscher, H.J. (1994) A quantitative method to study co-adhesion of microorganisms in a parallel plate flow chamber, basic principles of the analysis. J. Microbiol. Methods 20, 289–305.
[251] Bos, R., Van der Mei, H.C. and Busscher, H.J. (1996) Co-adhesion of oral microbial pairs under flow in the presence of saliva and lactose. J. Dent. Res. 75, 809–815.
[252] Landa, A.S., Van der Mei, H.C. and Busscher, H.J. (1997) Detachment of linking film bacteria from enamel surfaces by oral rinses and penetration of sodiumlauryl-sulphate through an artificial oral biofilm. Adv. Dent. Res. 11, 528–538.
[253] Bos, R., Van der Mei, H.C. and Busscher, H.J. (1996) Influence of temperature on the co-adhesion of oral microbial pairs in saliva. Eur. J. Oral Sci. 104, 372–377.
[254] Longman, C.M. and Pearson, G.J. (1987) Variations in tooth surface temperature in the oral cavity during fluid intake. Biomaterials 8, 411–414.
[255] Spiering, Th.A.M., Peters, M.C.R.B. and Plaschaert, A.J.M. (1984) Surface temperatures of oral tissues. A review. J. Biol. Buccale 12, 91–99.
[256] Abeygunawardana, C., Bush, C.A. and Cisar, I.O. (1990) Complete structure of the polysaccaride from *Streptococcus sanguis* J22. Biochemistry 29, 234–248.
[257] McIntire, F.C., Crosby, L.K. and Vatter, A.E. (1982) Inhibitors of coaggregation between *Actinomyces viscosus* T14V and *Streptococcus sanguis* 34, β-galactosides, related sugars, and anionic amphiphatic compounds. Infect. Immun. 36, 371–378.
[258] Bugg, C.E. (1973) Calcium binding to carbohydrates. Crystal structure of a hydrated calcium bromide complex of lactose. J. Am. Chem. Soc. 3, 908–913.
[259] Lal, R. and John, S.A. (1994) Biological applications of atomic force microscopy. Am. J. Physiol. 266 (Cell Physiol. 35), C1–C21.
[260] Schaefer, D.M., Carpenter, M., Reifenberger, R., Demejo, L.P. and Rimai, D.S. (1994) Surface force interactions between micro-meter size polystyrene spheres and silicon substrates during atomic force techniques. J. Adher. Sci. Technol. 8, 197–210.
[261] Beech, I.B., Cheung, C.W.S., Johnson, D.B. and Smith, J.R. (1996) Comparative studies of bacterial biofilms on steel surfaces using atomic force microscopy and environmental scanning electron microscopy. Biofouling 10, 65–77.
[262] Wit, P.J. and Busscher, H.J. (1998) Application of artificial neural networks in the enumeration of yeasts and bacteria adhering to solid substrata. J. Microbiol. Methods 32, 281–290.
[263] Vicente, A., Meinders, J.M. and Teixeira, J.A. (1996) Sizing and counting of *Saccharomyces cerevisiae* floc populations by image analysis, using an automatically calculated threshold. Biotechnol. Bioeng. 51, 673–678.
[264] Wigglesworth-Cooksey, B. and Cooksey, K.E. (1996) A computer-based image analysis system for biocide screening. Biofouling 10, 225–237.
[265] Lawrence, J.R., Korber, D.R., Hoyle, B.D., Costerton, J.W. and Caldwell, D.E. (1991) Optical sectioning of microbial biofilms. J. Bacteriol. 173, 6558–6567.
[266] Surman, S.B., Walker, J.T., Goddard, D.T., Morton, L.H.G., Keevil, C.W., Weaver, W., Skinner, A., Hanson, K., Caldwell, D. and Kuptz, J. (1996) Comparison of microscope techniques for the examination of biofilms. J. Microbiol. Methods 25, 57–70.